PETROLOGY AND GEOCHEMISTRY OF BUNDELKHAND GRANITES AROUND MAHOBA, DIST. HAMIRPUR (U.P.)

ABSTRACT

THESIS SUBMITTED FOR THE DEGREE OF

Doctor of Philosophy

IN

GEOLOGY

BY

ABDUL RAHMAN

DEPARTMENT OF GEOLOGY
ALIGARH MUSLIM UNIVERSITY
ALIGARH (INDIA)

1991

PETROLOGY AND GEOCHEMISTRY OF BUNDELKHAND GRANITES AROUND MAHOBA, DIST. HAMIRPUR (U.P.)

ABSTRACT

The Bundelkhand massif occupies the central portion of the Indian plate and forms a semicircular to triangular outcrop covering an area of 26,000 sq. kms. The massif is delineated by the Indo- Gangetic alluvium in the north, the Son-Narmada lineament in the south and the Great Boundary Fault in the west. The evolution of the massif has involved several phases of magmatic episodes from basic to felsic. The dominant rock types of the massif are represented by granitic rocks. Sarkar et al (1969) on the basis of K-Ar dating of hornblende and biotite suggested that granitization closed during the period of 2500 to 2400 Ma, however, Crawfrod (1970) using Rb-Sr technique placed the age of Bundelkhand granite at 2550 Ma.

The tectonic position of the Bundelkhand granite is significant in the regional framework of Indian sub-continent. The Bundelkhand granitic massif is a composite body of dominantly acid magmatic rocks; it has largely remained undifferentiated. Detailed geochemical study has not been undertaken to discriminate and delineate the different phases of granites. The tectonic environment of emplacement of the granites have also not been carried out so far. The proximity of Bundelkhand massif to the much debated Son-Narmada lineament deserves special attention. An understanding to the tectonic setting of emplacement of the granites and its relation

to the major Lineament may help in diciphering the erstwhile lithospheric plate configuration.

Five genetically different types of granite have been deciphered and delineated in the northeastern part of the massif around Mahoba. Xenoliths of varying sizes, shapes and orientations have been observed in the granitic rocks. The varying directions of the foliations in the xenoliths suggest that the xenoliths are the caught up fragments of the intruded rocks rather than ungranitised relicts of the country rocks.

The oldest granitic phase deciphered in the area is termed as hornblende granite. It is a dark grey coloured medium grained rock with small phenocrysts of feldspar. Enclaves of hornblende granite are encountered in all the younger granites. The hornblende granite is intruded by the foliated biotite granite which exhibits porphyritic texture with two generations of feldspar phenocrysts, pre-tectonic and syn-to post-tectonic. Porphyritic biotite granite, a coarse grained rock with large phenocrysts of feldspar, is intrusive into foliated biotite granite. The coarse grained leucogranite has intruded into the porphyritic biotite granite. The fine grained leucogranite is the youngest granite in the area and is intrusive into all the older types of granite.

All the five types of granite, in general, have similar mineralogy with difference in relative content of individual phases.

All of them are one-mica granite containing biotite only. The characteristic minerals of the older three types include hornblende, plagioclase and K-feldspars; the two younger leucogranites are conspicuous by the absence of hornblende.

Various types of perthite are observed in all the types of granite. Myrmekitic intergrowth is fairly common in all the granites except the older two, the hornblende granite and the porphyritic biotite granite where it is rare. Plagioclase in all the five types of granite except the oldest hornblende granite is generally sodic in nature. Relatively more calcic plagioclase is observed in the hornblende granite. Carlsbad twinning and normal zoning in plagioclase with calcic core intensely altered to sericite surrounded by sodic shell, are common features of the plagioclase.

The plots of the four younger types of Bundelkhand granite lie mainly in the granite field on the Streckeisen's (1976) classification diagram, however, the oldest hornblende granite extends from the granodiorite to granite field. Plots of all the five types of granite are concentrated mainly in the central part of the modal quartz-albite-orthoclase diagram; the field corresponds to low temperature trough. Restriction of the plots in and around the low temperature trough suggests that the granite cooled slowly maintaining equilibrium throughout.

The I-type nature of the Bundelkhand granite is revealed by various major and trace element discriminant diagrams. The plots of the Bundelkhand granites on Ga/Al vs $K_2O + Na_2O$, $(K_2O + Na_2O)$ / CaO, K_2O/MgO and FeO/MgO and Ga/Al vs Zr, Nb, Y and Zn lie in the orogenic (I- & S-type) granite field. Some plots of the youngest leucogranites, however, are scattered and extended into anorogenic A-type granite field. Plots on CaO vs SiO_2 diagram define a nagative linear correlation, an array characteristic of I-type plutons world over. On the classification scheme diagram of Debon and Le Fort (1983, 1988) based on the parameters: Q = Si/3 - (K + Na + 2Ca/3), P = K-(Na + Ca), A = Al-(K + Na + 2Ca), B = Fe + Mg + Ti and F = 555 - (Q + B), the plots of the older two types of Bundelkhand granite occupy the granodiorite and adamellite fields, whereas the three younger granites plot in the granite field. The older two granites are extended into the metaluminous domain; the three younger granites plot in the peraluminous domain. The trend of the Bundelkhand granite is similar to that of cafemic and alumino-cafemic rock association. The trend of the older granites indicates their calc-alkaline nature, whereas the younger leucogranites correspond to subalkaline potassic type. Debon et al (1987) concluded that the granites with cafemic and alumino-cafemic character and calc-alkaline to sub-alkaline nature are related with the oceanic subduction processes.

Trace element concentrations and their ratios in different types of Bundelkhand granite on Harker's variation diagram reveal a trend similar to that of granitic liquid produced by fractional crystallization. The figures show a good positive linear correlation with U, Th and Rb and strong negative linear correlation with Sr, Ba and V. The elemental ratios Rb/Sr and K/Ba show strong positive correlation, whereas negative correlation is observed for K/Rb and Ba/Rb. All these trends correlate with the trends observed for granitic melt produced by fractional crystallization from a common parental comagmatic source.

The chemical composition of Bundelkhand granite plotted on AFM diagram reveals its calc-alkaline affinity and the pattern corresponds to that of Sierra Nevada batholith which is considered to be calc-alkaline inland continental margin magmatism. Majority of the samples of Bundelkhand granite on Wright's (1969) alkalinity ratio vs SiO_2 diagram plot on the calc-alkaline field; a few, however, plot in the alkaline field. The plots of Bundelkhand granites on Rogers and Greenberg's (1981) diagram, based on SiO_2 vs Log (K_2O/MgO), occupy both calc-alkaline as well as alkaline fields and follow the trend similar to that of Sierra Nevada and Ben Ghnema batholiths, both of them are concluded to be related with continental margin magmatism. The three older granites on the Sylvester's (1989) discriminant diagram, based on $(Al_2O_3+CaO)/(FeO_T+Na_2O+K_2O)$ vs 100 $(MgO+FeO_T+TiO_2)/SiO_2$, plot in the calc-alkaline and strongly peraluminous fields, whereas the two

younger leucogranites lie in the highly fractionated calc-alkaline granitoid field which, according to Sylvester (1989), is a variety of alkaline granitoids.

Incompatible trace element pattern for Bundelkhand granites shows a relatively smooth pattern witth significant depletion in Y content for the oldest hornblende granite in relation to the other types. The pattern of the hornblende granite correlates with Y-depleted granitic rocks of East Antarctic shield which are inferred to be syn-collision granites. The patterns for the younger varieties of Bundelkhand granites, showing significant enrichment in Y content with larger negative Sr and Ti anomalies, are similar to undepleted granite of East Antarctic shield. The Y-undepleted granites of East Anatactic shield are believed to be syn-orogenic granites formed by melting of felsic crust during the collision of lithospheric plates.

The geochemical signatures of Bundelkhand granites reveal a spectrum of tectonic setting of intrusion. The oldest hornblende granite has a Y-depleted pattern, consistent with hydrous partial melting of hornblende and/or garnet bearing mafic source (Sheraton et al, 1985). Foliated biotite granite and porphyritic biotite granite show significant enrichment in Y with larger negative anomalies of Sr and Ti; other LILE are also enriched in relation to the oldest type. The late to post-orogenic melting event is represented by the youngest two leucogranites in the area. The leucogranites correlate with highly fractionated felsic I-type granite, which show

characteristics similar to A-type. The leucogranites show marked enrichment in Y, Zr, Th, K and Rb and depletion in P, Sr, Ti and Ba.

In the present study an attempt has been made to elucidate the tectonic setting of emplacement of Bundelkhand granite by employing Maniar and Piccoli's (1989) discriminant diagram based on major elements. The composition of Bundelkhand granites when plotted sequentially on the classification scheme proposed by them reveals the emplacement of the granites in a continental collision tectonic set-up. However, some of the plots of the two younger leucogranites lie in the post-orogenic granite field. It may be concluded that the Bundelkhand granites were emplaced in a continental collision tectonic setting. The younger leucogranites may be of post-collision setting.

From the tectonic map of India it is seen that the Indian plate is a composite one with recognisible three protoplates viz. Dharwar, Aravalli-Bundelkhand and Singhbhum, coalesced with a Y-shaped Son-Narmada-Godavari lineament in between them. These protoplates came into existence as discrete isolated nuclei in the Gondwanaland during pre-Gondwana period. It is concluded that these protoplates grew in size and later collided along Son-Narmada lineament; the emplacement of Bundelkhand granite is a result of this collision tectonics. This inference is supported by the calc-

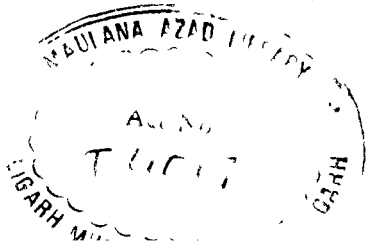

alkaline composition of the Bundelkhand granite and its close similarity with Sierra Nevada, Ben Ghnema and East Antarctic batholiths, all the batholiths are believed to be subduction related. The younger two leucogranites of Bundelkhand may be of post-collision setting.

PETROLOGY AND GEOCHEMISTRY OF BUNDELKHAND GRANITES AROUND MAHOBA, DIST. HAMIRPUR (U.P.)

THESIS SUBMITTED FOR THE DEGREE OF

Doctor of Philosophy

IN

GEOLOGY

BY

ABDUL RAHMAN

DEPARTMENT OF GEOLOGY
ALIGARH MUSLIM UNIVERSITY
ALIGARH (INDIA)

1991

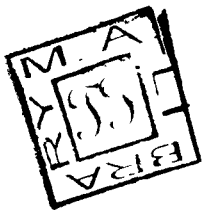

THESIS SECTION

DR. SYED M. ZAINUDDIN
M.Sc.,Ph.D. (Mich. State)
Sigma Xi (U.S.A.)
F.G.S. (India)

DEPARTMENT OF GEOLOGY
ALIGARH MUSLIM UNIVERSITY
ALIGARH — 202 002
PHONE : (0571) 5615
TELEX : 564-230-AMU-IN

Ref. No.....

Dated..April..8,..1991.....

CERTIFICATE

This is to certify that the work presented in this thesis, entitled **PETROLOGY AND GEOCHEMISTRY OF BUNDELKHAND GRANITES AROUND MAHOBA, DIST. HAMIRPUR (U.P.),** has been carried out and completed by Mr. Abdul Rahman under my supervision at the Department of Geology, Aligarh Muslim University, Aligarh.

This work is an original contribution to the knowledge of geochemistry and petrology of the Bundelkhand granites. The research work presented here has not been published anywhere in part or in full.

I recommend that Mr. Abdul Rahman be allowed to submit the thesis for the award of the degree of DOCTOR OF PHILOSOPHY IN GEOLOGY of the Aligarh Muslim University, Aligarh.

Syed M. Zainuddin

DR (SYED M. ZAINUDDIN)

ACKNOWLEDGEMENTS

The author extends his deep sense of gratitude to Dr. S.M. Zainuddin, Reader, Department of Geology, Aligarh Muslim University, Aligarh, under whose supervision and guidance this work was instigated and carried through. His personal interest in the study and guidance during the course of field work are gratefully acknowledged.

The writer would like to acknowledge the Chairman, Department of Geology, Aligarh Muslim University, Aligarh for providing necessary facilities.

The author is particularly grateful to Dr. Mohammad Ismail Bhat, Scientist 'C', Wadia Institute of Himalayan Geology, Dehra Dun for his unstinted cooperation. The help and cooperation of Dr. Anwar Rais, Geological Survey of India, Jaipur during the course of study are felt with special indebtedness.

Appreciations are due to the colleagues Messrs S.A. Rashid and M. Erfan Ali Mondal who helped in various phases of this work.

Acknowledgements are extended to Messrs Zakir Hussain Librarian, for his help in the course of study, Firoz Javed for chemical analysis, Salimuddin for drawing figures and Ziaur-Rehman for typing the manuscripts.

Abdul Rahman

ABDUL RAHMAN

TABLE OF CONTENTS

LIST OF TABLES

LIST OF FIGURES

INTRODUCTION

Purpose of Study

The granitic massif of Bundelkhand lies in the heart of Indian plate and forms a semicircular outcrop delineated by the Indo-Gangetic alluvium in the north and the Bijawars, the Vindhyans, the Gondwanas and the Deccan basalt in the south (Figure 1); the total outcrop area of Bundelkhand massif is 26,000 sq. kms.

Though the tectonic position of the Bundelkhand granite occupies a significant place in the regional framework of the Indian plate, yet not much work has been done to decipher the genesis, mode of emplacement and the tectonic setting of the granitic intrusion. The Bundelkhand granite covering a vast area has been mapped as a single body and has not been differentiated into genetically different types by the workers in the first half of the twentieth century. Various magmatic episodes in the area have not been deciphered and their effects on the host rock have also not been studied so far. Further, studies to determine the tectonic environment of the emplacement of the granites have not been carried out so far.

The proximity of Bundelkhand massif to Son-Narmada lineament may have some bearing on its genetic relationship. An understanding of the tectonic setting of the granitic emplacement and its relation to the Son-Narmada lineament may help in deciphering the configuration of the lithospheric plate in the Archean. An attempt

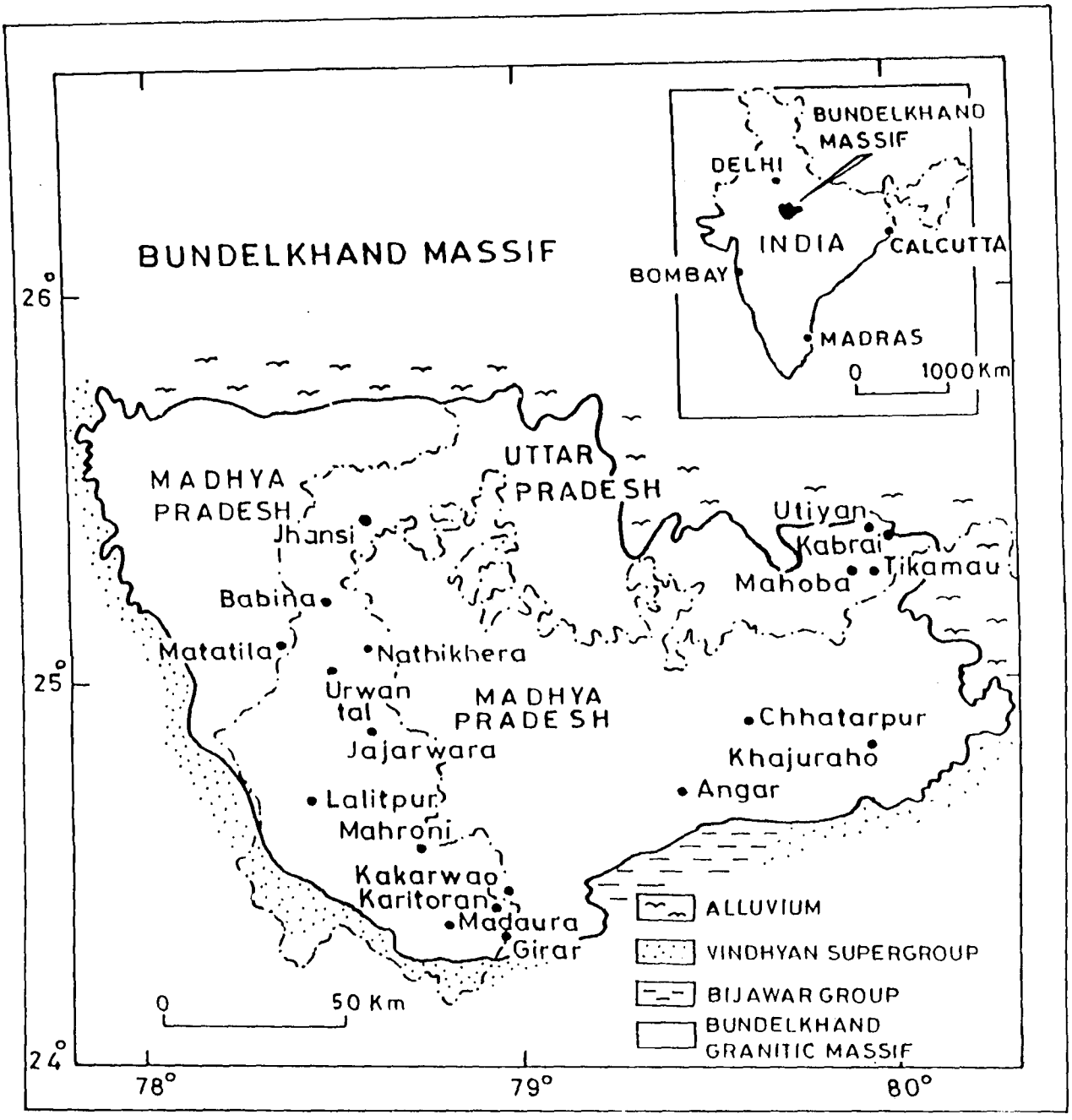

Fig. 1. Location map of Bundelkhand massif.

has been made to resolve this problem by petrological and geochemical study of the granitic massif.

Parts of Hamir Pur Distt. in U.P., where the granite is well exposed, constitute the proposed area of study. Geological mapping of the area was carried out using Survey of India toposheet No. 54 O/15 and 62 C/3 as base maps. Based on field evidence, five genetically different types of granite were deciphered and delineated.

Geography of the Area

The granitic rocks exposed in the area under present study constitute the northeastern margin of the Bundelkhand massif. The area is encompassed within latitudes 25°16'N and 25°26'N, and longitudes 79°47'E and 80°3'E. Figure 1 shows the area of study which includes Mahoba, Utiyan and Kabrai as some important localities. The climate of the area is semi-arid and the vegetation mostly xenophyric.

Most of the places are accessible by motarable roads. However, some places like, Daharra, Tikamau, Dharaun and Ganj are accessible by tracks only. At several places quarrying has been done for road and building material; these cuttings provide fresh and good exposures for field observations as well as sample collection.

The outcrop density is low; approximately 15-20% of the area has exposed rocks. The outcrops form isolated hills up to 2 km in length; the heights of the outcrop seldom exceed 300-400 feet above the surrounding terrain. The massive rocks are disintigrated along joint planes into blocks that range in size from few metres to tens of metres. Mechanical weathering due to extreme temperature variation appears to be dominant factor in the disintigration of the granite. The rocks weather into red loose soil, locally known as 'moram'.

Previous Work

The Bundelkhand massif situated in the northern part of Indian peninsula, has received attention of the geologists since mid-nineteenth century. The name, 'Bundelkhand gneiss' was proposed by Mallet (1869). The term, 'gneiss' was used for the coarse grained pink coloured granite of uniform composition showing poorly developed foliation and almost free from accessory minerals. Heron (1935) proposed the term, 'Bundelkhand granite' for the gneisses of the area. Fermor (1909) while discussing the granitic activity of Archeans, suggested a post-Dharwarian age for the Bundelkhand granite.

Heron (1935) believed that the massive granitoid gneisses of Bundelkhand and South India formed the floor over which the oldest

sedimentary beds of peninsula were deposited. However, Misra (1945, 1948) reported the presence of metasediments in the area which he believed to be older than granites. Saxena (1953, 1956) and Mathur (1954) agreed with the view of Misra (1945, 1948) regarding the presence of metasediments which are older than granites. They observed the presence of quartzite xenoliths in the granites and inferred that the quartzites were granitized. Saxena (1961) correlated the metasediments with the middle Dharwarian rocks. He considered the granitic activity in Bundelkhand as equivalent of Closepet granite.

Jhingran (1958) distinguished ten types of granite in the area on the basis of colour of feldspar, grain size, and variation in the content of ferromagnesian minerals. He observed xenoliths of various rock types in the granite and suggested an intrusive magmatic origin of the granite; the granite liquid having formed by anatexis of earlier sedimentary rocks. However, a metasomatic origin of the granites in Bundelkhand region was later proposed by Saxena (1961).

On the basis of petrochemical study of Bundelkhand granites, Misra and Sharma (1974) distinguished two principal types of granite in the area, a k-poor and a k-rich variety. They also reported that the average composition of metasedimentary raft corresponds to the composition of granites.

Misra and Sharma (1975) observed the presence of metasediments, quartzites, limestones, granites, syenites, carbonatites,

dolerites and keratophyres in Bundelkhand region and suggested that the assemblage may be referred to as 'Bundelkhand Complex' and the lithostratigraphic unit as 'Bundelkhand Group'. They divided the Bundelkhand Complex into four formations, namely: (1) Kuraicha formation which comprises of amphibolites, quartzites and migmatites, (2) Palar formation including quartzites, phyllites and ferruginous quartzite and pyrophyllite and diaspore deposits (3) Bundelkhand granites, ranging in composition from granite, granodiorite to syenite, cover about sixty percent of the total outcrop area; and (4) Bundelkhand basic intrusives comprising dolerite dykes which occur in a regular pattern throughout Bundelkhand. Five phases of folding were identified; the F_1, F_2 and F_3 deformations show excessive flowage of material without the development of cleavage in the rocks. The F_4 and F_5 folding episodes took place after the deposition of Palar formation.

Sharma (1982 and 1983) reviewed the lithostratigraphy and structure of the Bundelkhand complex. He opined that Bundelkhand region is composed of a variety of rocks which have undergone metamorphism contemporaneous with several pulses of deformation. All these rocks being intimately related, bear common imprints of major episodes of metamorphism and deformation. As such, they have been classified into one group, called Bundelkhand Group which has been divided into seven formations. These include (1) Kuraicha formation, (2) Palar formation, (3) Peron meta-acid volcanics,

(4) Garhmau granites, (5) Matatila granites, (6) Mahoba dolerites and (7) Madaura ultrabasics.

The petrological evolution of the Bundelkhand Group has been through the Archean time; the volcanogenic sediments constitute the oldest crustal material. The Bundelkhand craton can be classified into two divisions on the basis of the degree of metamorphism; the older rocks have been metamorphosed to the upper medium grade facies, whereas the rocks of younger division correspond to low grade metamorphic facies (Sharma, 1982). The earlier crust was separated into a deeper amphibolitic layer and an upper gneissic layer; the gneissic layer through anatexis has given rise to different types of granite.

The structures developed in the Bundelkhand massif are a result of lateral compression and vertical movement of the craton. The style and attitude of folds, trends of foliation and domal features, north and northeast trending lineaments, west and northwest trending lineaments, faulted contact with the Bijawar and the Vindhyan, and regional tectonic framework correspond with the major tectonics of the Narmada-Son lineament, boundary faults of the Aravalli and normal faults of the Indo-Gangetic trough (Sharma, 1982).

Sharma (1983) suggested that the Narmada-Son lineament is a tectonic zone dissecting the Indian shield into northern and southern segments. The movement along this tectonic zone and its strain

history have an important bearing on the tectonics of the Bundelkhand complex. Roday and Bhatt (1980) attributed the deformation in the Narmada valley to the longitudinal tangential strain and flexure slip. The gash and tension fractures opening upward whose trends are parallel to the lineament, have been interpreted as a product of the buckling of the crust. The granite occurring in this tectonic zone, parallel to the lineament are possible remnant of an old crust that has been cut by transverse and longitudinal faults. These granites are not considered to be intrusive in the fault zones (Sharma, 1983). However, Das et al (1982) found a positive correlation of K_2O vs Al_2O_3 plots of Buldelkhand granite and attributed this to an igneous origin of the granite. They also observed a proportionate enrichment of U in younger granites indicated by gradual decrease in U/Th ratio. This order, they thought, may be taken as the possible sequence of emplacement of various granites.

Several episodes of granitic activity in the Bundelkhand massif were deciphered by Basu (1986). On the basis of field relationship corroborated by petrography and geochemical study, he distinguished twenty episodes of igneous activity which included three main types of granite, (1) Porphyritic coarse grained granite (2) Porphyritic medium grained granite and (3) non-porphyritic to sparsely porphyritic medium to fine grained leucogranites. Besides these types of granite, a number of other varieties have also been reported by him. He observed a similarity in geochemistry of the different

intrusive granites of Bundelkhand massif and opined that these were possibly derived from the same melt. He also reported the conspicuous absence of any enclaves of schist and high grade rocks within the granitic plutons. Basu inferred that the magmatism has been the principal mechanism of rock generation and concluded that the quartz reefs are intrusive veins in contrast to the sedimentary origin claimed by some of the earlier workers. Lack of muscovite in the granite indicates medium to upper level formation of granites.

On the basis of K-Ar dating of hornblende and biotite from the amphibolite and biotite schists of the Kuraicha formation, Sarkar et al (1964) and Sarkar et al (1969) suggested that the Bundelkhand orogeny, regional metamorphism and granitization closed during the period of 2500 to 2400 Ma. However, Crawford (1970), using Rb-Sr method, considered the granitic rocks of Bundelkhand and Berach to be coeval at 2550 Ma. The granites have intruded the older undated sediments in the area.

Various earlier workers working on parts of the Bundelkhand massif proposed different views regarding the origin of Bundelkhand granites. There is a controversy on the number of phases of igneous activity and their tectonic set-up. Present study is aimed to differentiate the genetically different granitic episodes and to determine the tectonic setting of emplacement in relation to the Son-Narmada lineament.

CHAPTER II

GEOLOGICAL SET-UP

The Bundelkhand granitic massif situated in the northern part of peninsular India, is a semicircular outcrop, surrounded by the Bijawar, the Vindhyans, the Gondwanas and the Deccan traps in the south and by the Indo-Gangetic alluvium in the north. It is believed that the massif extends to the Narmada-Son lineament in the south, the Great Boundary Fault of the Aravallis in the west and the Himalayas in the north (Naqvi and Rogers, 1987). Geophysical investigations reveal the northeasterly extension of the granitic massif below the alluvium designated as the Faizabad (sub-surface) Ridge (Sastry et al , 1971). The outcrops in the terrain of the massif are scattered and isolated. A wide variety of rocks are exposed in the area; the most dominant being the granitic rocks of several generations which cover more than sixty percent of the total outcrop area.

Pascoe (1950) and Chatterji et al (1971) have correlated the regional stratigraphic sequence of the Bundelkhand massif with the adjoining areas (Table 1).

Table 1: Stratigraphic succession in the Bundelkhand region.

Malwa Deccan Traps (Cretaceous - Eocene)
Vindhyan Supergroup (1500 - 500 Ma)
----------Unconformity----------
Bijawar and Gawalior group (2400-2300 Ma)
----------Unconformity----------
Bundelkhand granitic complex (2600 Ma)
Mahroni Formation (Archean)

The earlier workers have carried out studies in different parts of the massif; stratigraphic successions determined by different workers are given in Table 2.

The present study area lies in the northeastern part of the massif around Mahoba, Distt. Hamirpur. The granitic rocks are well exposed in the area in the form of isolated hillocks; their heights seldom exceed 300-400 feet above the surrounding country. The outcrops are detached and scattered due to intense and deep weathering. Small jointed and fragmented blocks of different sizes are common in the area. Based on field relationship, five genetically different types of granite were identified and delineated

able 2 : Stratigraphic Successions of the Bundelkhand Massif

Pascoe, 1950	Jhingran, 1958	Saxena, 1961	Prakash et al, 1975	Misra & Sharma, 1975	Sharma, 1982	Basu, 1986
eridotites, pyroxenites partially altered to erpentinite and ilcactinolite schists) trusive dolerite-trap kes e-Dharwar Bundel- and Granite mplex with quartz ef.and with inclusions Mahroni schists	Basic dykes Quartz reefs Granites (of ten mega-scopic types) Relict metasediments #Dharwars(?)	Dolerite and other basic dykes Quartz reefs Pink granites, migmatites ---Unconformity--- Metasedimentary rocks	Madaura Formation (Pre-to post-Bijawar age) a dolerite dykes, granite member, quartz vein, pegmatite, graphic granite b Gabbro member coarse to medium grained gabbro, pillow lava, ultrabasic member Milky dense sheared vein quartz Bundelkhand granite Formation dull pink dense fine grained to porphyritic granite coarsely crystalline pink unfoliated granites and migmatites ----------Unconformity---------- M a Bijawar Formation: Iron-h rmations, carbonate rock, n ceous green slates, o uartzite quartzite and n conglomerate 1 ---------Unconformity--------- G Madaula Formation r sedimentation-volcanism o amphibolites, biotite-u feldspar foliated p gneisses.	i) Bundelkhand Basic Intrusives dolerites, keratophyres, lamprophyre, other basaltic rocks, carbonatites ii) Bundelkhand granites gneisses, grey and pink granites granodiorites syenite porphyritic granites quartz veins and feldspathic veins iii) Palar Formation (low grade metamorphics) quartzite spotted phyllites, sericite schists talc-schists, phyllites black shales, limestones, ferruginous quartzites with traces of chalcopyrite, galena, pyrophyllite and diaspore deposits --------Unconformity------ iv) Kuraicha Formation, (high grade metamorphics) migmatites gneisses, para-ortho-, and augen gneisses amphibolites chlorite and biotite schists and quartzites	B Madaura Ultrabasics U N Mahoba Dolerite D E Matatila Granite L K Garhmau Granite H A Baron Meta-acid Volcanics N D Palar Formation G R O U P ----Unconformity--- Kuraicha Formation	Dolerites Quartz reefs (with pyrite, chalcopyrite, pyrophyllite and diaspore) Aplite Esmeraldite Porphyries Pegmatites Leucocratic granites Migmatite Syenites Medium grained porphyritic granites Coarse grained porphyritic granites Coarse biotite granite Gneisses --------Unconformity-------- Banded iron-formations Metabasites

in the area. The geology of the study area is shown in Figure 2; the structural data and sample locations are plotted in Figure 3. The age relationship of different types of granite as inferred by field obserevations is given in Table 3.

Table 3: Stratigraphy of the Bundelkhand Massif around Mahoba.

Dolerite Dykes
Quartz Reefs
Aplites and Pegmatites
Fine Grained Leucogranite (FLG)
Coarse Grained Leucogranite (CLG)
Porphyritic Biotite Granite (PBG)
Foliated Biotite Granite (FBG)
Hornblende Granite (HG)
Basement Rocks

Basement Rocks

The oldest rock encountered in the area is a dark coloured biotite rich rock, compact and hard, exhibiting perfect foliation. The constituent minerals identified in the rock are biotite, quartz, plagioclase, apatite and opaques; biotite is dominant with numerous

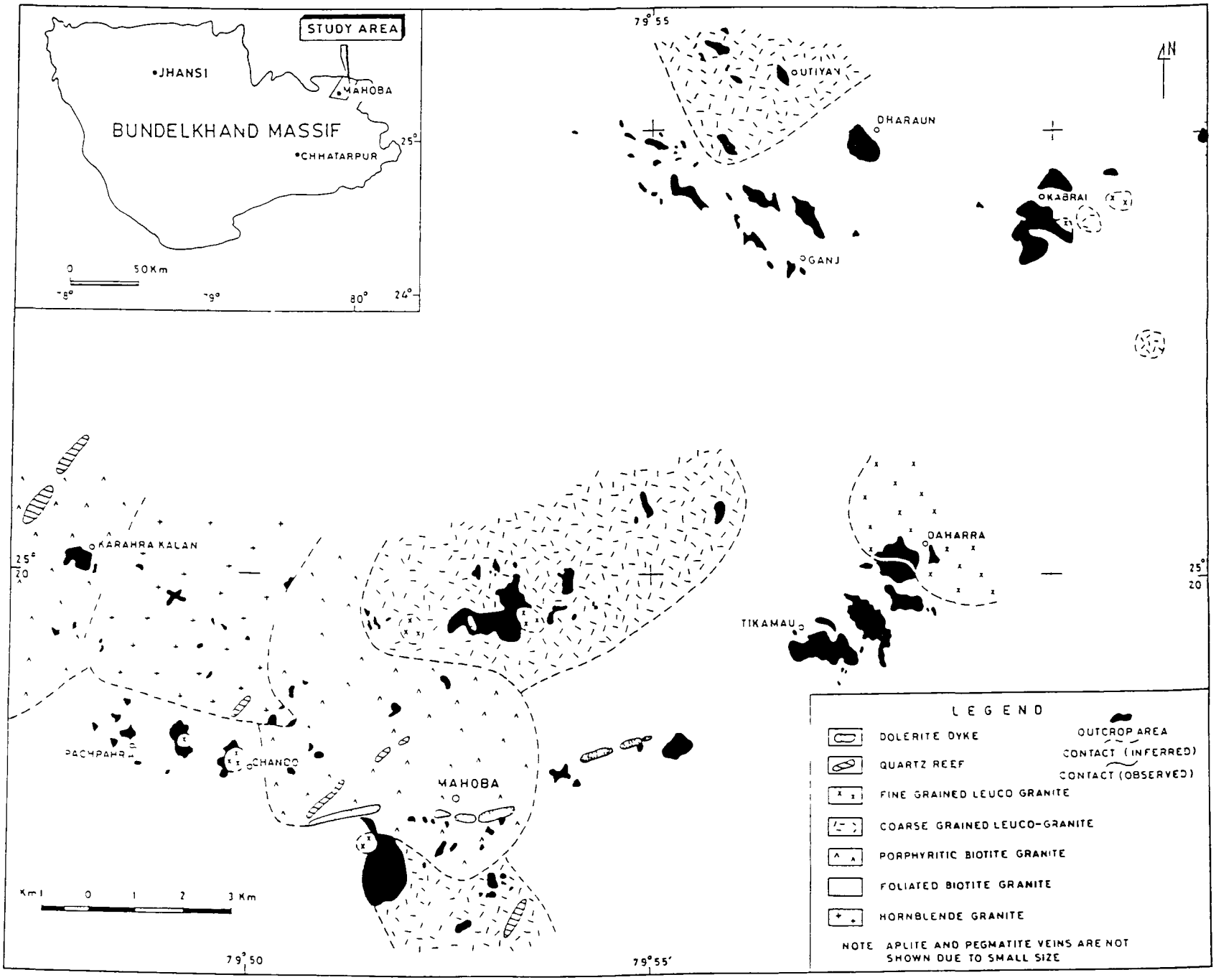

Figure 2. Geological map of Bundelkhand massif around Mahoba, Dist. Hamirpur,(U.P.)

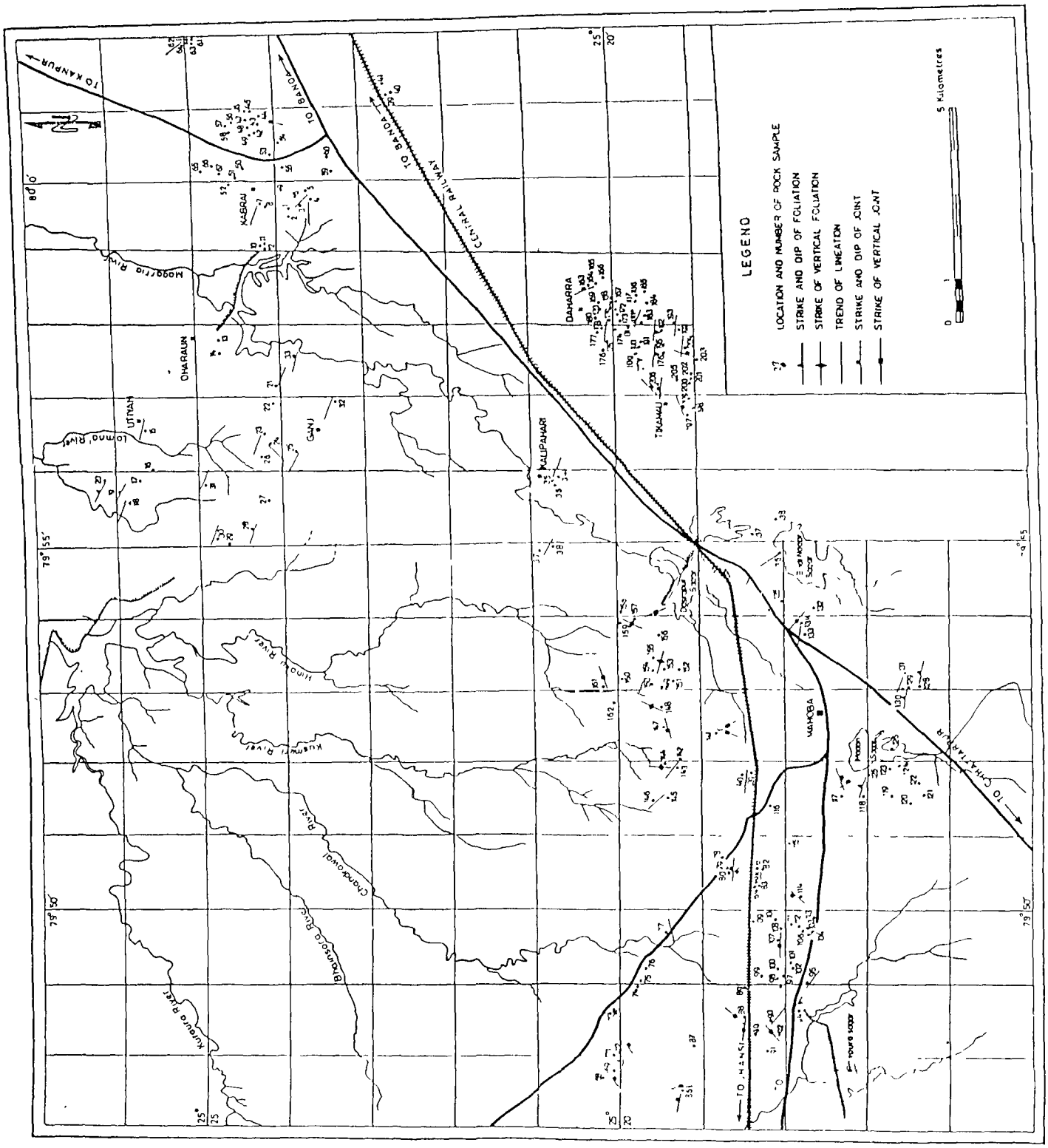

Fig. 3. Map of Mahoba area showing sample locations

inclusions of apatite. Crystals of biotite exhibit parallel orientation (Figure 4).

Xenoliths of varying sizes of the biotite rich rock have been found in the granitic rocks. Generally the xenoliths have sharp contacts with the enclosing granite and show no evidence of any visible reaction between them. At places chilled contacts are observed. The enclaves occur in different orientations in the granite as is indicated by the varying direction of foliation in the xenoliths within a small outcrop. This suggests that they are caught up fragments of intruded rocks rather than ungranitised relicts of the older country rock. Xenoliths of quartzites are rare, sometimes they exhibit alternate fine lamellae of mafic minerals with quartz bands. Enclaves of basement rocks mainly occur in the older types, whereas the xenoliths in younger varieties are rare.

Hornblende Granite

The granitic rocks of the oldest phase in the area under present investigation is a medium grained rock, light to dark grey in colour with small phenocrysts of feldspar. The concentration of ferromagnesian minerals in the rock is high.

The most prominent outcrop in this granitic body is located along Mahoba-Charkhari road where it occurs in the form of small

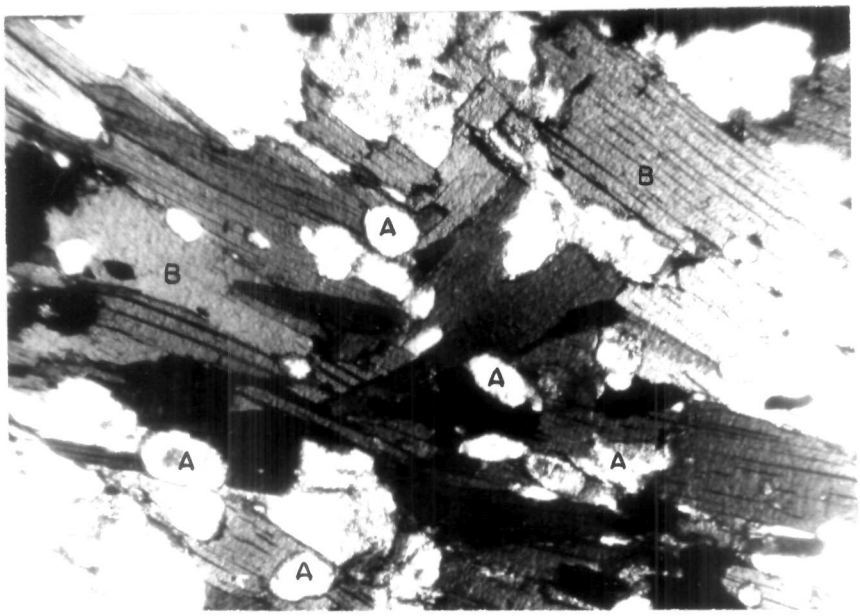

Figure 4. Photomicrograph showing parallel orientation of biotite (B) with inclusions of apatite (A) in xenoliths of basement rock.

hillocks. Small isolated outcrops of hornblende granite are also found around Daharra, northeast of Mahoba where it is intruded by the foliated biotite granite; mixture of the two rock types formed a hybrid rock. The hornblende granite also occurs in the form of xenoliths of varying shapes and sizes in the younger granites of the area.

Xenoliths of dull black coloured biotite rich basement rocks are common in the granite (Figure 5). Small fragments of basaltic rocks present in the granite, impart a spotted appearance. The size of basaltic fragments are commonly less than 1 cm but sometimes it is as large as 4 cm in length. The rock is intruded by several generations of quartz veins (Figure 6). Towards east of Karehra Kalan, the porphyritic biotite granite and the fine grained leucogranite are found to have intruded into the hornblende granite; the hybrid rock produced by the mixture of these granites appears like a migmatite. Three prominent sets of joints are present, their trends are NNW-SSE, N-S and NE-SW.

Foliated Biotite Granite

The foliated biotite granite is the most dominant type of granite occuring in the area. The rock forms large ridges around Pachpahra and Chandu villages towards west of Mahoba, and around Tikamau in the northeast of Mahoba. The granite occupies a large

Figure 5. Xenolith of basement rock in hornblende granite (HG). Small veins of HG traverse the xenolith.

Figure 6. Hornblende granite is intruded by several generations of quartz veins.

area around Kabrai, Ganj and at Dharaun, about 20 km. north of Mahoba.

The granite is grey in colour, generally light but at places it ranges from light to dark grey. The rock is coarse grained with a porphyritic texture having tabular phenocrysts of feldspars. The groundmass is medium grained, composed of quartz, feldspar and small crystals of biotite. The granite locally exhibits foliation; alternate bands of biotite and feldspar impart a gneissic texture to the rock. Foliation is well developed in the granite exposed at Tikamau northeast of Mahoba and towards south of Dharaun. Dark coloured ferromagnesian minerals are segregated into thin streaks which together with parallelism of elongated crystals of feldspar phenocrysts impart a banded appearance to the rock. Feldspar phenocrysts in the rock are of two generations, the pre-tectonic feldspar phenocrysts have a high length to width ratio ranging from 5:1 to 7:1, whereas the dimentions of the post- and syn-tectonic phenocrysts, varies from 4 x 1.8, 5 x 2.5 to 3 x 1.3 centimetre and the general foliation trend is NW-SE.

Joints are the prominent structural features of the rock; five sets of joints have been identified in the granite. Three sets of joints, however, are more prominent. Weathering along the joints has resulted into the development of tabular blocks. The degree of weathering along the joints varies considerably within a single outcrop. Veins of aplite and quartz have intruded along the joints.

Xenoliths of varying shape and size of old metabasic rocks are common in the granite (Figure 7). The granite also contains xenoliths of hornblende granite (Figure 8), which indicate an older age of the hornblende granite. The foliated biotite granite, in turn, is intruded by the porphyritic biotite granite with a sharp contact between the two granites as observed at Mahoba near Madan Sagar (Figure 9). Veins of porphyritic biotite granite within the foliated biotite granite, have physical continuity with the main body of the porphyritic biotite granite. This indicates the intrusion of the porphyritic biotite granite into the foliated biotite granite and hence a relatively younger age and a magmatic origin of the porphyritic biotite granite.

Porphyritic Biotite Granite

Large outcrops of porphyritic granite are seen at Karehra Kalan and Mahoba. The rock is coarse grained having large phenocrysts of feldspars. The colour of the granite varying from pink to grey shows gradational change within short distances. The variation in colour has probably no genetic significance and may only be a superficial feature. Three sets of joints, trending NW-SE, NNW-SSE and E-W, are prominent.

The rock is not very compact, it weathers by exfoliation easily. The outcrops form gentle slopes. The nature of weathering

Figure 7. Metabasic xenoliths (basement rock) in foliated biotite granite.

Figure 8. Xenoliths of hornblende granite (HG) in foliated biotite granite.

Figure 9. Sharp contact (weathered) between foliated biotite granite (FBG) and porphyritic biotite granite (PBG).

Figure 10. Xenoliths of metabasites, cut across by later pegmatite vein, in porphyritic biotite granite.

of the porphyritic biotite granite is different from that of other varieties. On weathering, the granite forms a deep red coloured soil, locally known as 'moram' which is used in building construction. Major parts of the outcrops of the granite in the area is highly weathered and has been changed to 'moram'.

Xenoliths of metabasites, migmatites and sometimes metasediments (Figure 10 & 11) occur in porphyritic biotite granite. At Karehra Kalan, xenoliths of hornblende granite are very commonly observed in porphyritic biotite granite (Figure 12). The contact of granite with xenoliths is very sharp which indicates that the magma was not very hot at the time of intrusion. A few large porphyroblasts of feldspar extend across the contact of porphyritic biotite granite and xenoliths of metabasites; they have probably formed at a later stage by reaction between the granitic liquid and the xenoliths.

The porphyritic biotite granite is intruded by the coarse grained leucogranite, as seen towards the north of Mahoba along Mahoba-Bilbai road, the contact between the two is sharp (Figure 13). This suggests an older age of porphyritic biotite granite in relation to coarse grained leucogranite.

Coarse Grained Leucogranite

The granite is exposed in a large part of the area, north of Mahoba and at Kalipahari along Mahoba - Kabrai road. In the

Figure 11. Xenolith of migmatite in porphyritic biotite granite.

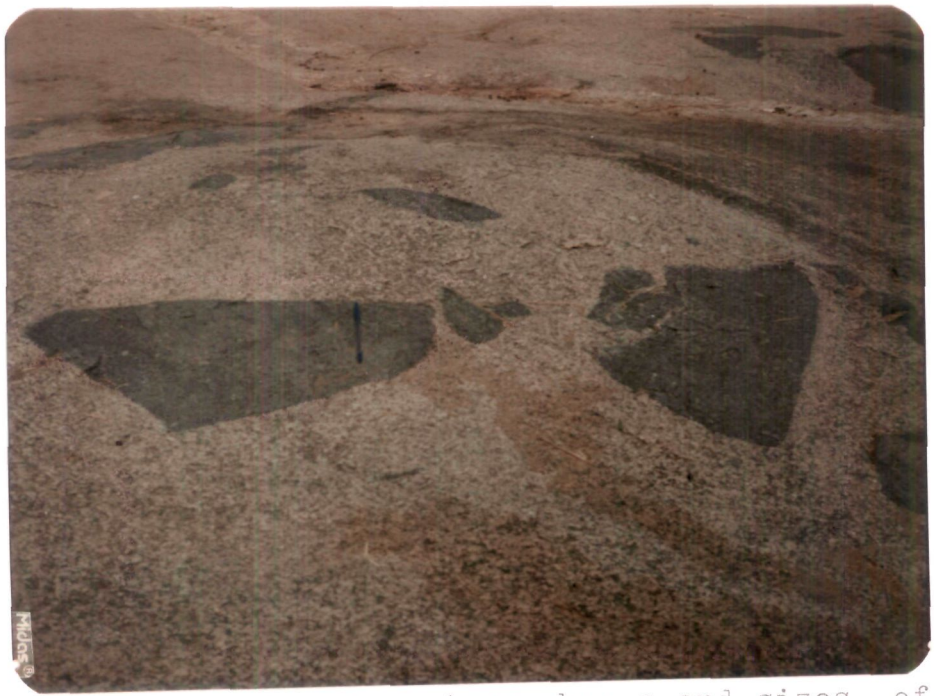

Figure 12. Xenoliths of various shapes and sizes of hornblende granite (HG) in porphyritic biotite granite (PBG) indicating younger age of PBG.

Figure 13. Vein of coarse grained leucogranite (CLG) in porphyritic biotite granite (PBG) indicating an older age of PBG.

Kabrai area, the outcrop of the granite is seen at Utiyan. The leucogranite is a massive medium grained rock comprising mainly of quartz and pink coloured feldspars; ferromagnesian minerals constitute a small proportion of the rock.

Xenoliths of fcliated biotite granite, found in the rock indicate younger age of the leucogranite. This is supported by the intrusive relation of the leucogranite into porphyritic biotite granite. The coarse grained leucogranite has been intruded by aplitic granite which has been termed as fine grained leucogranite.

Biotite is the common ferromagnesian mineral in the rock which exhibits preferred orientation at places. The trend of foliation is parallel to the NW-SE joint.

Fine Grained Leucogranite

This is the youngest granitic rock exposed in the area. It is a compact leucocratic rock of brown to grey colour. The granite is intrusive into all the older types of granite and occurs in the form of veins and dykes ranging in thickness from a few cm to a few metres. At Daharra towards northeast of Mahoba, it forms the most prominent outcrop where it occurs in the form of small hillocks. Veins of aplite and pegmatite are also common at Daharra.

Joints are poorly developed in the granite, the most prominent of them being in NE-SW direction.

The granite is uniformly fine grained and is mainly composed of quartz and feldspar. Biotite, the only ferromagnesian mineral present in the rock, is in much less concentration than in the other four types of granite. The granite is observed to have been intruded into the metabasites and all the other types of granite occuring in the area; at places enclaves of the older granites (Figure 14 & 15) are found in the fine grained leucogranite. The composition of the rock has been modified by the assimilative reaction of the granite with the host rock.

Figure 14. Photograph showing sharp contact between foliated biotite granite (FBG) and fine grained leucogranite (FLG) with xenoliths of hornblende granite (HG) in FLG.

Figure 15. Enclaves of foliated biotite granite (FBG) in fine grained leucogranite.

CHAPTER III

PETROLOGY OF THE GRANITES

Modal Analysis of the Granites

Determination of the mineral composition and their relative proportions in the various types of granitic rock exposed in the area were carried out to differentiate and classify the granite types on the basis of their mineralogy. K-feldspars in thin sections were stained using the method suggested by Baily and Stevens (1960) to differentiate them from untwinned plagioclases. The thin sections were etched by concentrated hydrofluoric acid and then dipped into a solution of Sodium Cobaltinitrite. As a result, the K-feldspars were stained yellow. Modal compositions of the five types of granite were determined by the point count method of Chayes (1956). Fifty thin sections, ten of each type of granaite were studied to determine the modal abundance of the constituent minerals.

The five types of granite have similar mineral composition. However, differences in the relative proportion of various minerals in the different types of granite can be observed. The range and average modal composition of the five types of granite are presented in Table 4.

The variation in the relative proportions of different minerals in the various types of granite is evident. The three older granites are enriched in ferromagnesian minerals including biotite and

Table 4: Mineral Composition of the Five Types of Granitic Rocks (values in mode %).

	Hornblende Granite (10 samples)		Foliated Biotite Granite (10 samples)		Porphyritic Biotite Granite (10 samples)		Coarse Grained Leucogranite (10 samples)		Fine Grained Leucogranite (10 samples)	
Mineral	Mean	Range	Mean	Range	Mean	Range	Mean	Range	Mean	Range
Quartz	29.60	24.81-36.54	30.94	24.67-37.89	32.68	24.62-38.81	36.09	30.12-45.4	37.60	32.51-41.83
Plagioclase	36.70	30.26-43.30	36.98	32.22-41.34	24.76	19.08-26.56	23.12	17.10-30.45	24.39	19.83-32.75
Microcline	20.10	16.15-25.02	25.25	19.55-29.00	39.42	33.45-44.60	37.22	31.50-45.06	34.46	30.41-36.57
Biotite	6.35	4.23-11.50	4.27	0.02-6.46	2.74	1.0-5.26	1.92	0.45-3.94	2.22	0.16-4.6
Hornblende	3.15	0.40-9.83	0.94	0.00-3.91	0.70	0.00-3.08	-	-	-	-
Chlorite	-	-	0.10	0.00-0.39	0.47	0.00-2.38	0.43	0.00-1.80	0.42	0.00-1.19
Sphene	0.70	0.70-1.28	0.36	0.00-1.11	0.12	0.00-0.38	0.24	0.00-1.17	0.09	0.00-0.29
Zircon	0.32	0.00-0.90	0.16	0.00-0.33	0.07	0.00-0.18	0.16	0.00-0.80	0.09	0.00-0.50
Apatite	0.33	0.16-0.60	0.20	0.00-0.44	0.23	0.05-0.74	0.03	0.00-0.13	0.04	0.00-0.45
Epidote	0.28	0.00-0.46	0.47	0.00-1.26	0.10	0.00-0.58	0.25	0.00-0.87	0.16	0.00-0.32
Opaque	1.17	0.70-2.00	0.31	0.00-1.00	0.27	0.04-1.39	0.50	0.19-0.90	0.49	0.19-1.00

hornblende and have high content of plagioclase, whereas K-feldspar is relatively low. In the younger granites, the content of ferromagnesian minerals and plagioclase decreases with concomitant increase in K-feldspar and quartz. The two older granites have a higher plagioclase : K-feldspar ratio, whereas the younger granites have a plagioclase: K-feldspar ratio of less than 1. Absence of hornblende in the younger two leucogranites is significant.

The modal quartz, potash feldspar and plagioclase (recalculated to 100%) were plotted on the Orthoclase-Albite-Quartz phase diagram (Figure 16) of James and Hamilton (1969). Plots of all the five types of granite are concentrated mainly in the central part of the diagram. However, the plots of the two older granites, having a plagioclase : k-feldspar ratio of more than 1, are distinctly restricted towards the plagioclase field, whereas the three younger granites plot towards k-feldspar field.

These plots are also restricted in and around the area of low temperature trough suggesting that the granites cooled slowly maintaining equilibrium throughout the cooling.

Modal values of quartz, albite and orthoclase were plotted on the Streckeisen's (1976) classification diagram (Figure 17). The plots of the hornblende granite extend from the granodiorite to granite field, whereas the plots of foliated biotite granite, porphyritic biotite granite, coarse grained leucogranite and fine grained leucogranite are restricted to the granite field.

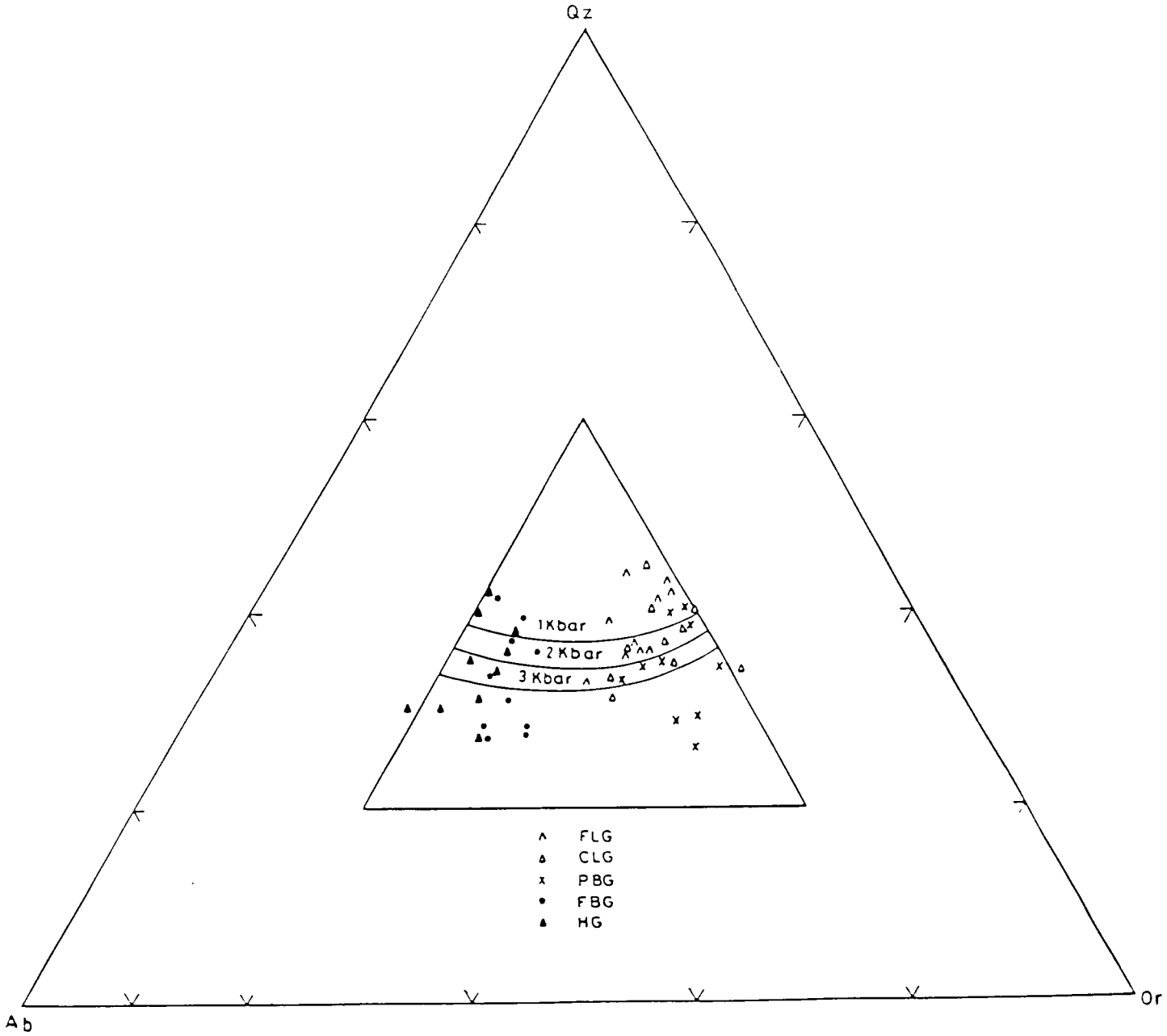

Figure 16. Ternary quartz-albite-orthoclase plot for the Bundelkhand granites.

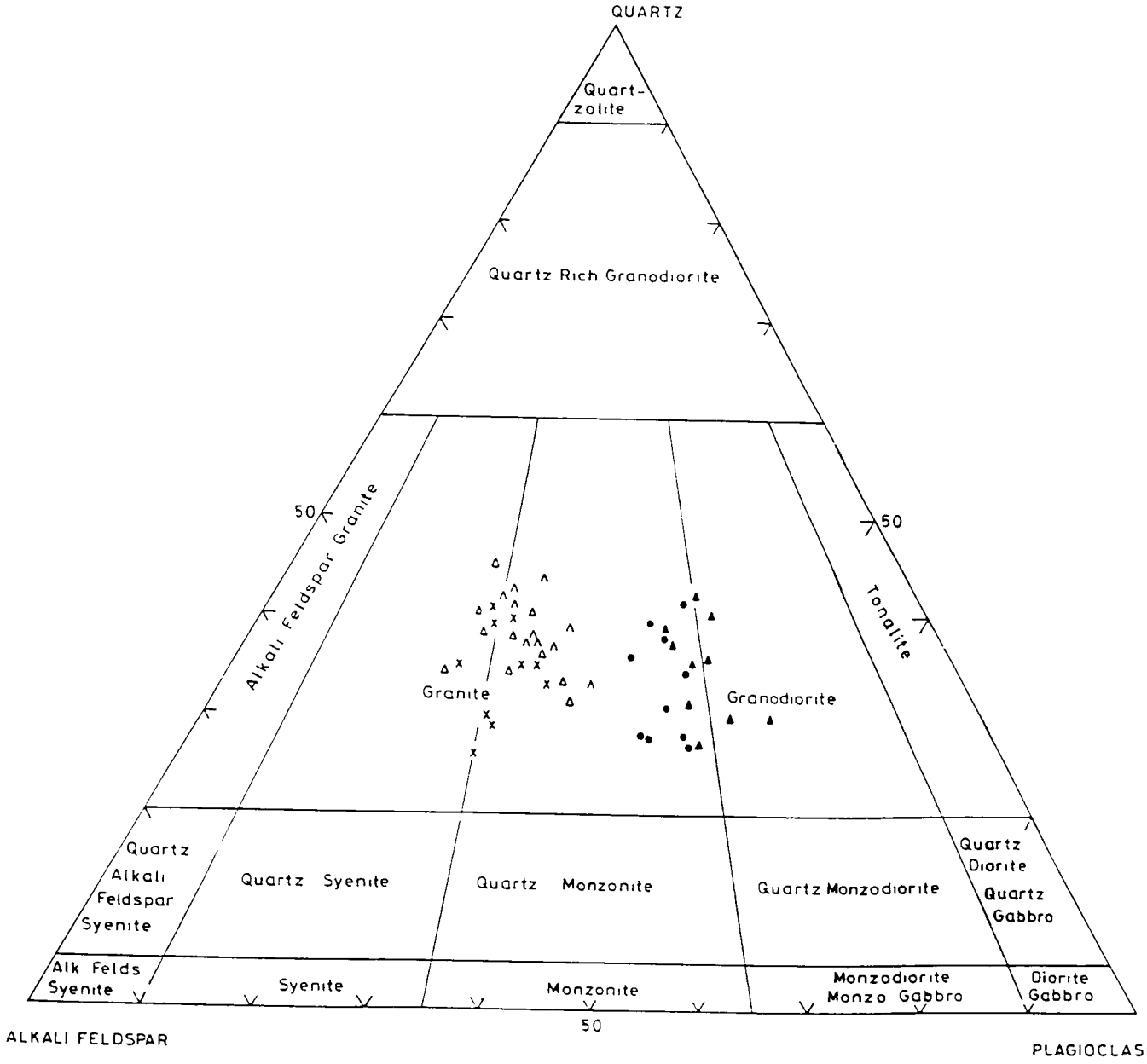

Figure 17. Modal values of Bundelkhand granites plotted on Streckiesen's (1976) classification diagram (symbols as in Figure 16).

Petrography of the Granitic Rocks

Hornblende Granite

On the basis of field relationship, the hornblende granite is inferred to be the oldest granite in the area. Xenoliths of hornblende granite are found in all the younger types.

It is a medium grained rock generally showing hypidiomorphic granular texture, at places, small phenocrysts of plagioclase are found in the rock. The clusters of ferromagnesian minerals impart a spotted appearance to the rock.

Plagioclase is the dominant mineral and constitute about 30.3% to 43.3% of the rock by volume; the average being 36.7%. The plagioclase is sodic in composition, ranging from An_9 to An_{18}. Zoning in plagioclase is common, the calcic core being relatively more altered than the rims in the zoned plagioclases (Figure 18). Antiperthitic intergrowth of microcline is commonly observed in the rock; most of the microcline grains within the plagioclase crystals show similar optical orientation (Figure 19). The formation of the antiperthite may be attributed to the growth of microcline on low energy surfaces of ealrier formed plagioclases. Sometimes plagioclase grains are partially enclosed within the biotite crystals (Figure 20) which indicates the earlier crystallization of plagioclase. Myrmekitic intergrowth is very rare, a few plagioclase grains show enclaves of quartz which is believed to be of exsolution origin.

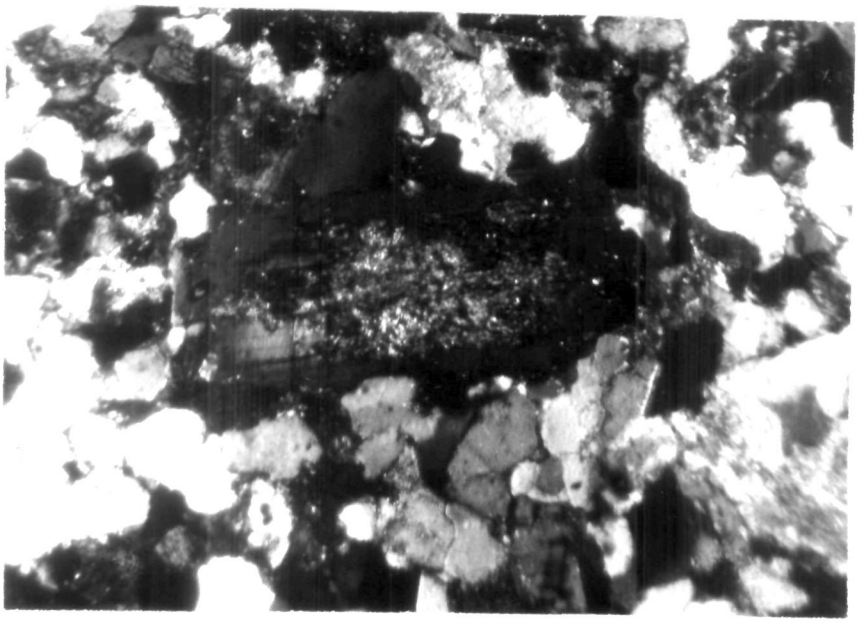

Figure 18. Zoning in plagioclase with an altered calcic core and a clear sodic rim. Crossed polars.

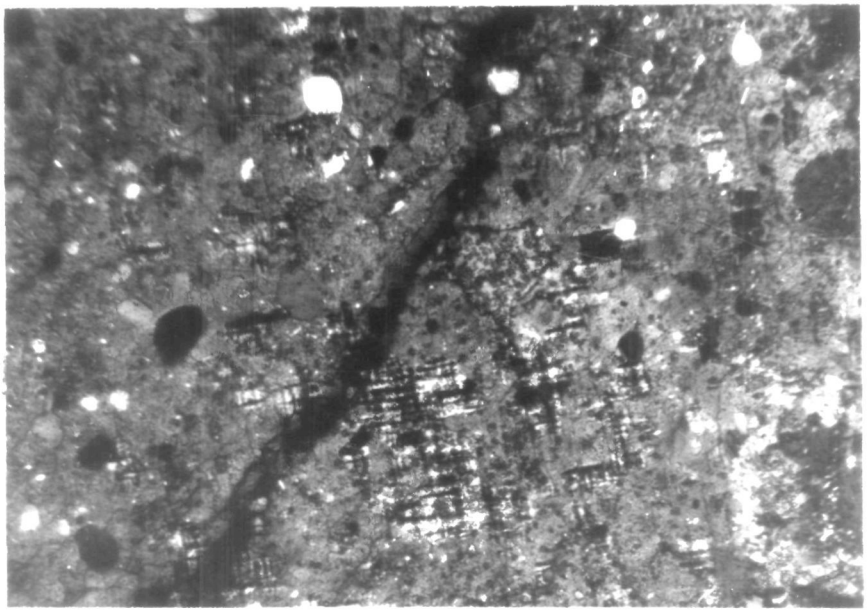

Figure 19. Antiperthitic intergrowth of microcline. Most of the microcline grains show similar optical orientation. Crossed polars

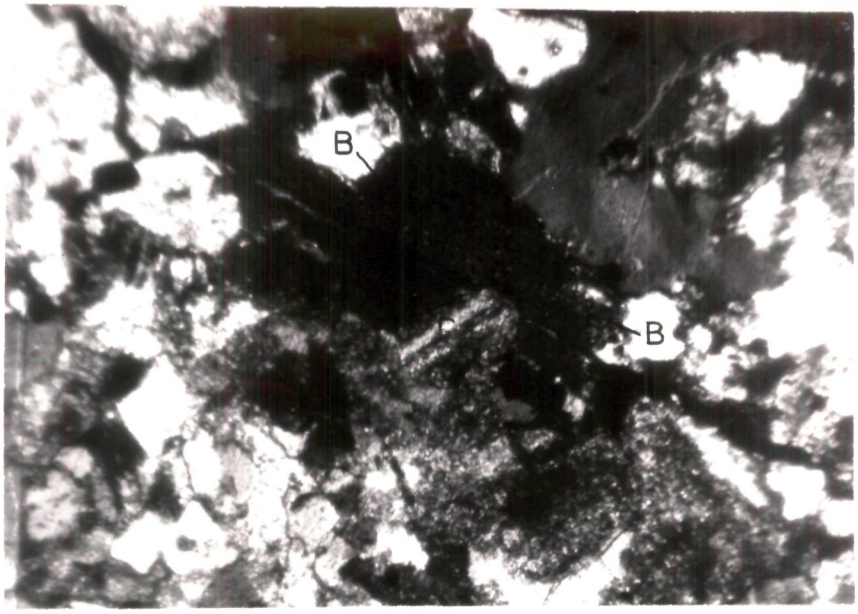

Figure 20. Plagioclase (P) partially enclosed within biotite (B) crystals. Crossed polars.

Quartz is also fairly abundant in the rock, it has a modal concentration of 24.8 to 36.5%, with an average of 29.6% by volume. Quartz occurs in the form of subhedral to anhedral grains, the contact between the quartz crystals are highly embayed.

K-feldspar, mainly microcline, is relatively less abundant and constitutes an average of about 20% of the rock by volume. Untwinned orthoclase crystals in the rock are very rare. Vein perthite is also observed which is inferred to be of exsolution origin.

Biotite and hornblende comprise an average of 6.3% and 3.1% of the rock, respectively. Alteration of biotite to chlorite is common. Sphene, zircon, apatite and magnetite are common accessories; sometimes these minerals occur as inclusions in biotite.

Foliated Biotite Granite

The general texture of the rock is hypidiomorphic granular. The rock sometimes exhibits porphyritic texture with phenocrysts of microcline set in the matrix of quartz, plagioclase, microcline and biotite. Plagioclase is the dominant mineral in the rock having mean modal abundance of 37%, quartz comprises 30.9% and K-feldspar 25.2% of the total rock.

Plagioclase in the rock ranges in composition from An_6 to An_{16}. Normal zoning is also observed in some of the plagioclase crystals,

the calcic core being intensely altered to sericite. K-feldspars are relatively less altered and are generally perthitic in nature. Several types of perthite have been reported to occur simultaneously in perthitic microcline (Smith, 1974).

Adamson (1942) and Smith (1974) observed that the perthites from plutonic rocks show a range of textures which appears to depend on the bulk chemistry and on the tectonic environment. Michot (1961) invented the term mesoperthite for a special type of microperthite whose lamellae are so intimately interrelated that neither phase appears to dominate. Anderson (1966) opined that the two components of mesoperthite tend to occur equally. Soldatos (1962) studied microcline perthite from Yxsjeveberg, Sweden and observed two generations of micro-albite, the coarser may be termed as film perthite and the finer one, string perthite. The various types of perthite occuring in the rock are shown in Figures 21 and 22. Sometimes veins of albite from plagioclase extend into K-feldspar suggesting its exsolution origin (Figure 23).

Myrmekitic intergrowth is also observed; it is characteristically restricted along the contact of K-feldspar and plagioclase. In a few cases, quartz occurs as elongated band in K-feldspar. Most of the myrmekites have a covex margin towards K-feldspar. The vermicules of quartz are uniformly distributed and typically thicker at the boundary of plagioclase and become vanishingly thinner towards the K-feldspar boundary (Figure 24). Qurtz also occurs as irregular droplets in K-feldspar. The quartz

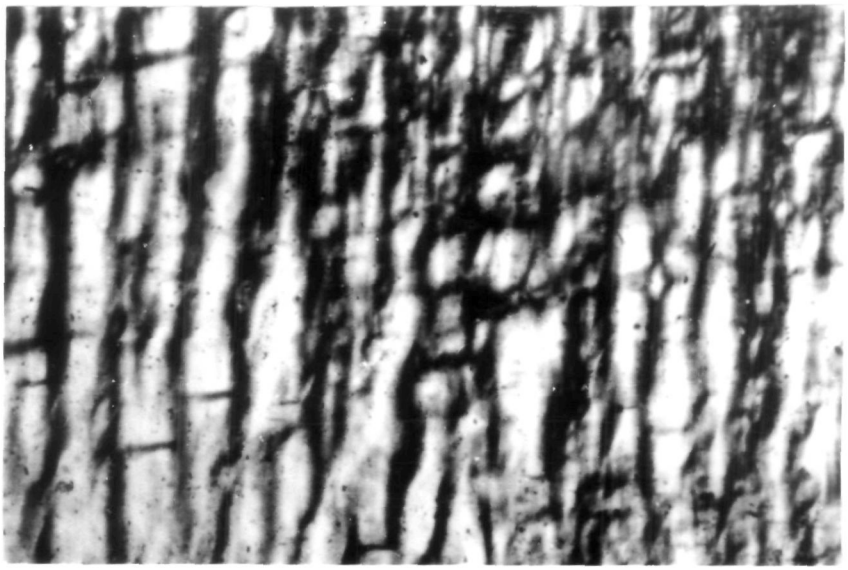

Figure 21. Mesoperthite with intimately interrelated lamellae. Crossed polars.

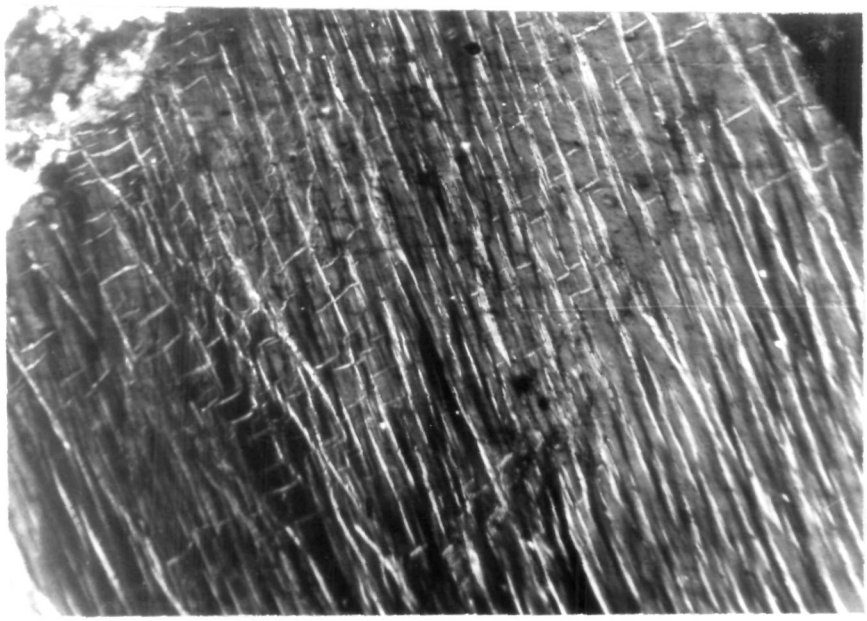

Figure 22. Two generations of micro-albite, the coarser one, film perthite and the finer one, string perthite. Crossed polars.

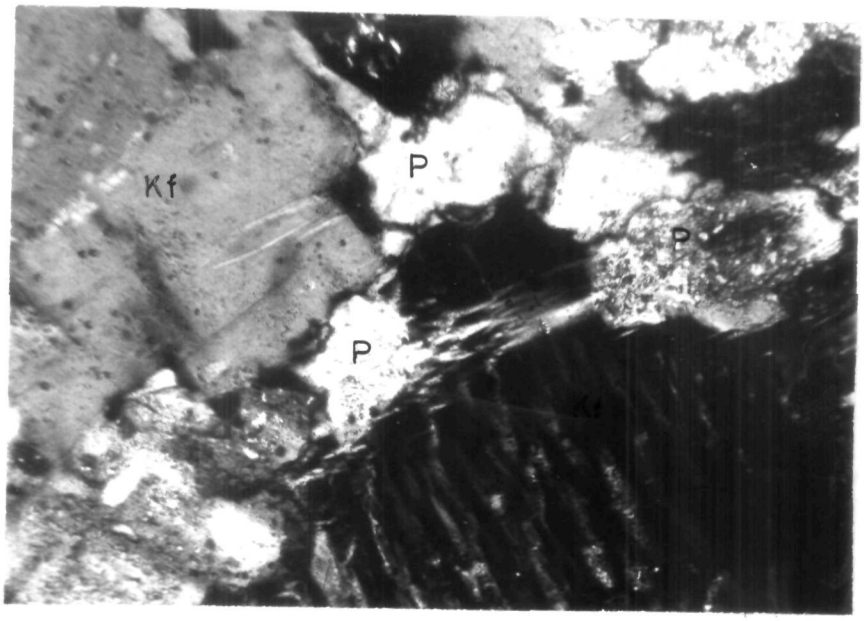

Figure 23. Veins of albite from plagioclase extend into K-feldspar (Kf). Crossed polars.

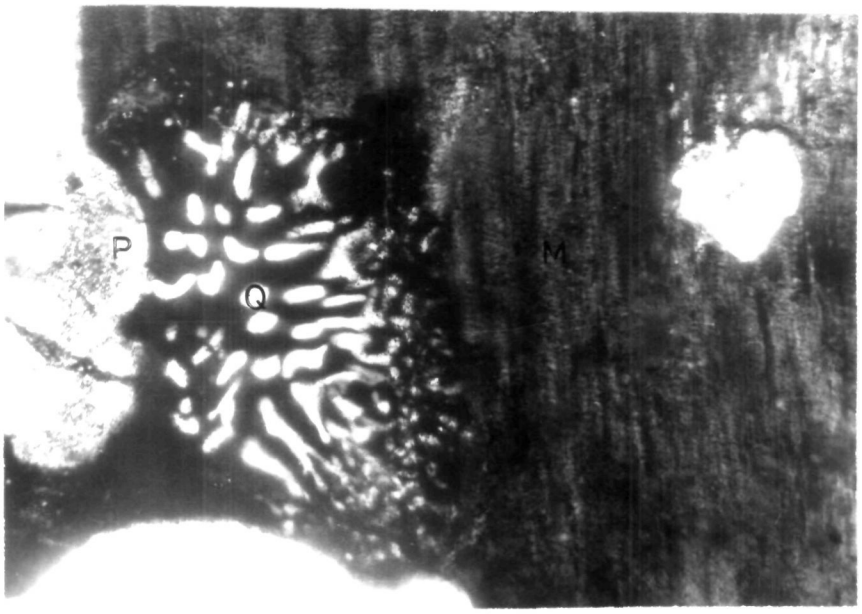

Figure 24. Myrmekite intergrowth with vermicules of quartz uniformly distributed in plagioclase. Crossed polars.

rods were concluded to be younger than the enclosing plagioclase and older than the K-feldspar (Sarma and Raja, 1958, 1959). Myrmekite occuring at the boundary of K-feldspar in contact with plagioclase is concluded to have formed as a result of corrosion (Drescher-Kaden, 1948). He also opined that the myrmekite may signify a metasomatic origin. Graphic intergrowth of quartz and microcline is also observed in a few samples (Figure 25).

Biotite is the most dominant accessory mineral and constitute 4.3% of the rock by volume; some crystals of biotite are partially altered to chlorite. At places, biotite encloses apatite and zircon grains which may indicate the growth of biotite crystals within a melt (Noyes et al, 1983). Grains of zircon have well developed crystal faces and are zoned (Figure 26). Zoning of zircon indicates the evolution of magma by fractional crystallization process (Martin, 1987).

The deformation of the rock is manifested by the strained quartz grains and fracturing of plagioclase twin lamellae.

Porphyritic Biotite Granite

The granite is very coarse grained with a porphyritic texture, the large phenocrysts of microcline are set in the groundmass composed of small grains of feldspar, quartz and biotite.

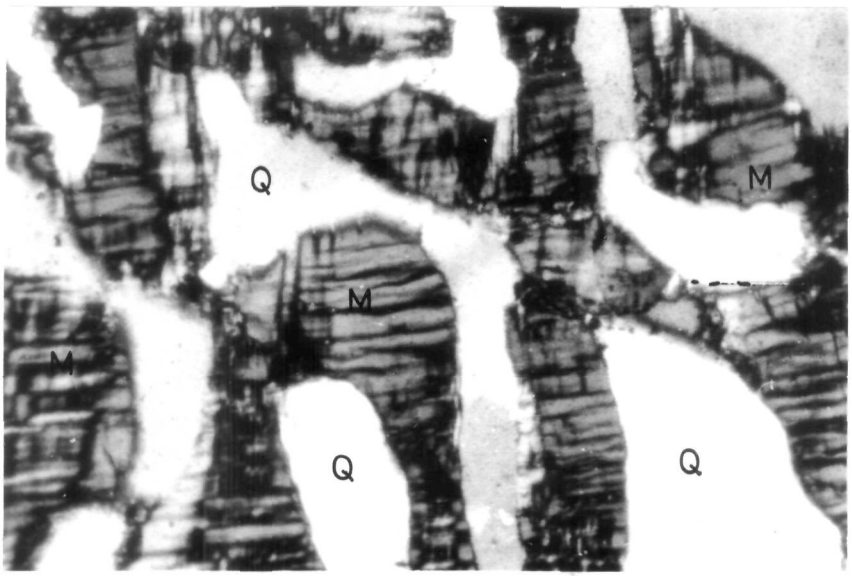

Figure 25. Graphic intergrowth of quartz (Q) and microcline (M). Crossed polars.

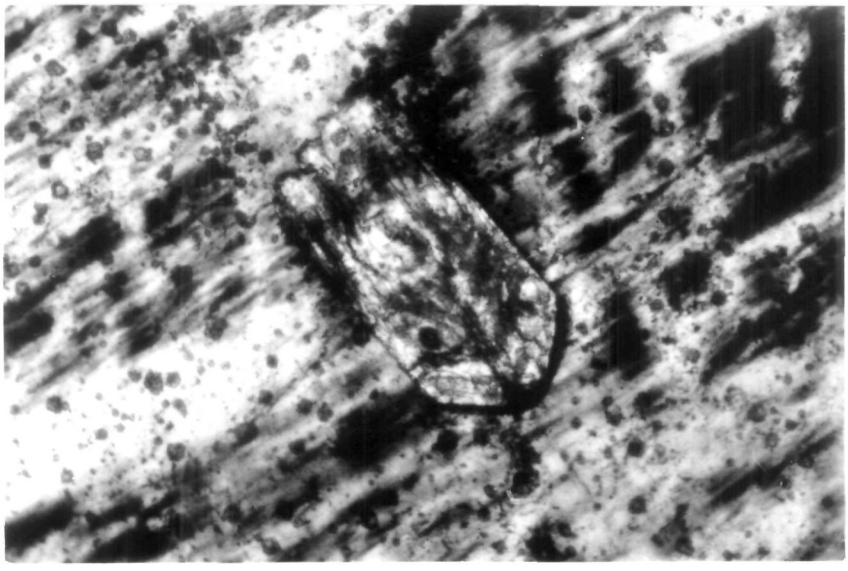

Figure 26. Zoned euhedral zircon. Crossed polars.

K-feldspar is the dominant mineral constituting about 39.4% of the rock by volume. Quartz has a mean modal abundance of 32.7%, whereas plagioclase, occuring as subordinate to both the K-feldspar and quartz, forms an average of 24.7% of the rock. Quartz grains are generally subhedral with embayed outline. Post-crystallization deformation of the rock is indicated by the bending of the biotite crystals (Figure 27).

Plagioclase ranges in composition from An_6 to A_{11}. Normal zoning in plagioclase is common, the altered calcic core is mantled by clear albite rim. Abundance of carlsbad twinning in plagioclases suggests a mgmatic origin of the granite. Vermicular intergrowth of quartz in plagioclase is rare.

Microcline occurs both as large phenocrysts and as small grains in the groundmass; this may be attributed to the polybaric crystallization of the granitic magma. Large crystals of microcline are generally perthitic which is considered to be of replacement origin. Veins and stringers of albite extend from plagioclase into microcline (Figure 28). It is inferred that the perthite forming solutions have infiltrated the K-feldspar along the interleptonic spaces provided by cracks and cleavages.

Biotite, generally green in colour, constitutes about 2.7% of the rock by volume. The accessory minerals include apatite, sphene, epidote and zircon.

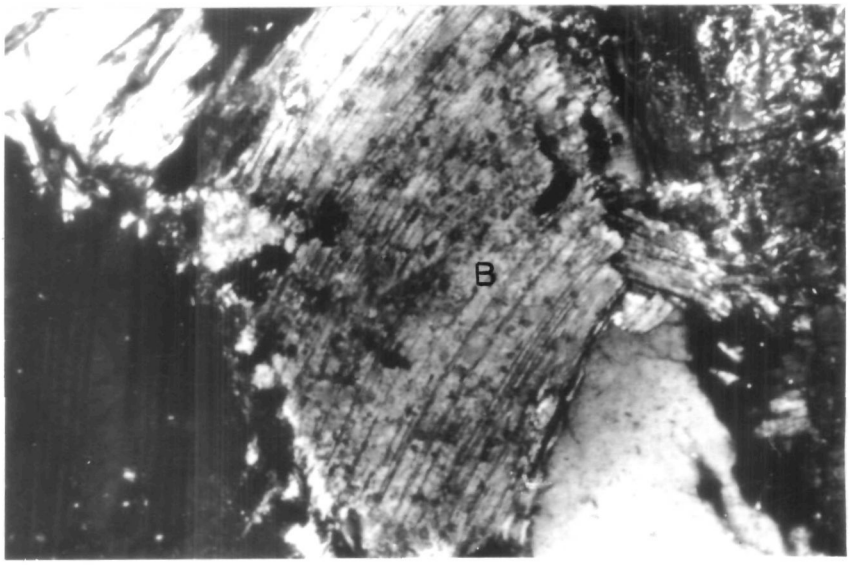

Figure 27. Post-crystallization deformation of the rock manifested by the bending of biotite (B) crystals. Crossed polars.

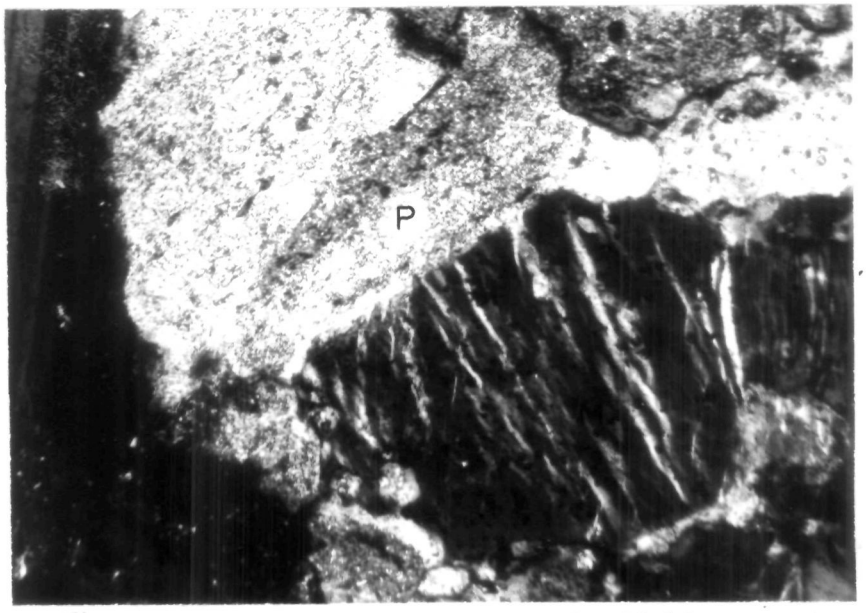

Figure 28. Veins and stringers of albite extend from plagioclase (P) into microcline (M). Crossed polars.

Coarse Grained Leucogranite

It is a medium to coarse grained massive rock composed mainly of potash feldspar and quartz which constitute an average of 37.2% and 36.1% of the rock by volume, respectively. Majority of the microcline grains are perthitic in nature. The perthites are of variable type and are inferred to have formed by replacement as well as exsolution processes. Myrmekitic intergrowth, generally restricted at the microcline-plagioclase contact (Figure 29), suggests an exsolution origin of the myrmekite (Hubbard, 1966, 1967). Quartz also occurs as inclusion in plagioclase and microcline.

Plagioclase is subordinate to both K-feldspar and quartz and constitutes an average of 23.1% of the rock; the grains are generally weathered to sericite. Plagioclase composition ranges from An_8 to An_{14}. Inclusion of plagioclase crystals within K-feldspar suggest earlier crystallization of plagioclase. Normal zoning and Carlsbad twinning in plagioclases suggest a magmatic origin of the granite.

Biotite is the major ferromagnesian mineral, it constitutes about 1.9% of the rock. Hornblende, in contrast to older types, is conspicuously absent. Zircon crystals are generally euhedral in shape. The presence of zoned crystals of zircon (Figure 30) suggests evolution of magma through fractional crystallization process (Martin, 1987). Sphene, epidote and apatites are common accessories.

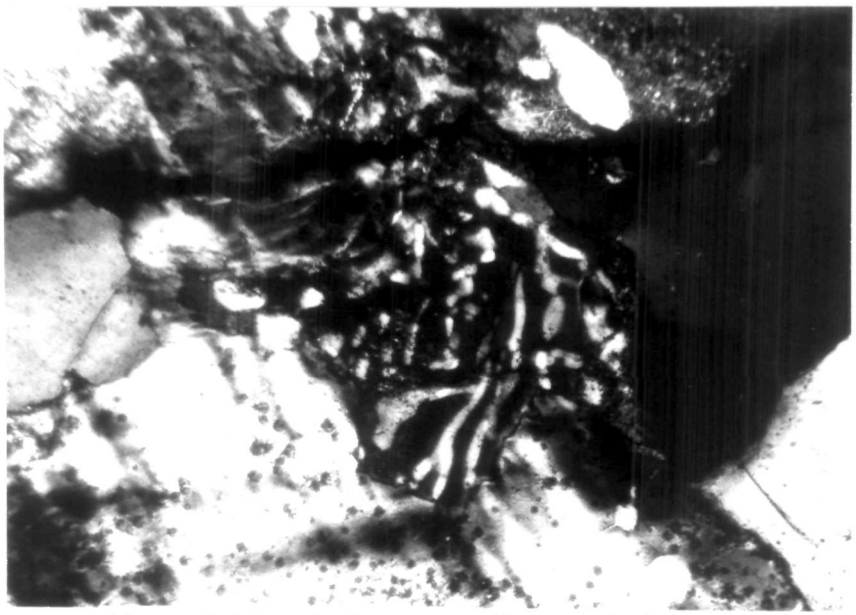

Figure 29. Myrmekite intergrowth restricted at the microcline-plagioclase contact. Crossed polars.

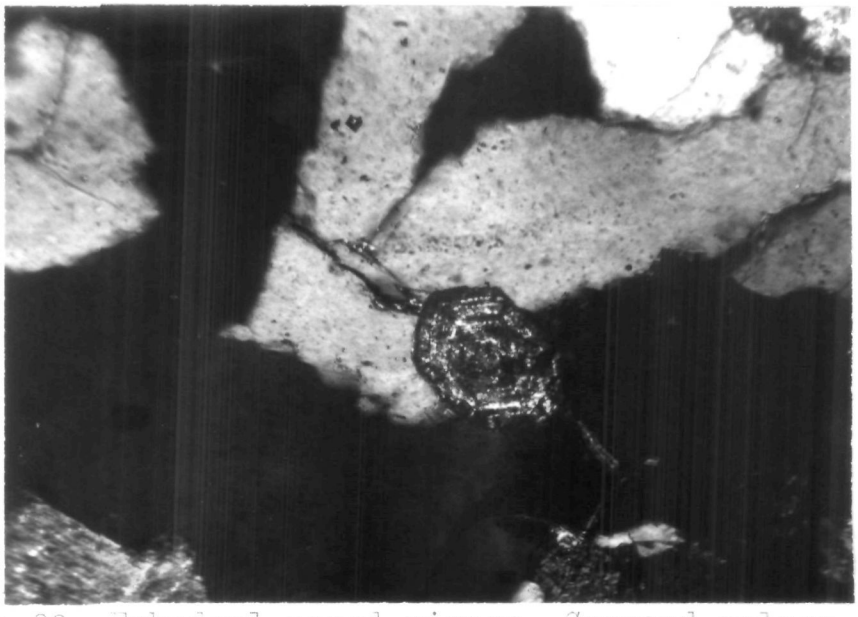

Figure 30. Euhedral zoned zircon. Crossed polars.

Fine Grained Leucogranite

The fine grained leucogranite is the youngest granite in the area; it is observed to have intruded into all the older types of granite. The rock is massive having hypidiomorphic granular texture and shows similarity with foliated biotite granite. However, it is finer grained and has lower content of ferromagnesian minerals.

The granite is composed mainly of quartz and microcline which constitutes an average of 37.6% and 34.5% of the rock by volume, respectively. Plagioclase is subordinate in amount to both quartz and potash feldspar. Microcline is generally perthitic with veins of albites distributed uniformly throughout the grain. The textures of perthites suggest its origin by exsolution as well as replacement processes.

Plagioclase ranges in composition from An_7 to An_{16}, some plagioclase crystals show normal zoning having a relatively more altered calcic core (Figure 31). Myrmekitic intergrowth is common; in some cases quartz blebs are observed to extend from plagioclase across the contact into microcline (Figure 32). Stress may have been responsible for promoting exsolution and migration of exsolved quartz to grain boundaries. Smith (1974) opined that the stress accompanying rock deformation provide channels for migration of solutions, partly by generating regions of usually high and unusually low pressure which favour appropriate material.

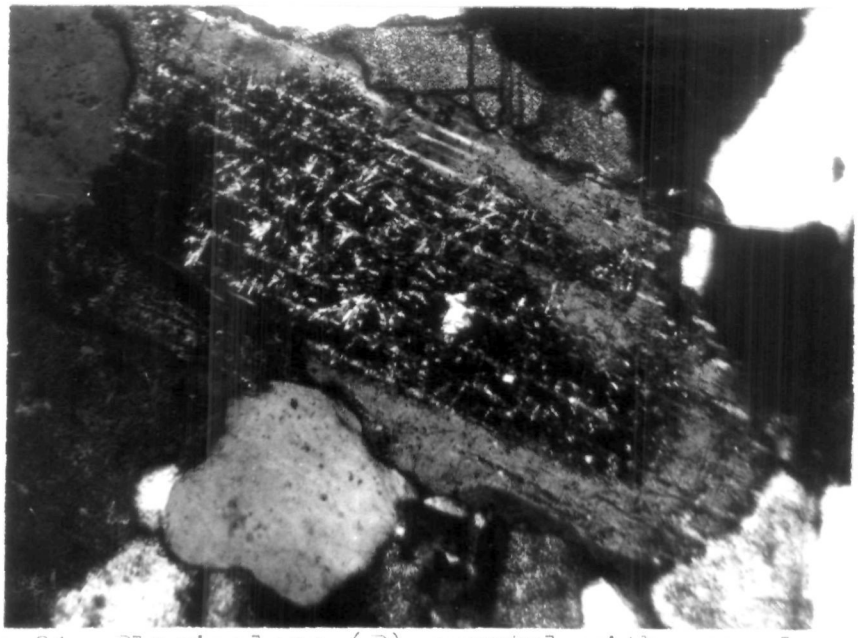

Figure 31. Plagioclase (P) crystal with normal zoning. Crossed polars.

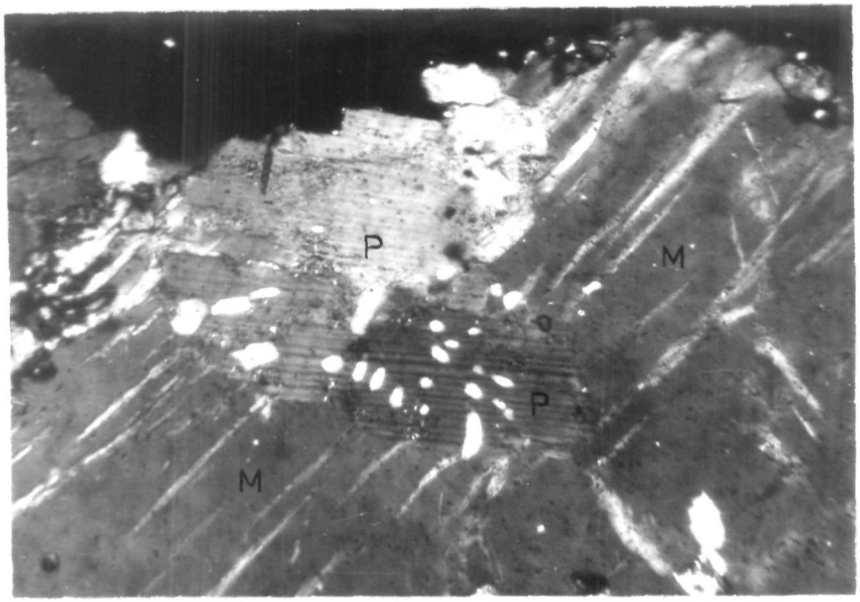

Figure 32. Myrmekite intergrowth with bleb of quartz extending from plagioclase (P) across the contact into microcline (M). Crossed polars.

Biotite is the only major ferromagnesian constituent of the rock, the average modal value being 2.2%. Similar to coarse grained leucogranite, hornblende is significantly not found in the rock. Sphene, zircon, and apatite are very rare, whereas the opaques are commonly distributed throughout the rock. Garnet and muscovite is observed only in one sample. The granite shows little effect of deformation.

An-Content of Plagioclase

The plagioclase composition is a very significant indicator of the physico-chemical condition of rock formation. Barth (1969) suggested that plagioclase of low pressure-temperature formation is nearly pure albite but plagioclase of higher pressure-temperature varies in the composition. Kuno (1956) opined that at high temperature albite is always contaminated with appreciable amount of anorthite in solid solution.

The composition of plagioclase in 50 samples, 10 of each of the five types of granite, was determined by the Rittman method (Emmons, 1943). The result is presented in Table 5.

Table 5 : Plagioclase composition in the five types of granite.

Rock Type	An-content
Hornblende granite	An_9 - An_{18}
Foliated biotite granite	An_6 - An_{16}
Porphyritic biotite granite	An_6 - An_{11}
Coarse grained leucogranite	An_8 - An_{14}
Fine grained leucogranite	An_7 - An_{16}

It is evident from Table 5 that there is not much difference in the An-content of plagioclases among the five types of granite; the plagioclase is generally sodic in composition. Hornblende granite, however, has slightly more calcic plagioclases than the other types.

Plagioclase Twinning

The nature and type of twinning in plagioclase provides important clues about the origin of the rock; the nature of plagioclase twinning in igneous rocks differs from the twinning in metamorphic plagioclases (Gorai, 1951; Vance, 1961; Tobi, 1962; Seifert, 1964).

Gorai (1951) observed a characteristic difference in the type of plagioclase twin in magmatic and metamorphic rocks. He classified the plagioclase twinning into two types, A-type and C-type. A-type twinning is found both in igneous and metamorphic rocks; it includes lamellar albite, acline and pericline twins, alone or in combination. Secondary glide twins formed due to deformation by external forces after the growth of the crystal are also grouped in A-type twins. The C-type twins include Carlsbad, albite-Carlsbad and penetration twins which are developed in the crystal during growth and is restricted in the magmatic rocks. Abundance of C-type Carlsbad twinning in plagioclases in all the five types of Bundelkhand granite may indicate their magmatic origin. A similar conclusion was also drawn by Alam (1979).

Zoning in Plagioclase

The plagioclase crystals in all the five types of Bundelkhand granite are zoned; the calcic core being intensely altered to sericite. The presence of zoning in the plagioclase grains may suggest a magmatic origin of the granites. Normal zoning in plagioclases (sodic shells around calcic cores) indicates a magmatic origin. In a magmatic system as crystallization proceeds, a series of compositional changes is induced by regularly decreasing temperature. At the initial high temperature, calcic plagioclase is in equilibrium with

the chemical environment. With decreasing temperature, successively more sodic rims are developed, the result being a zoned plagioclase with a calcic core surrounded by a series of shells of increasing sodium content towards the circumference (Barth, 1962; Smith, 1974).

CHAPTER IV

GEOCHEMISTRY

Trace elements provide useful tool for modelling or tracing igneous fractionation processes (Gast, 1968; Haskin et al, 1970; Zielinski and Frey, 1970; Hubbard et al, 1971; Weill et al, 1974). Tausan (1965) opined that a number of important problems in petrogenesis may be solved by using data on the nature of the distribution of the trace elements in igneous rocks. The data can be utilized in determining age sequence of individual intrusive phases. Valsov (1966) observed that rocks are more clearly distinguished with the help of trace elements than with common rock forming minerals.

The trace elements, present in the magma in small quantity, rarely form their own mineral. These elements substitute for different cations and are widely distributed in the structures of common minerals of rock. Mason and Moore (1985) suggested that the fate of an element during magmatic crystallization is linked with its concentration in the magma and the nature of the structural lattices that may form. The silicon and aluminium content of the magma and temperature are the factors controlling the sequence of crystal lattices which act as a sorting mechanism for the cations.

In a mineral, each major element is present in a definite proportion and in a particular ratio with the other constituent elements with which they bear close relationship in terms of ionic radii, electronegativity, and ionization potential under a particular set of physical conditions. Varying content of certain trace elements in a mineral is related to the course of crystallization and changes in the physical conditions.

Tauson (1968) observed that the processes of crystallo-differentiation in abyssal batholiths lead to a higher concentration of some elements and a sharp decrease in others. The acid differentiates intensively accumulate elements crystallochemically associated with potassium (Rb, Cs, Tl etc) or those which build up stable compounds with volatile (Li, Ba, U etc) but are depleted in the content of elements crystallo-chemically related to magnesium and iron (Zn, Cu, Ni, Co etc). The geochemical history of the rare elements in magmatic processes and specially their distribution in rocks depends mainly on the ratio of their atoms which are in a state of crystallochemical dispersion to those which remain in solution. This ratio will change with composition, size and depth of intrusion.

Geochemical analyses of 54 samples of granites were carried out to determine the nature of the granites, their composition and genesis. Major and trace elements were analysed by the modified

rapid analysis method of Shapiro and Brannock (1962); the U.S.G.S. Standards, G_2, GSP_1, and AGV_1 were used as internal standards.

One gm. of sample was digested in hydrofluoric acid and then it was transferred to 100 ml volumetric flask to prepare the solution B which was used to determine the concentration of major elements, Na_2O, K_2O, CaO, MgO, total Iron, and MnO on Double Beam Atomic Absorption Spectrophotometer. The trace elements, Rb, Ba, Sr, Cu, Co, Ni, Cr, Zn, Pb and Li were determined on Atomic Absorption Spectrophotometer directly from the solution B. Concentrations of V, Y, Nb were determined on ICP and Zr, Ga, U and Th were analysed by XRF. P_2O_5 and TiO_2 were determined by Spectrophotometer using colour ions of respective elements and measuring the absorbance on selected wavelengths.

Solution A was used to determine the concentration of SiO_2 and Al_2O_3 in the rock; it was prepared by fusion of 0.1 gm of rock powder with NaOH pellets in nickel crucible. The solution was mixed with 1:1 HCl and then transferred to one litre volumetric flask. The concentration of SiO_2 and Al_2O_3 was determined by spectrophotometer using colour ions of respective elements and measuring the absorbance on selected wavelength, 640 mu for SiO_2 and 475 mu for Al_2O_3. The concentrations of major elements as oxides and trace element in the different types of Bundelkhand granite are presented in Table 6. Complete analytical data is given in Appendix A.

Table 6 : Mean Chemical Composition of Major and Trace Elements and Their Ratios in the Five Types of Bundelkhand Granite.

Major Elements (Oxide Wt. %)	Hornblende Granite (8 samples)	Foliated Biotite Granite (14 samples)	Porphyritic Biotite Granite (8 samples)	Coarse Grained Leucogranite (13 samples)	Fine Grained Leucogranite (10 samples)
SiO_2	65.54	69.79	70.91	72.64	74.03
TiO_2	0.57	0.34	0.39	0.28	0.16
Al_2O_3	15.86	14.59	14.96	15.17	15.13
Fe_2O_3*	4.47	2.15	2.37	1.50	1.02
MnO	0.068	0.054	0.047	0.029	0.025
MgO	1.38	0.91	0.66	0.45	0.57
CaO	3.07	1.94	1.48	0.98	0.85
Na_2O	3.72	3.81	3.32	3.31	3.36
K_2O	4.34	4.41	5.55	5.78	5.78
P_2O_5	0.23	0.14	0.16	0.09	0.06
Total	99.25	98.13	99.85	100.23	100.99
Trace Elements (ppm)					
Ba	899	465	219	334	136
Rb	201	325	318	451	489
Sr	293	190	142	94	67
Cr	54	43	36	28	45
Ni	36	30	24	22	30
Cu	13	9	10	9	8
Zn	74	60	66	56	45
Co	20	22	22	25	30
Pb	15	21	22	38	28
Li	35	39	45	29	28
V**	57	48	38	25	14
Nb**	21	21	27	24	27
Y**	24	34	41	35	46
Zr**	182	224	276	223	142
Ga**	12	16	14	15	14
U**	4	14	14	18	26
Th**	12	44	49	68	62
$Al_2O_3/CaO+Na_2O+K_2O$	1.42	1.49	1.46	1.50	1.52
K_2O/Na_2O	1.17	1.27	1.66	1.76	1.69
K/Rb	181	124	117	110	105
K/Ba	41	106	246	147	544
Rb/Sr	0.725	1.88	2.84	5.29	8.25
U/Th	0.36	0.31	0.29	0.27	0.44
Ni/Co	1.63	1.48	1.17	1.01	1.07
Zr/Y	10.15	6.10	6.92	5.49	3.06
Ti/Zr	18.8	10.91	8.78	7.54	5.99
Ti/Nb	175.75	120.98	100.41	73.35	34.81

* Fe_2O_3 was determined as total iron.

** Number of samples vary from 1 to 6.

The behaviour of Si, Al, Na, Ca, K, Fe, and Mg are very helpful to determine the history of magma evolution and the process of differentiation. The concentrations of major elements in all the five types of Bundelkhand granite are plotted on Harker's (1909) diagram to decipher the process of formation of magma, whether by partial melting or differentiation. All the plots (Figure 33) exhibit a linear correlation with respect to age. It is evident from the figure that the abundance of Al_2O_3 and Na_2O in all the five types of granite have very little variation, the trend, however, shows a poor negative correlation. The plots of K_2O is somewhat scattered. However, a progressive enrichment of K_2O in younger varieties of granite can be observed. The trend of CaO, MgO, Fe_2O_3 TiO_2, MnO and P_2O_5 shows a strong negative linear correlation with respect to age, from older to younger granites.

The trend of major element obtained on Harker's diagram appears to be consistent with the process of differentiation in the evolution of magma.

The trace elements are partitioned more strongly than major elements into either the crystalline or liquid phase making them more sensitive indicator of both degree and mechanism of differentiation (Drake & Weill, 1975). Probably the most important advantage in the study of trace element over the major elements is that the trace elements are diluted in the solid or liquid solutions in which they are dissolved and their thermodynamic activity

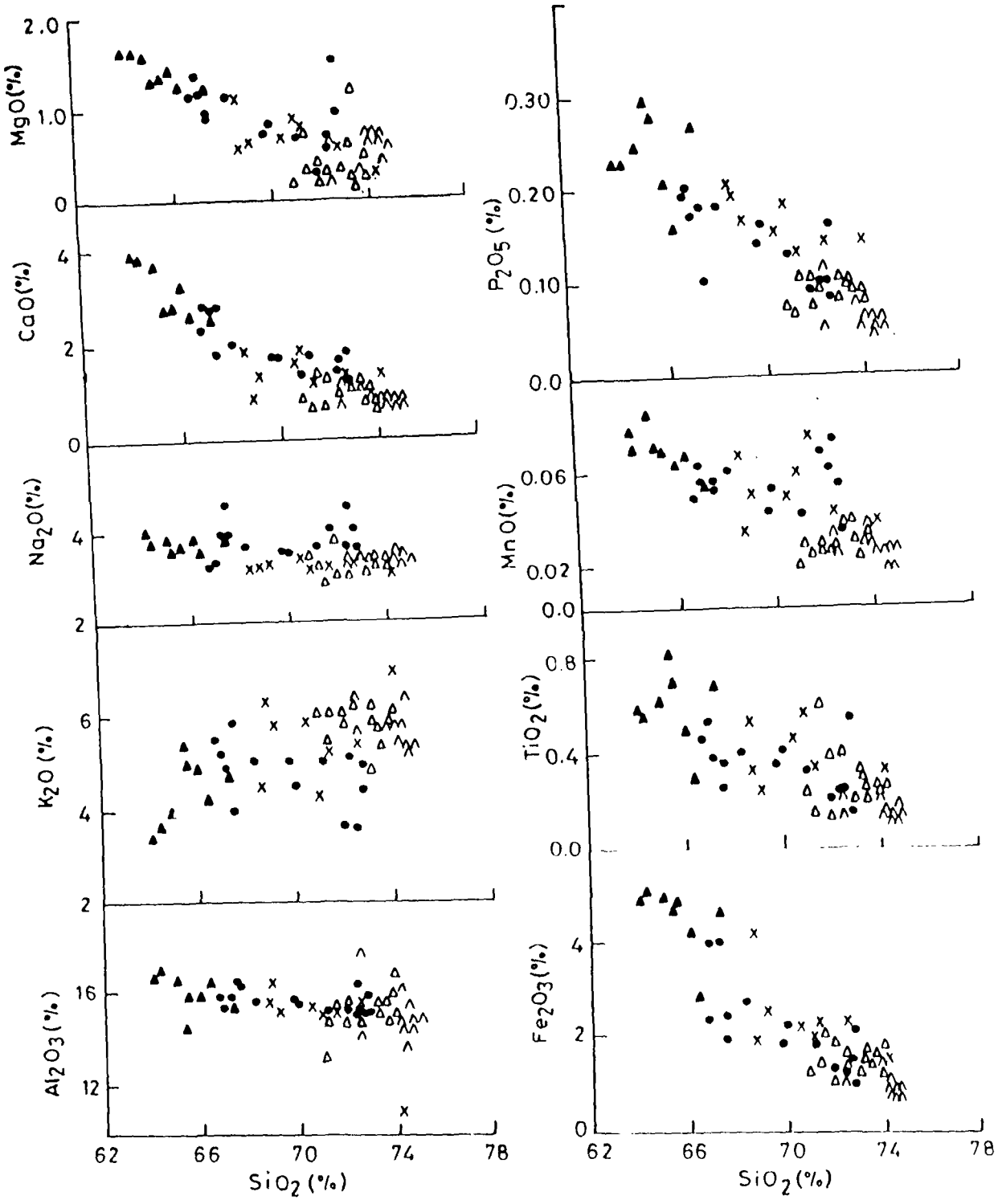

Figure 33. Harker's variation diagrams of major elements in granitic rocks of Bundelkhand massif.

is directly proportional to its mole fraction; this simplifies the thermodynamic analysis of interphase partitioning.

Trace elements, particularly the immobile elements, are relatively more resistant to post-crystallization secondary processes. The ratio of trace elements with corresponding major elments with which they bear close relationship, such as K/Rb, Ba/Rb, Rb/Sr, Ca/Sr etc. are widely utilised in the interpretation of sequence of differentiation of granitic rocks and their relative ages (Taylor and Heier 1960; Zlobin and Lebedev, 1960).

Rb is considered to be a good indicator of differentiation because it does not form its own minerals but replaces K in the K-bearing minerals (Stavrov, 1971; Zlobin and Lebedev, 1960; Valsov, 1966). Due to its lower ionization potential and electronegativity, Rb is more mobile and is one of the most chemically active element. Its ionic radius and other crystallochemical properties exhibit close relationship with K(Valsov, 1966).

The progressive enrichment of Rb in residual magmas can lead to concentration of 500 ppm or more, and K/Rb ratio of less than 100 in late stages of granites and rhyolites (Taylor et al, 1956). The crustal abundance of Rb is 90 ppm, the average K/Rb ratio is 230. The common anomaly, low K/Rb ratio indicating Rb enrichment is found specially in pegmatites (Heier and Taylor, 1959; Taylor

and Heier 1958, 1960) and some later stage granites (Taylor et al, 1956). Taylor (1965) suggested that an increase in rubidium relative to potassium in a sequence of granites intrusions can be interpreted as indicating the order of intrusion.

Butler et al. (1962) have discriminated the granites of Northern Nigeria having closely similar mineralogy and major element contents into sequence of intrusion on the basis of K/Rb ratios. They conclude that as granite approach the ternary minimum in the system SiO_2 - $NaAlSiO_4$ - $KAlSiO_4$, the major element composition will tend towards uniformity and hence it is the trace elements that provide the evidence to separate the stages of differentiation. They have also suggested that other highly fractionated elements, such as, Cs, Th, Ba, or Sr should also prove valuable as differentiation indices. Erlank (1968) opined that the greatest potential use of the K/Rb ratio will probaby be for interpreting and comparing differentiation sequences. K/Rb ratio has also been used to understand petrogenesis and mode of evolution of granitic magma (Arth and Hanson, 1975; Whitney et al, 1976; Onion and Pankhurst, 1978; Imeokparia, 1984; Charoy, 1986; Santosh and Drury, 1988).

The K/Rb ratio in the Bundelkhand granites may be applied to discriminate the granites on the basis of the degree of differentiation. All the plots on the K vs Rb diagram (Figure 34) lie between K/Rb ratio of 200 and 75; the ratio progressively decreases in younger varieties because of the Rb enrichment in late

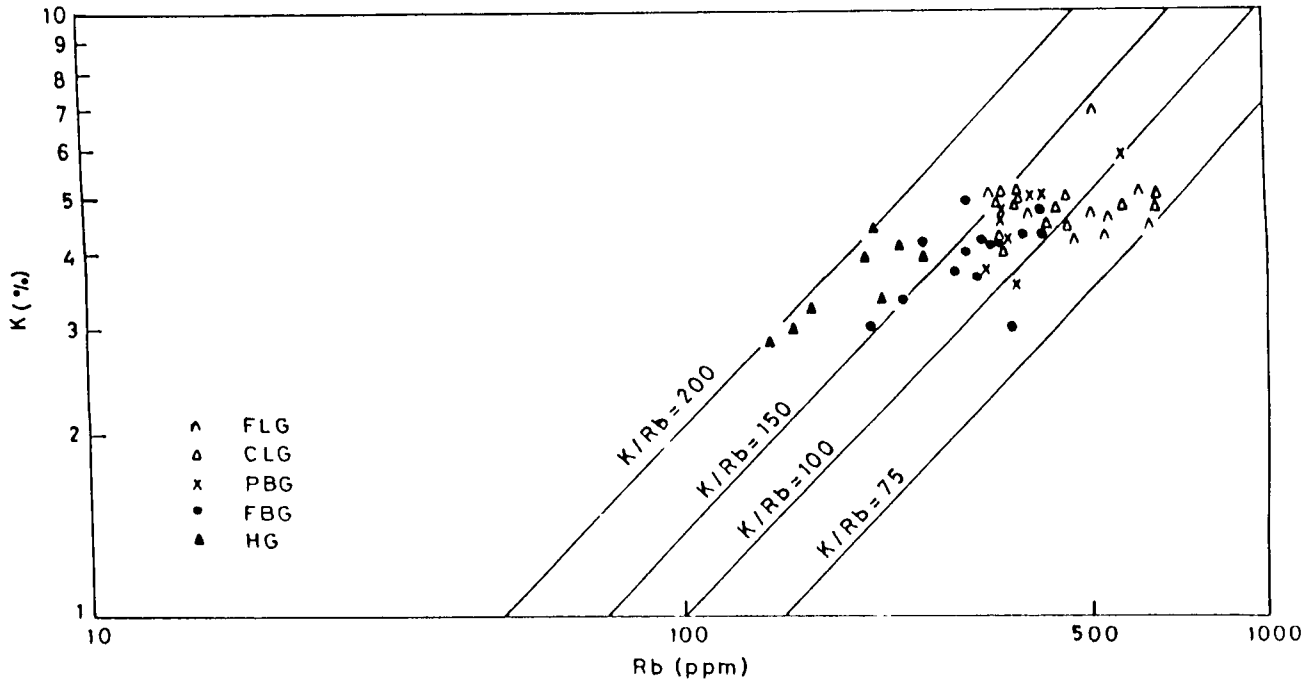

Figure 34. Plots of K vs Rb of Bundelkhand granites.

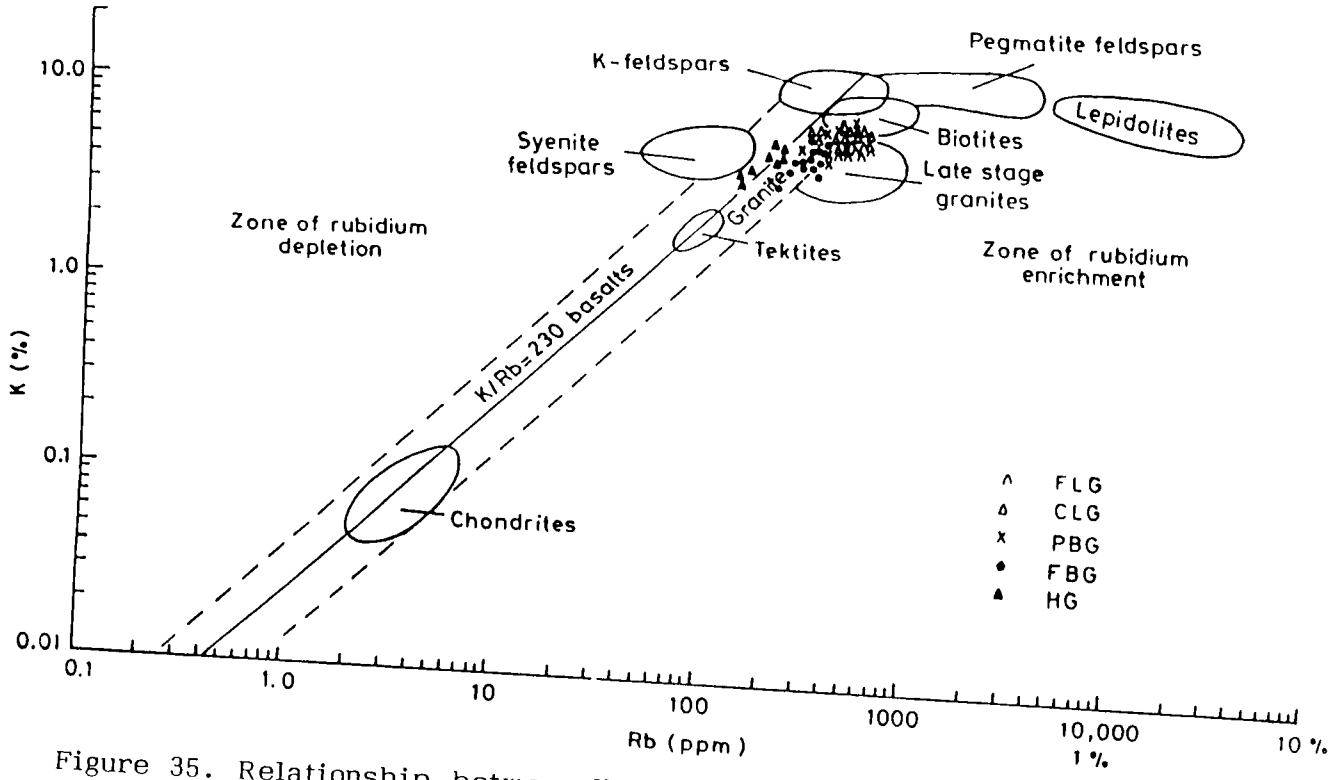

Figure 35. Relationship between K and Rb in Bundelkhand granites. (after Taylor, 1965).

stage of magma formation. The average K/Rb ratio of the different types of granite varies from 181 for the oldest to 105 for the youngest granite. The K vs Rb plots of the three older granites in Bundelkhand on Taylor's (1965) diagram lie in the granite field whereas plots of coarse grained leucogranite are more concentrated towards late stage granaite field, and those of the youngest granite lie within the late stage granite field (Figure 35).

The K/Rb ratio plotted against SiO_2 (Figure 36) shows a good negative linear correlation with respect to age of the granite, as determined by field observations. Taylor and Heier (1960) observed that Rb and Ba in K-bearing minerals provide a critical index of fractionation because Ba has a tendency to be captured in the earlier K-minerals, wheras Rb is enriched in the residual melts. Ba, Rb, and Sr are considered useful for modelling in granite system because they occur only in the major silicate minerals (McCarthy and Hasty, 1976). Hanson (1978) proposed a petrogenetic modelling of the granitic rocks by using mineral/melt distribution coefficient of Rb, Ba, Sr and REE and applied it to discriminate the mode of evolution of granitic magma, either by partial melting or differentiation.

The behaviour of Rb, Ba and Sr and their ratios have been used to interpret the process of evolution of the granitic rocks (Arth and Hanson, 1975; MacCarthy and Fripp, 1978; Onion and Pankhurst,

1978; Noyes et al, 1983; Tuach et al, 1986; Kleemann and Twist 1989; Eby and Kochhar, 1990).

Trace element concentrations and their ratios in different types of Bundelkhand granite were plotted on Harker's diagram (Figure 36,& 37). The figures show a good positive linear correlation with U, Th and Rb and strong negative linear variation with Sr, Ba and V. Among elemental ratios, Rb/Sr and K/Ba show a strong positive correlation, whereas negative linear correlation is observed for K/Rb and Ba/Rb. The trend is in accordance with the production of granite melt by the fractional crystallization of a common parental comagmatic source. Mittlefehldt and Miller (1983) observed a decreasing trend in Ba and Sr with increase in Rb content in the Sweetwater Wash pluton. They concluded that the trend is produced by fractional crystallization. Imeokaparia (1984), also suggested that the trend indicates the production of granitic liquid by fractional crystallization.

Sr and Ba show a positive correlation with CaO, whereas Rb has a negative relation (Figure 38); the plots follow the trend of fractionation. K/Rb vs Rb/Sr plots for Bundelkhand granite also follow the trend of fractional crystallization as indicated by the decrease in K/Rb ratio with concomitant increase in Rb/Sr ratio (Figure 39).

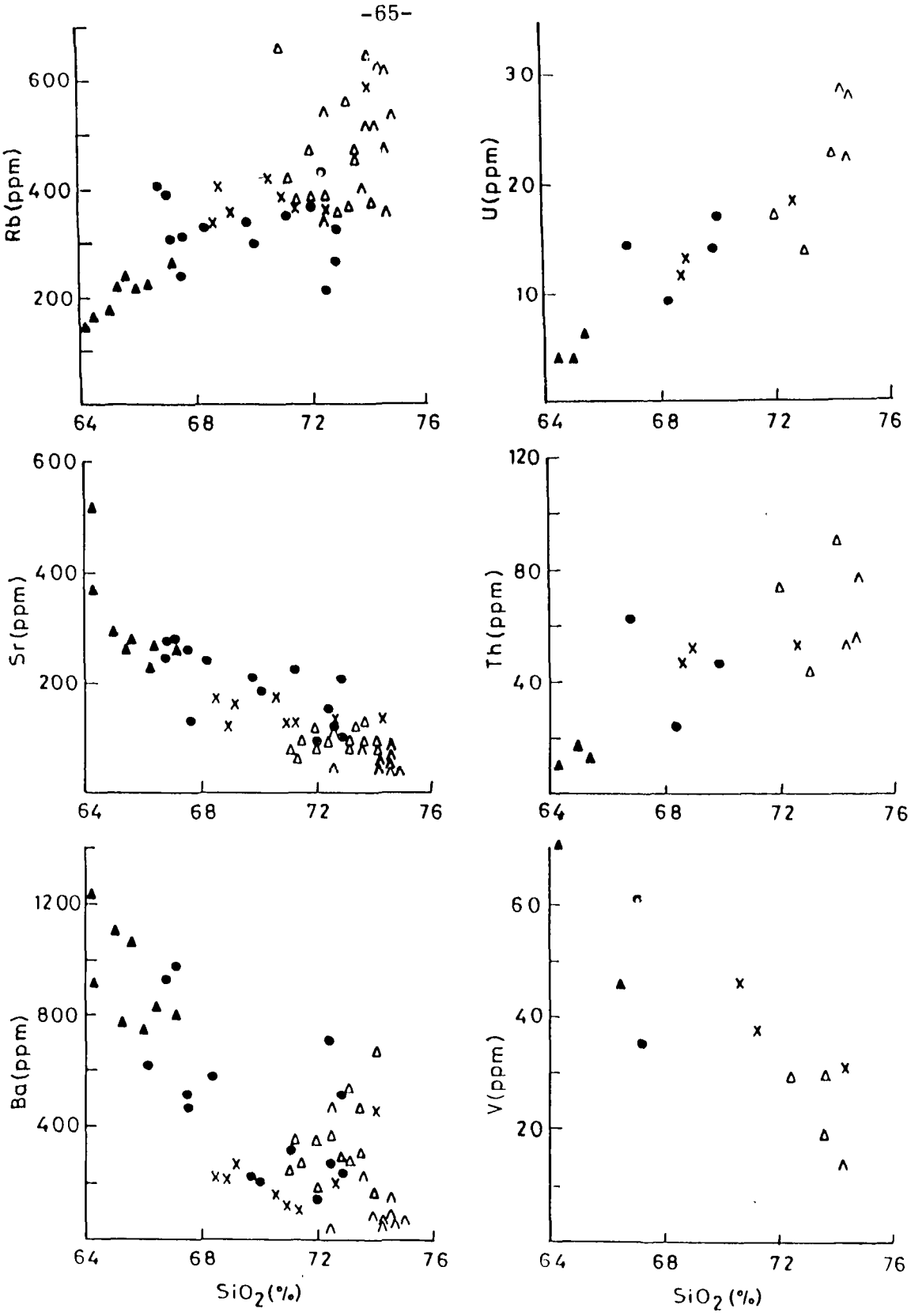

Figure 36. Harker's diagrams of trace elements in Bundelkhand granites. (symbols as in Figure 35).

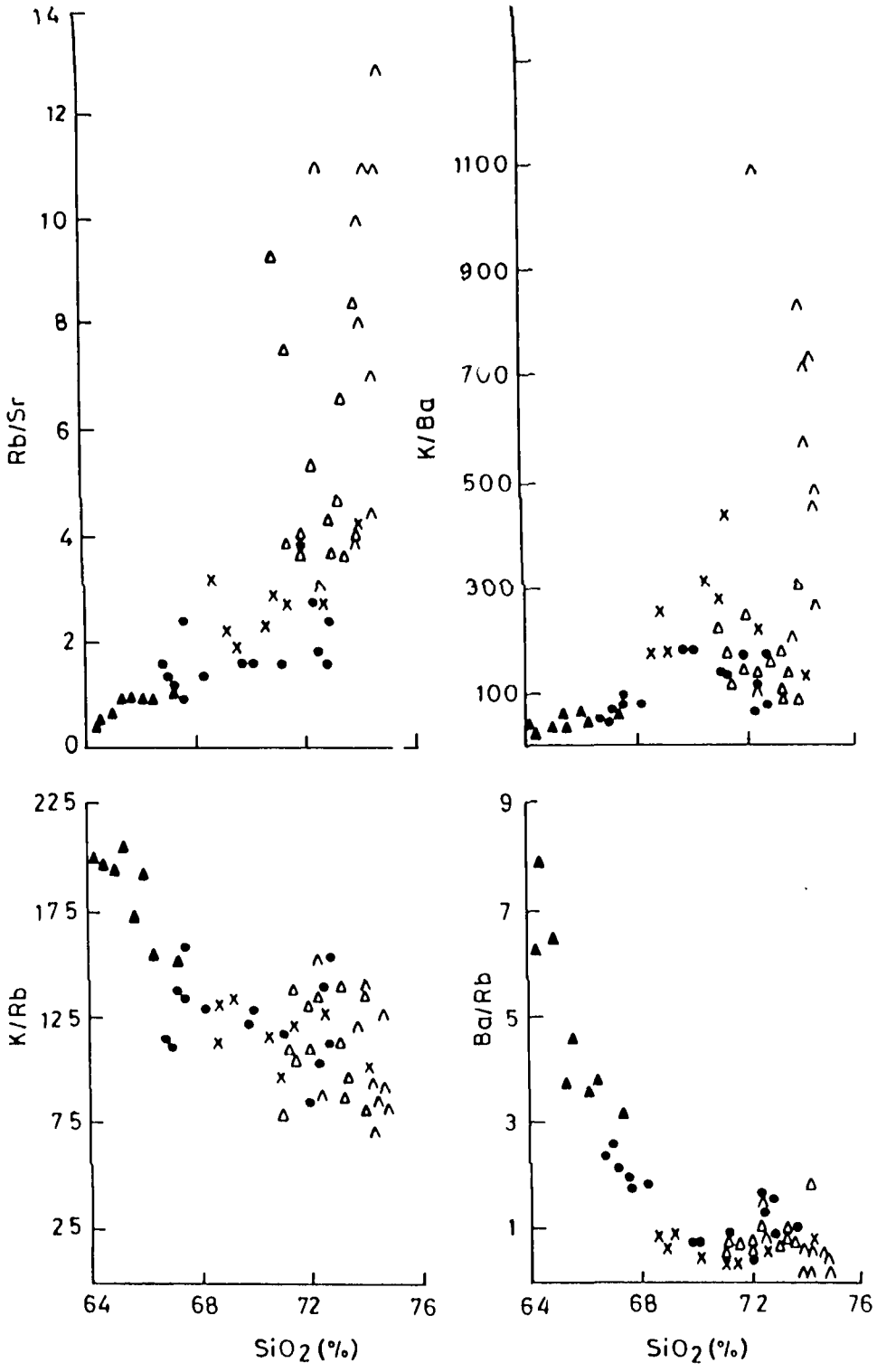

Figure 37. Variation diagrams of trace element ratios.

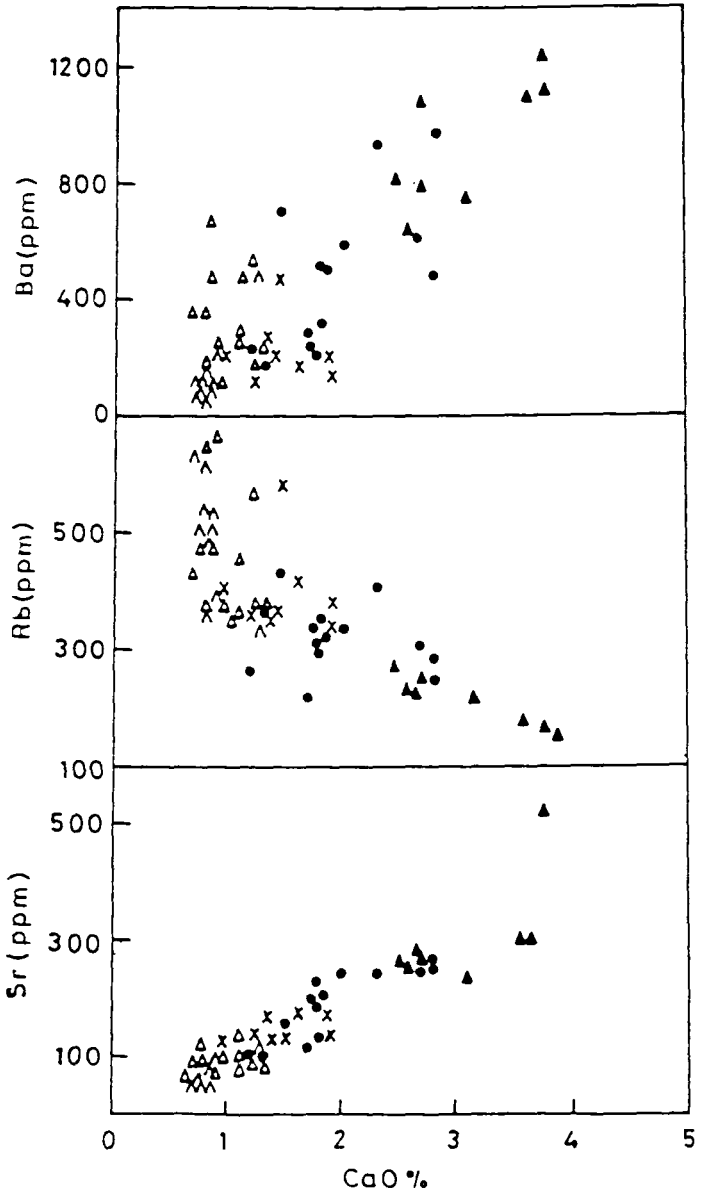

Figure 38. Plots of CaO vs Sr, Rb and Ba(symbols as in Figure 37).

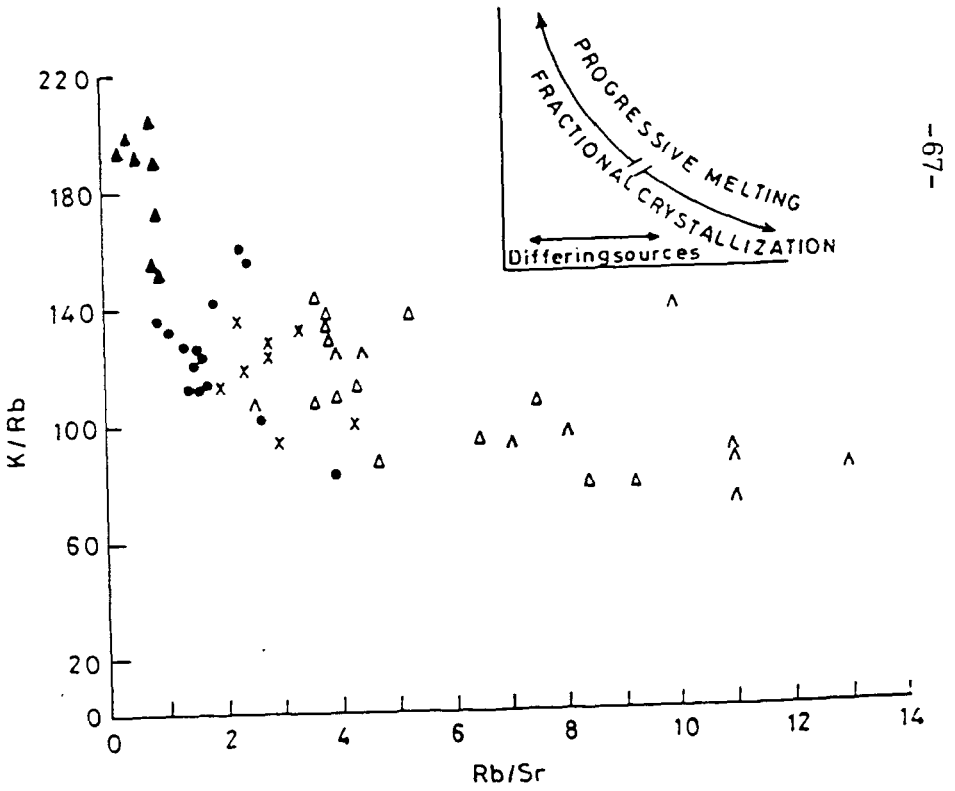

Figure 39. Plots of Rb/Sr vs K/Rb in Bundelkhand granites (sumbols as in Figure 37).

Rb vs Sr plots of Bundelkhand granites show a progressive increase in Rb/Sr ratio in the younger granites (Figure 40). The Rb/Sr ratio in the oldest type is less than 1, whereas the fine grained leucogranite has a ratio of more than 4. The plots of Ba vs Sr depict a falling Ba/Sr ratio with progressive fractionation from older to younger granites (Figure 41).

El-Bouseilly and El-Shokkary (1975) plotted the Rb, Ba, and Sr values (ppm values recalculated to 100%) on a ternary diagram to determine the differentiation trend of the granitic rocks. The ternary plots of Rb, Ba, and Sr for Bundelkhand granite (Figure 42) defines a continuous variation that extends from the Ba apex to the Rb apex. The plots of the hornblende granite lie within the anomalous granite field, whereas the plots of the younger granites follow the differentiation trend, progressively from older to younger in age.

It may be concluded that the distribution pattern of Ba, Sr, Rb and their relationship on variation diagrams in the Bundelkhand granite together with the trend of major and trace elements and their ratios on Harker's diagram follow a trend similar to that of granites formed by fractional crystallization.

The plots of Bundelkhand granites on K_2O vs Na_2O variation diagram (Figure 43) exhibit a progressive enrichment trend in K_2O concentration in the younger granites. The K_2O/Na_2O ratios in the two older granites are less than 1.5; their plots mainly lie in the

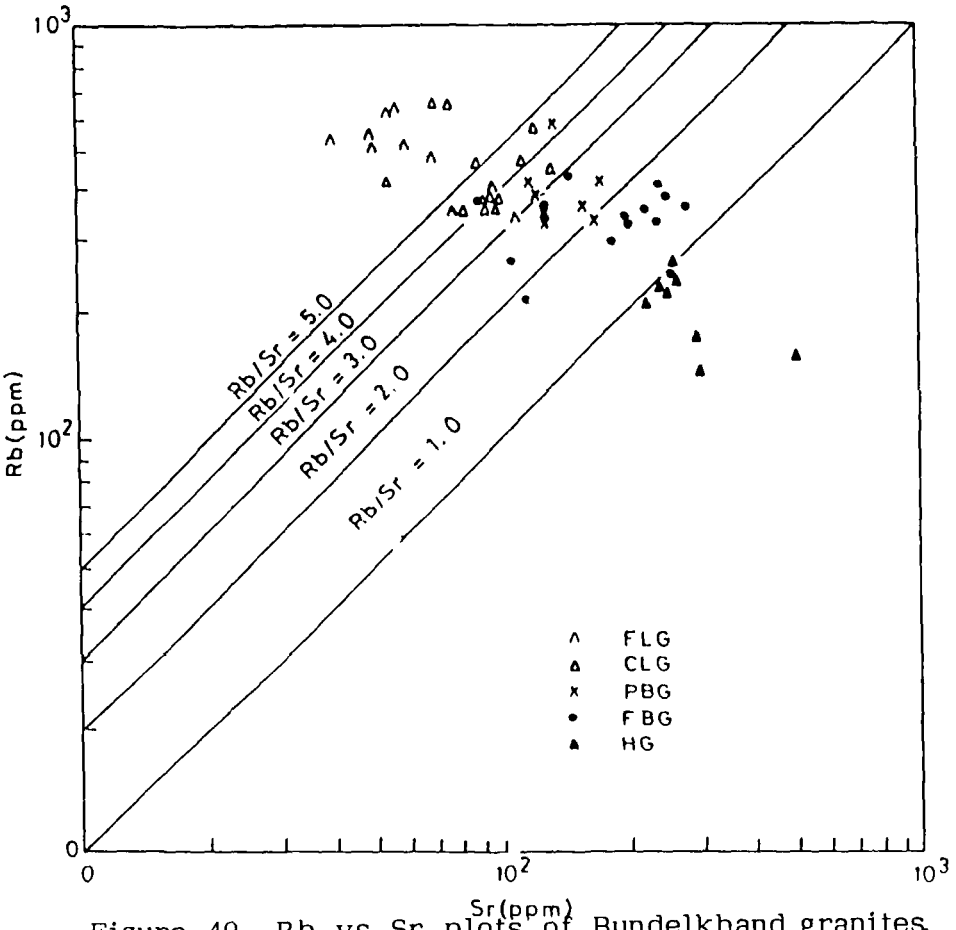

Figure 40. Rb vs Sr plots of Bundelkhand granites.

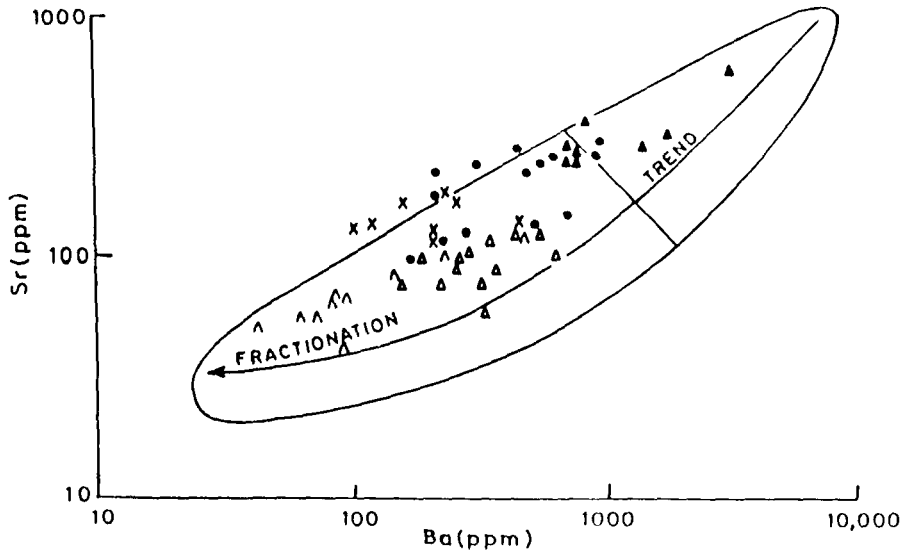

Figure 41. Plots of Bundelkhand granites on Ba vs Sr diagram (after Heier and Taylor, 1959), (symbols as in Figure 40).

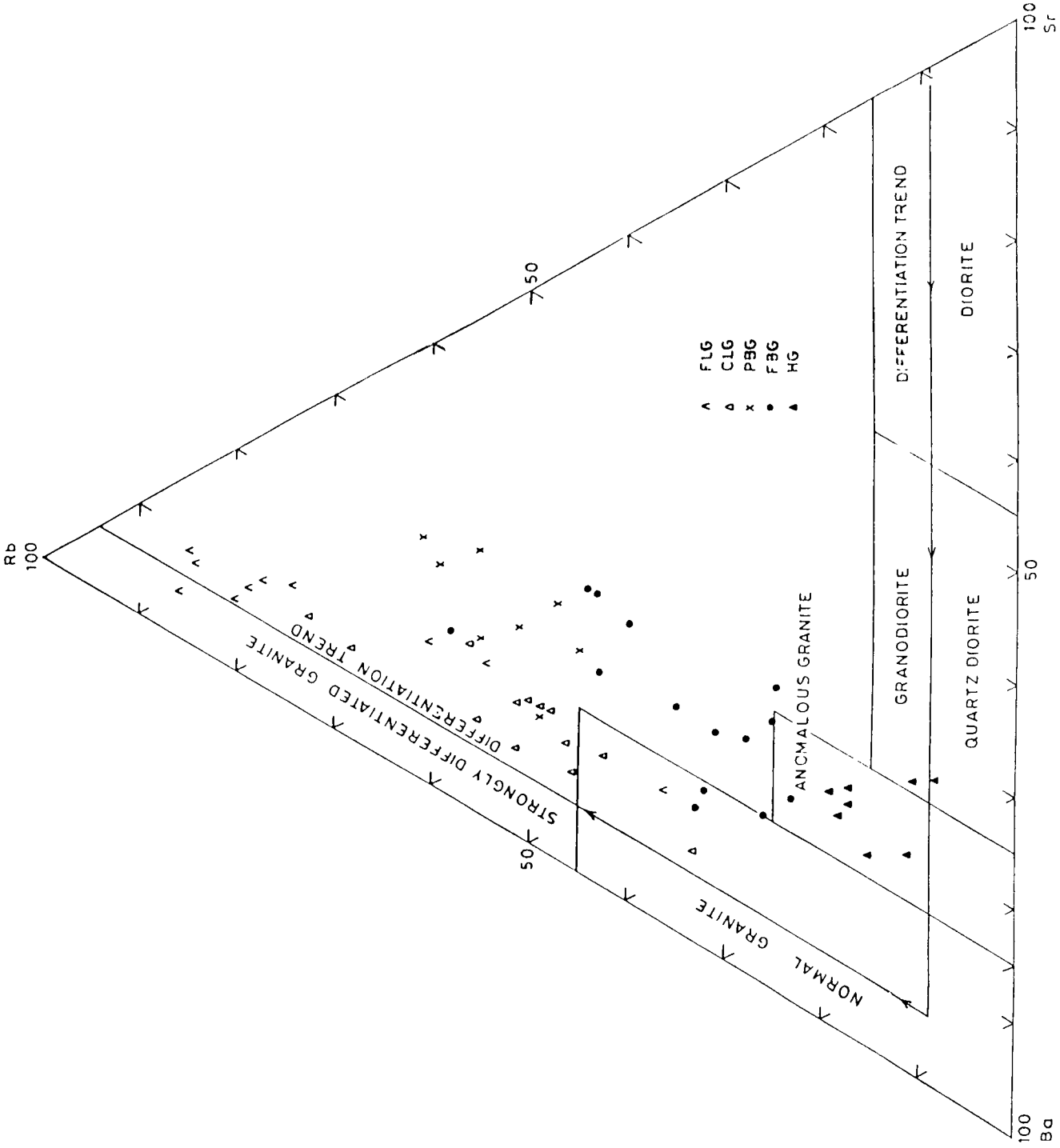

Figure 42. Rb-Sr-Ba ternary diagram for Bundelkhand granites (after El Bouseily & El Sokkary, 1975).

adamellite field, whereas the ratio exceeds 1.5 in the three younger granites which plot in the granite field. Similar trend is also observed in the Na_2O- K_2O - CaO ternary diagram (Figure 44) where the two older granites plot in quartz monzonite field and the younger granites are clustered in the granite field. This correlates with Taylor's (1985) view who observed the abundance and domination of sodium-rich granites in the early Archean; the later granites are found to be potassium rich.

The potassium enrichment with relation to younger intrusions in the Precambrian granites of South India has also been reported by Raju et al, (1983) who have attributed the phenomena to the increasing K_2O concentration in the source material from Archean to Proterozoic. The source for Archean granitoids is believed to be Na-rich and that for the Proterozoic and younger granitoid was relatively K-rich.

Geochemical Classification of the granites

Chappell and White (1974) classified the granites into I-and S-types on the basis of the nature of source material. The identification of source on the bsis of chemical and mineralogical characteristics was further discussed by White and Chappell (1977 and 1983), Hine et. al, (1978), Chappell (1984), and Clemens and Wall, (1988). Backinsale (1979) opined that the I-type and S-type granites

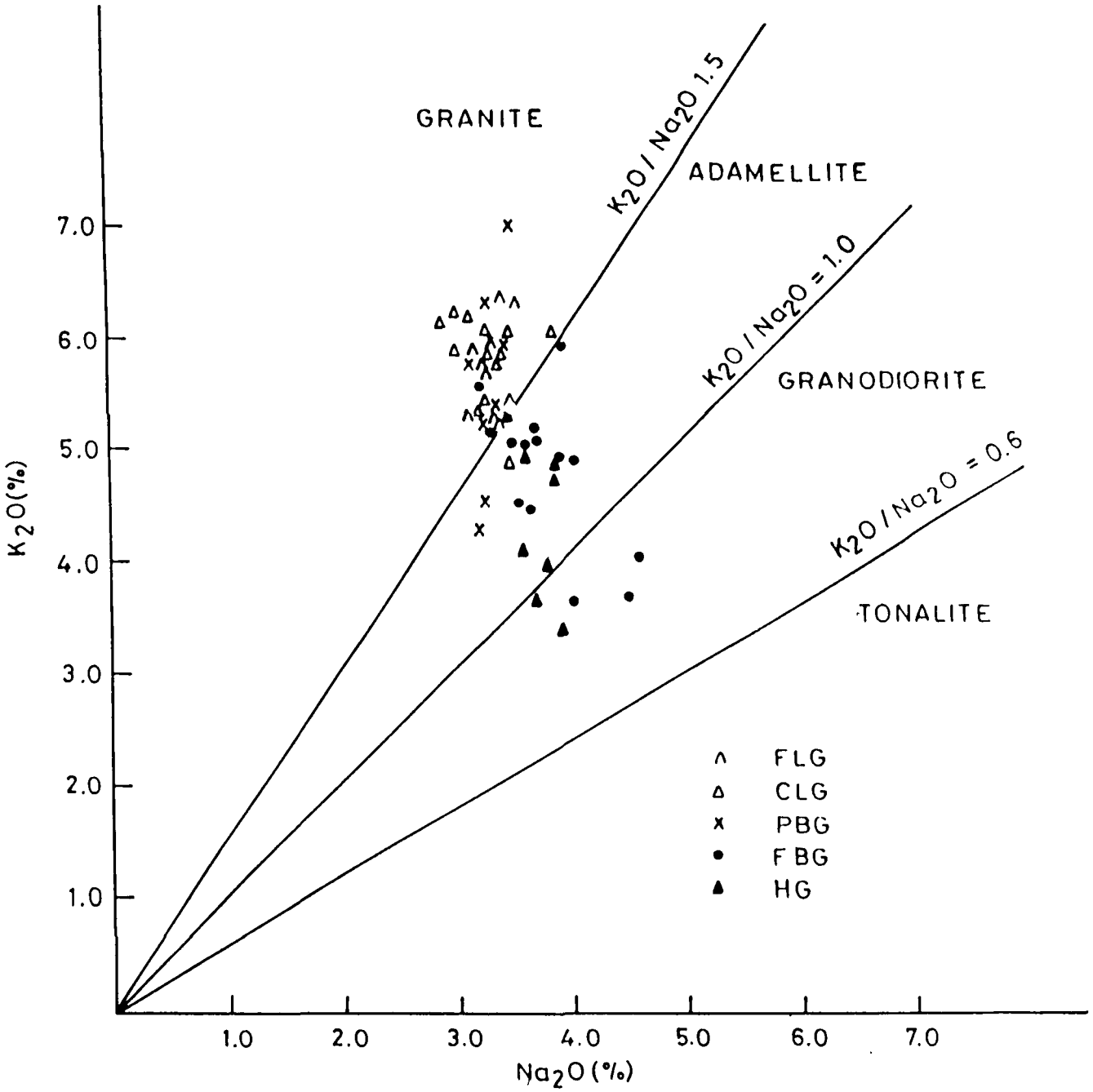

Figure 43. Plots of Na_2O and K_2O contents of the Bundelkhand granites.

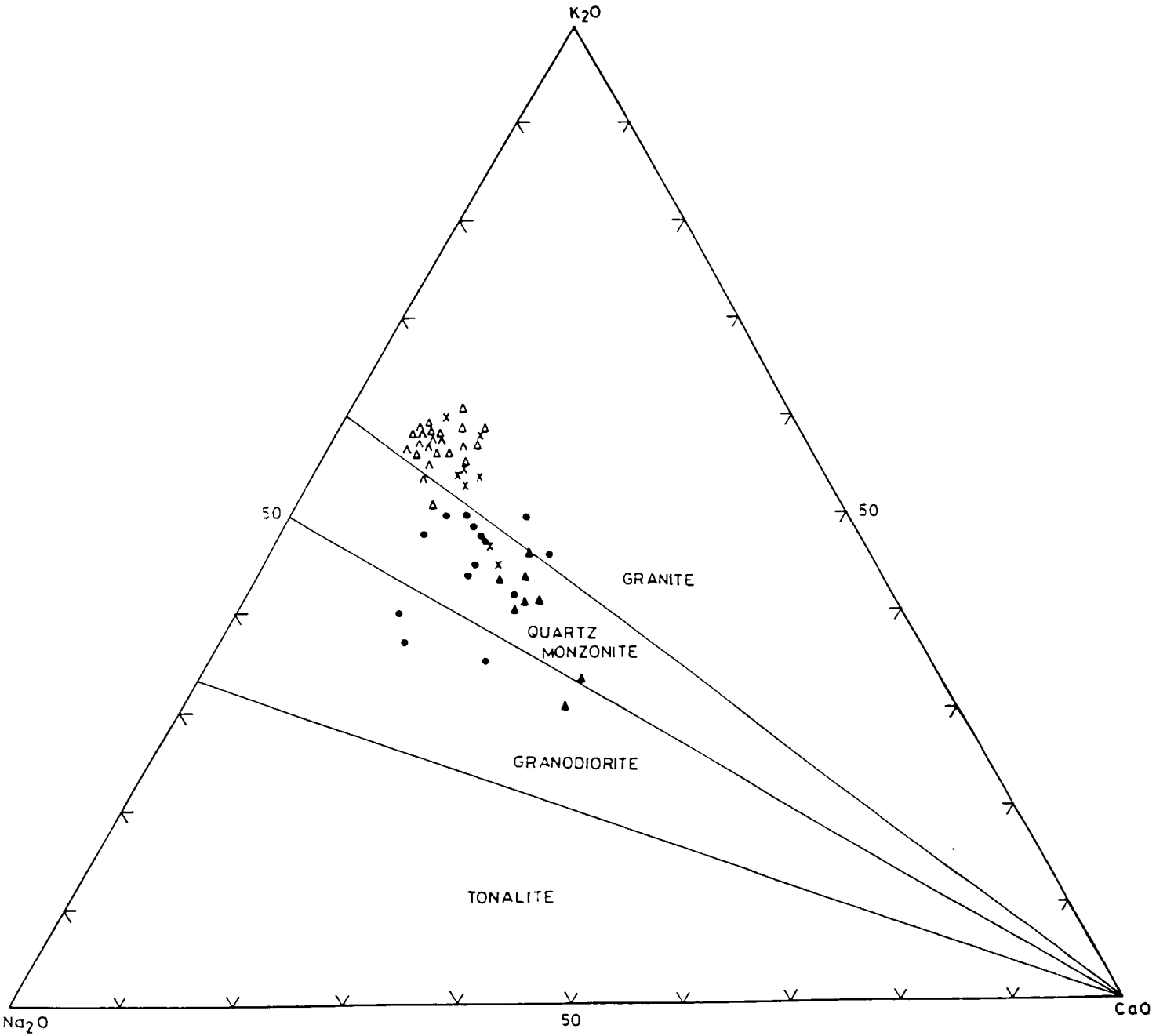

Figure 44. K_2O-Na_2O-CaO ternary diagram for Bundelkhand granites (symbols as in Figure 43).

are approximately equivalent to the magnetite series granite and ilmenite series granite, respectively of Ishihara (1977). Debon and Le Fort (1983) suggested that the cafemic and aluminous association of rocks, distinguished by their nomenclature scheme, are approximately equivalent to I- and S- types respectively of Chappell and White (1974), though the genetic interpretation may differ. The I- and S- type granites are calc-alkaline in nature and are associated with the convergent plate boundaries (Middlemost, 1985). Loiselle and Wones (1979) proposed a third type of granite, the A- type, which is related with the anorogenic environment (tensional stress regime). They suggested that the A- type granite is produced along rift zone and within stable continental blocks.

Pitcher (1982), on the basis of the tectonic setting characteristics of the various orogenic granites subdivided the I- type granite into three types; (a) M-type, (b) I- (cordilleran) type and (c) I- (caledonian) type. The M-type or mantle type granites are developed in ocean island arcs from mantle derived parent magmas; the rock ranges in composition from gabbro to tonalite.

Herms et al. (1981), Collins et al. (1982), and Jackson et al. (1984) reported that for a given SiO_2 content. A-type granite contains higher concentrations of Fe and Na + K and highly charged cations, such as Ga, Nb, Y, Zr and REE. Eby (1987) observed that in many tensional magmatic environments, the A-type granites are accompanied by the granites of different chemical characteristics which often show

features similar to I- and S- type granites. Whalen et al. (1987) also observed this phenomenon and proposed a discrimination diagram using plots of Ga/Al ratio vs selected major and trace elements to distinguish the orogenic (I- and S- type granites) from A-type granite; high Ga/Al value is diagnostic of A-type granite. They have also suggested the application of Zr+Nb+Ce+Y vs FeO/MgO and K_2O + Na_2O/CaO plots to discriminate the anorogenic A-type granites from the orogenic I- and S- types. Sometimes highly fractionated felsic I- or S- type granites have similar geochemical characteristics as a typical A-type granite and they overlap the field of A-type granites on the discrimination diagram proposed by Whalen et al (1987). However, linear increase in Rb, Rb/Sr, Rb/Ba, Ga/Al and Nb with decreasing Ba, Sr, Zr, Y and Ce in the felsic I-or S- type granites reveals their fractionated nature, whereas the A-type granites do not indicate evidence of strong fractionation (Whalen, 1983).

The plots of Bundelkhand granites on Ga/Al vs K_2O + Na_2O, (K_2O + Na_2O)/CaO, K_2O/MgO and FeO/MgO (Figure 45) and Ga/Al vs Zr, Nb, Y, and Zn (Figure 46) lie in the orogenic (I- & S-type) granite field. However, some plots on the Ga/Al vs K_2O + Na_2O and Ga/Al vs Nb diagrams are scattered and extend into anorogenic A-type granite field which has been observed to be the field of fractionated felsic I-type granite also (Whalen et al, 1987). Fractionated nature of the Bundelkhand granite is evident from the different major and trace elements variation diagrams (Figures 36, 37& 42).

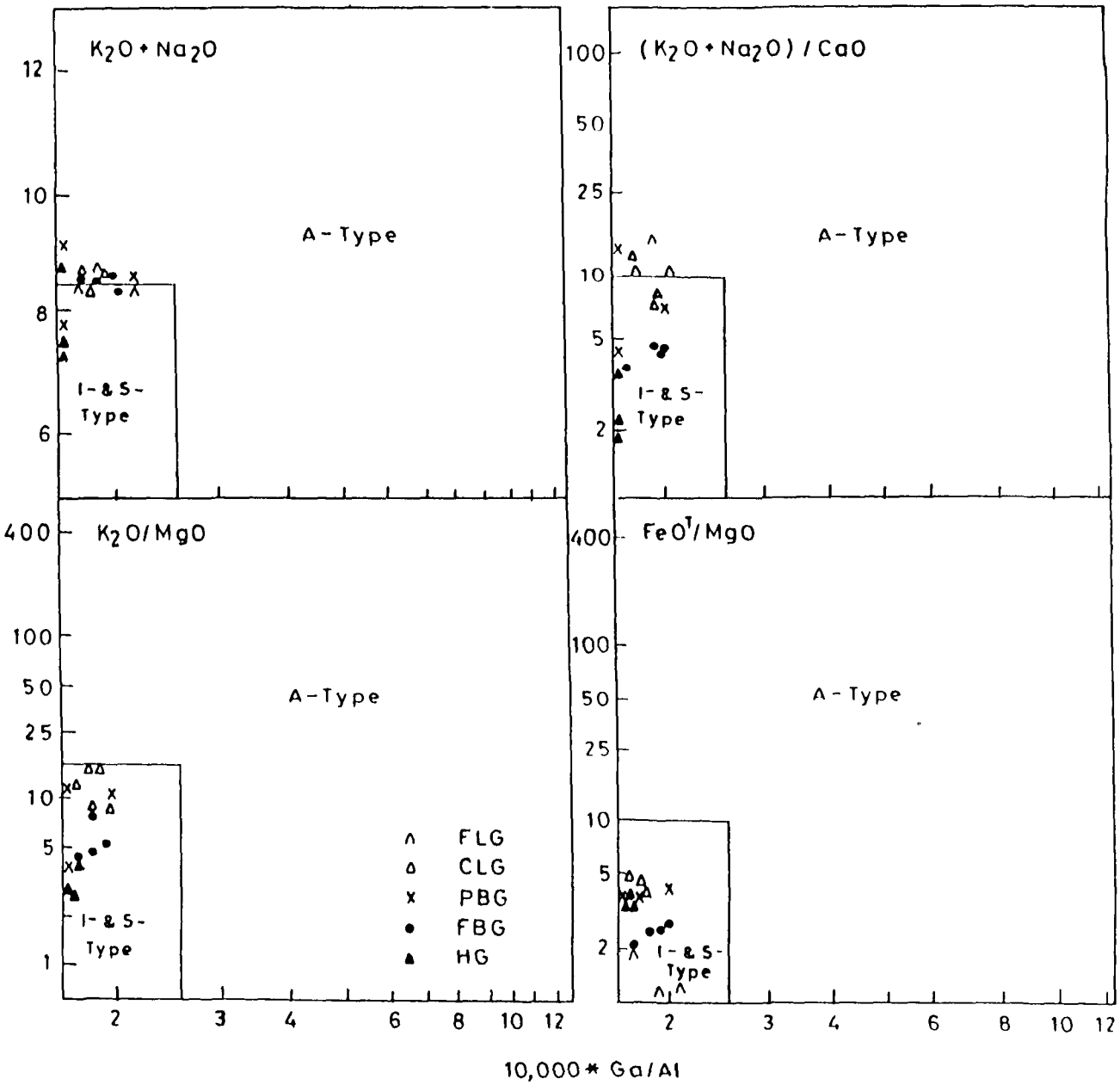

Figure 45. 10,000 * Ga/Al vs (K_2O+Na_2O), (K_2O+Na_2O)/ CaO, FeO/MgO and K_2O/MgO plots of Bundelkhand granites (after Whalen et al, 1987).

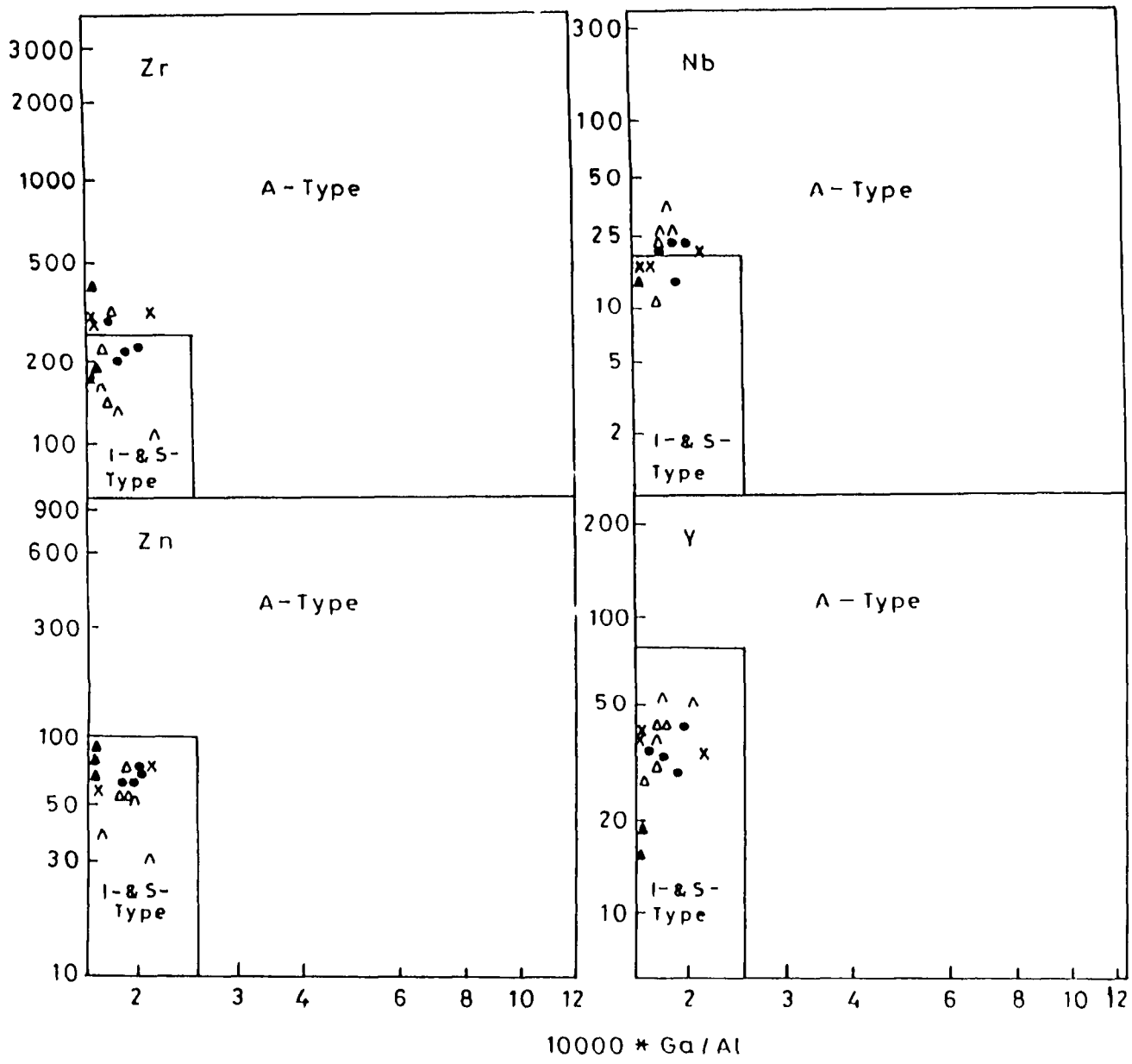

Figure 46. Plots of 10,000 * Ga/Al vs Zr, Nb, Y, and Zn on the discriminant diagram (after Whalen et al, 1987), (symbols as in Figure 45).

Kleemann and Twist (1989) differentiated the felsic rock of Bushveld complex into A-type and I-type on a discrimination diagram using SiO_2 vs Zr, Nb, Y and Ce, and Al_2O_3 vs Ga. They have demarcated the boundaries between I- type and A-type granites based on the data of Collins et al. (1982). Chemical composition of Bundelkhand granites plotted on the Kleemann and Twist's (1989) diagram (Figure 47 & 48) reveals its I-type affinity. However, the Nb vs SiO_2 plots are scattered and occupy both the fields of I- and A-type granites. Rogers et al (1980) observed that the Nb concentrations do not show any trend throughout the differentiation sequence in Ben Ghnema batholith thereby casting doubt on the usefulness of Nb in discrimination diagrams.

The Bundelkhand granites exhibit well defined negative linear correlation between CaO and SiO_2 on Harker's diagram (Figure 33). This type of linear array is characteristic of I-type pluton world over (Czamanske et al, 1981).

A significant characteristics of the Bundelkhand granite is its peraluminous composition. Various processes have been proposed for the formation of peraluminous magma (Cawthorn et al 1976; McCarthy and Groves, 1979; Halliday et al, 1981; White and Chappell, 1983; Miller, 1985).

Millar (1985) discussed the source and criteria for the evolution of peraluminous magmas and concluded that sedimentary input of any

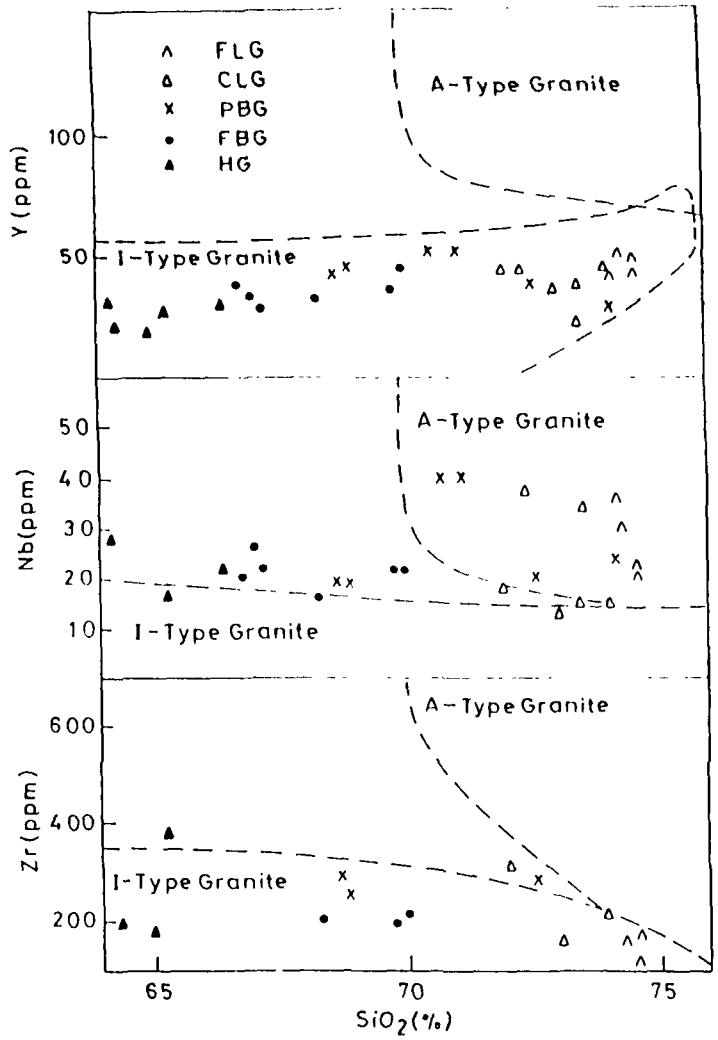

Figure 47. Plots of Zr, Nb and Y against SiO_2 to discriminate between I-type and A-type granites, (after Kleemann and Twist, 1989).

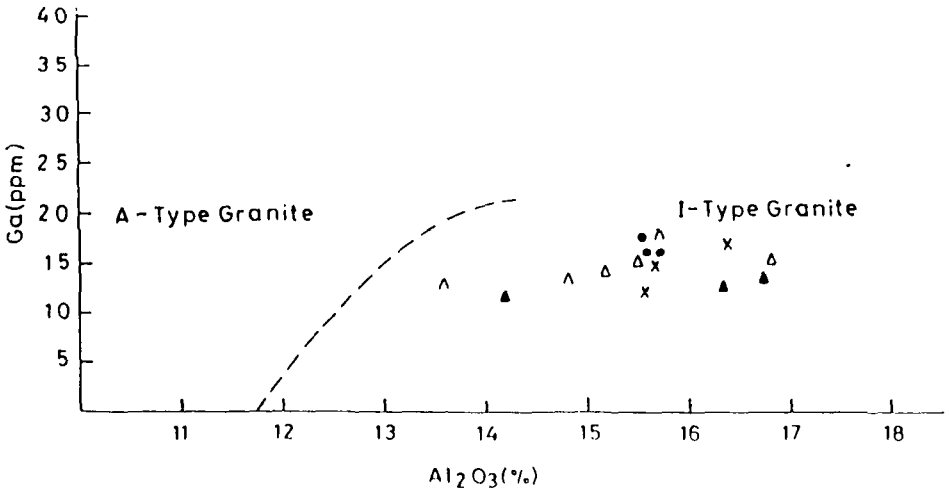

Figure 48. Bundelkhand granites plotted on Ga vs Al_2O_3 discriminant diagram (after Kleemann and Twist, 1989), (symbols as in Figure 47).

sort is not required to produce peraluminous composition; many strongly peraluminous rocks had little or no contribution from pelitic sediments. Lack of muscovite, garnet or cordierite and presence of hornblende, sphene and magnetite in the Bundelkhand granites are not consistent with the sedimentary parentage for the peraluminous composition.

Cawthorn and Brown (1976) have shown that calc-alkaline magmas as a whole grade, with increasing silica from metaluminous to peraluminous or even to strongly peraluminous. They attribute this change to fractionation of hornblende which they suggest may persist until the liquid is strongly peraluminous. A similar opinion is held by Abott (1981) which is consistent with the experimental results of Naney (1983). Zen and Hammarstrom (1982) believe that epidote fractionation can also drive liquid compositions into the strongly peraluminous field. Similar effect may be obtained by the fractionation of sphene. Any peraluminous magma produced in these ways should have "normal" calc-alkaline isotopic signature (Miller, 1985).

Variation trends of major and trace elements in Bundelkhand granites are consistent with the variations produced by fractional crystallization. A tendency towards increase in alumina with increase in SiO_2 suggests that this mechanism may have been important in the evolution of peraluminous composition of granite magma in the Bundelkhand massif. A similar mechanism has been proposed by Barr et al (1986) for Cheticamp pluton.

Plots of Bundelkhand granites on the modified ACF diagram of White and Chappell (1977) lie in the biotite-muscovite-plagioclase field with a well defined trend towards A (Al-Na-K) apex in relation to age (Figure 49). This distribution is not consistent with the assumption of simple mechanical mixing of melt and residue (Charoy, 1986). The regular decrease of Mg content indicates that more magnesium phases were stable at liquidus temperature (Abbott and Clarks, 1979; MacRae and Nesbitt, 1980). Bundelkhand granites are felsic, I-type and peraluminous in nature. This is consistent with the fact that minimum partial melts of basaltic rocks are peraluminous (Helz, 1976). Taylor and McLennan (1985) also advocated that fractionated I-types or only minimum temperature melts may be peraluminous. Some important features of Bundelkhand granite compared with the I- S- and A-type granite are given in Table 7.

It is evident from Table 7 that the Bundelkhand granite correlates with the I-type granite as indicated by the presence of hornblende, magnetite, sphene and absence of muscovite, garnet and codierite. It is further evidenced by linear variation trends on various variation diagrams, less than 15% mode of biotite and presence of metabasic xenoliths in Bundelkhand granite.

Debon and Le Fort (1983, 1988) proposed a cationic classification scheme of plutonic rocks and their magmatic associations based on the parameters Q=Si/3 - (K+Na+2Ca/3), P=K-(Na+Ca), A=Al- (K+Na+2Ca), B=Fe+Mg+Ti, and F=555-(Q+B) which are plotted in a set of three

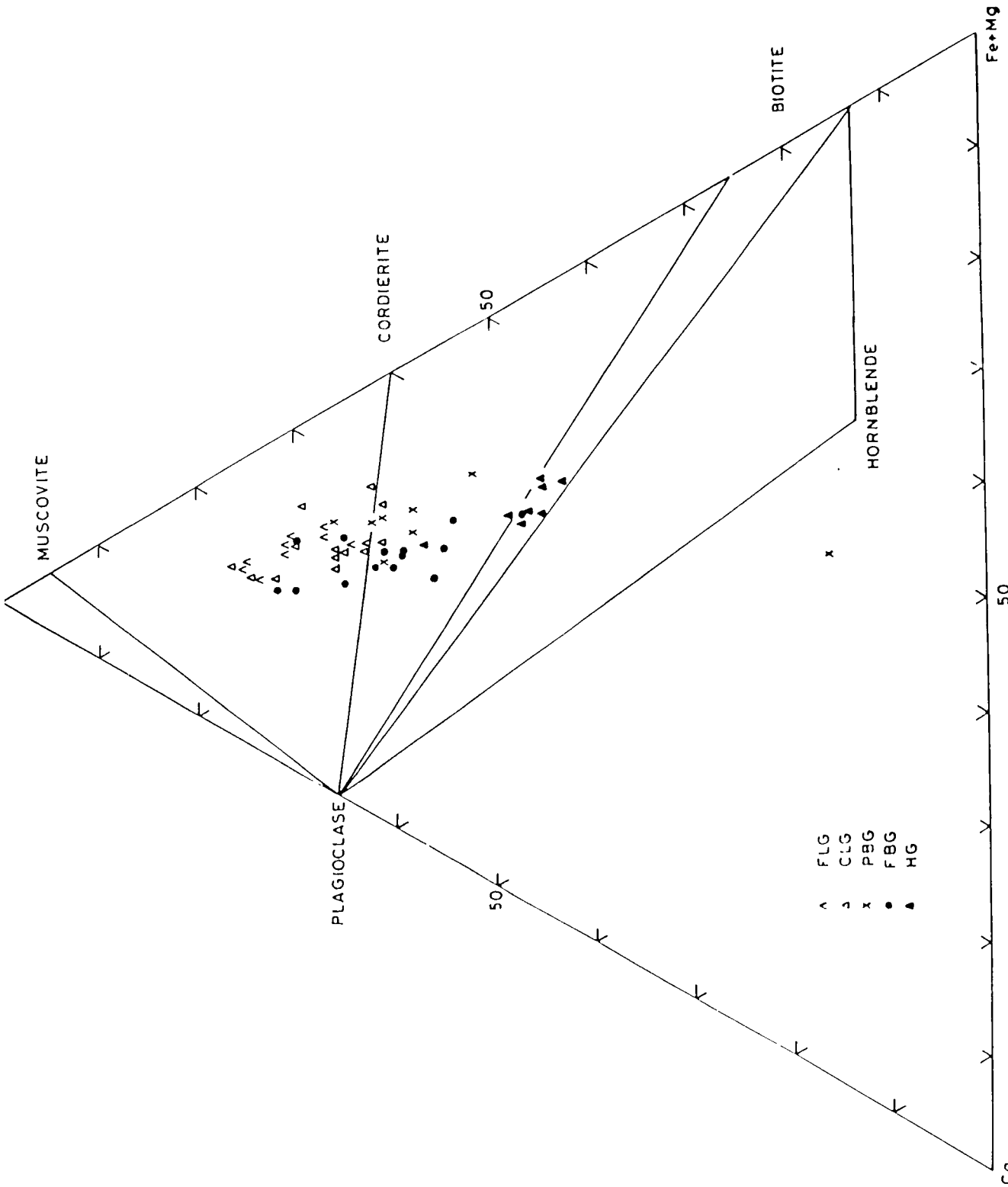

Figure 49. Bundelkhand granite compositions plotted in terms of Al-Na-K, Ca and Fe+Mg (after White and Chappell, 1977).

Table:7 Characteristics of S-, I- and A-type granites compared with Bundelkhand granite.

	S-type	I-type	A-type	Bundelkhand granite
Tectonic regime	Orogenic	Orogenic	Anorogenic	Orogenic
Xenoliths	Abundant sediment derived thoroughly recrystallized xenoliths	Mafic hornblende bearing xenoliths in more mafic granites. No sedimentary xenoliths.	Xenoliths accidental Magmas were completely molten, no restite.	Xenolith present biotite rich rock, rare metasediments
Hornblende	Not present	Common in mafic types, may also be present in felsic types.	Interstitial with high content of Fe and low Mg.	Present in the three older types and absent in two younger leucogranites.
Muscovite	Common	Generally no primary muscovite.	No primary muscovite.	Absent (noprimary muscovite)
Biotite	15-20% of mode in mafic varieties.	Generally $<$ 15% of mode.	Interstitial anninite rich biotite.	$<$ 15% of mode.
Al_2O_3/Na_2O+K_2O+CaO	High (>1.05) and increase as the rock becomes more mafic.	Normally low (<1.1) (only minimum temperature melts or fractionated I-type rocks may be per aluminous).	Low, 1.0	More than 1.1 per aluminous, granites are fractionated in nature.
Binary variation	Irregular	Linear or near linear.	Linear or near linear.	Linear

Source : Kleemann and Twist (1989); Taylor and McLennan (1985).

diagrams. The method involves two sequential steps, the first step is concerned with individual sample, the second one aims at defining the type of magmatic association to which the sample belongs.

Three main types of associations are distinguished: cafemic, from source material mainly or completely derived from mantle, aluminous, mainly or completely derived from anatexis of continental crust; and alumino-cafemic, intermediate between the other two types. Cafemic and alumino —cafemic associations are further divided into subtypes; tholeiitic, calc-alkaline (granodioritic), subalkaline (monzonitic), alkaline and peralkaline.

The clssification scheme of Debon and Le Fort (1983, 1988) was applied on Bundelkhand granite. On the "Q-P" diagram (Figure 50), the plots of hornblende granite and foliated biotite granite lie in granodiorite and adamellite field which is plagioclase rich,whereas the younger granites plot within and near the granite field. The trend of the older two types indicates calc-alkaline nature of the granite, whereas the younger leucogranites correspond to subalkaline potassic type. On the characteristic minerals "A-B" diagram (Figure 51), trend of Bundelkhand granite is similar to cafemic and alumino-cafemic association. The older two granites are extended in the metaluminous domain and lie in sector (iv). The three younger granites plot in the peraluminous domain. The youngest, fine grained leucogranite plots in the leucogranitoid field.

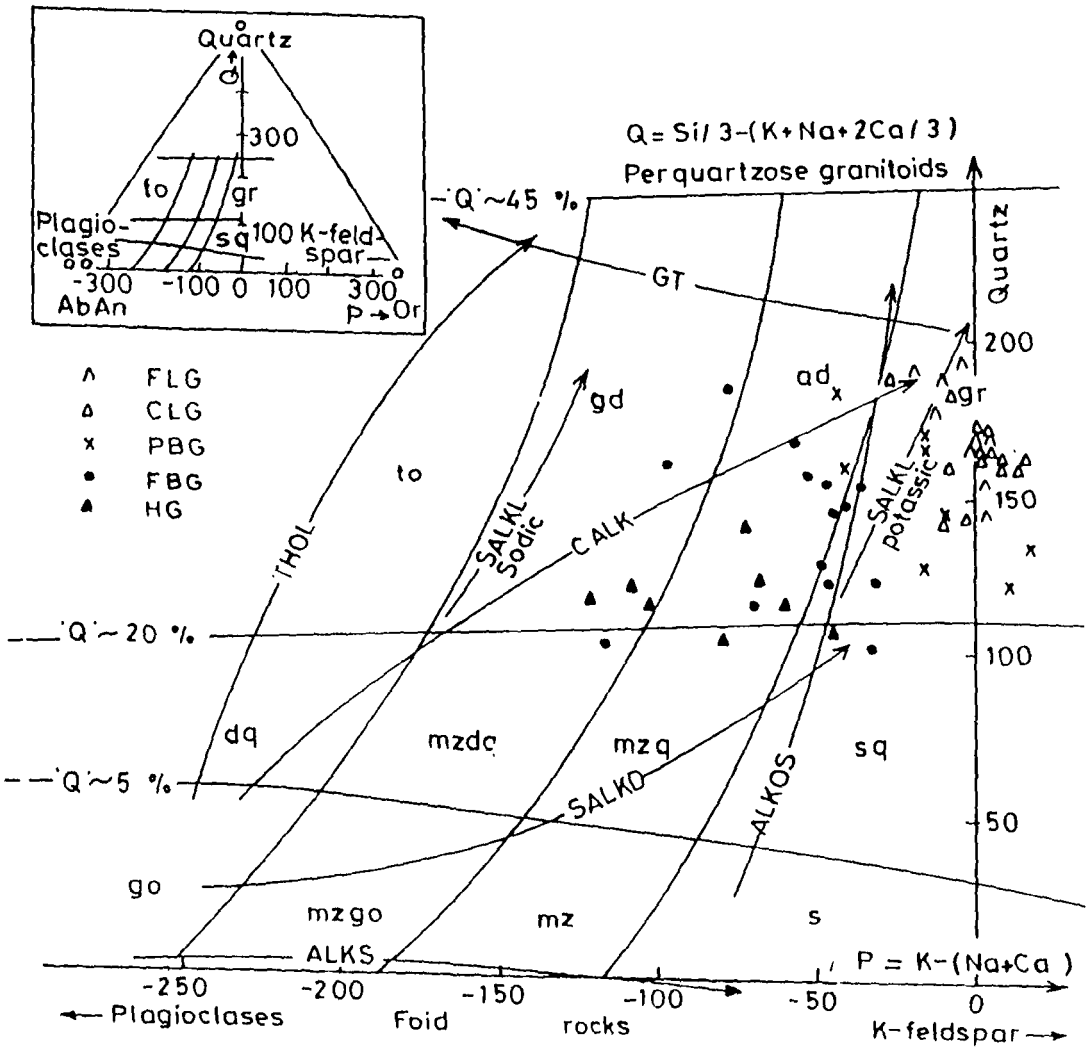

Figure 50. Distribution of the five types of the Bundelkhand granite in the 'nomenclature' diagram proposed by Debon & Le Fort (1983). The two parameters are in millications. Each field correspond, to a rock type: gr granite, ad adamellite, gd granodiorite, to tonalite, sq quartz syenite, mzq quartz monzonite, mzdq quarts monzodiorite, dq quartz diorite, a syenite, mz monzonite, mzgo monzogabbro, go gabbro. Typical trends of different subtypes of cafemic or alumino-cafemic associations are shown: THOL tholeiitic, CALK calk-alkaline, SALKD, SALKL dark and light-coloured subalkaline respectively, ALKS ALKOS alkaline saturated and oversaturated respectively.

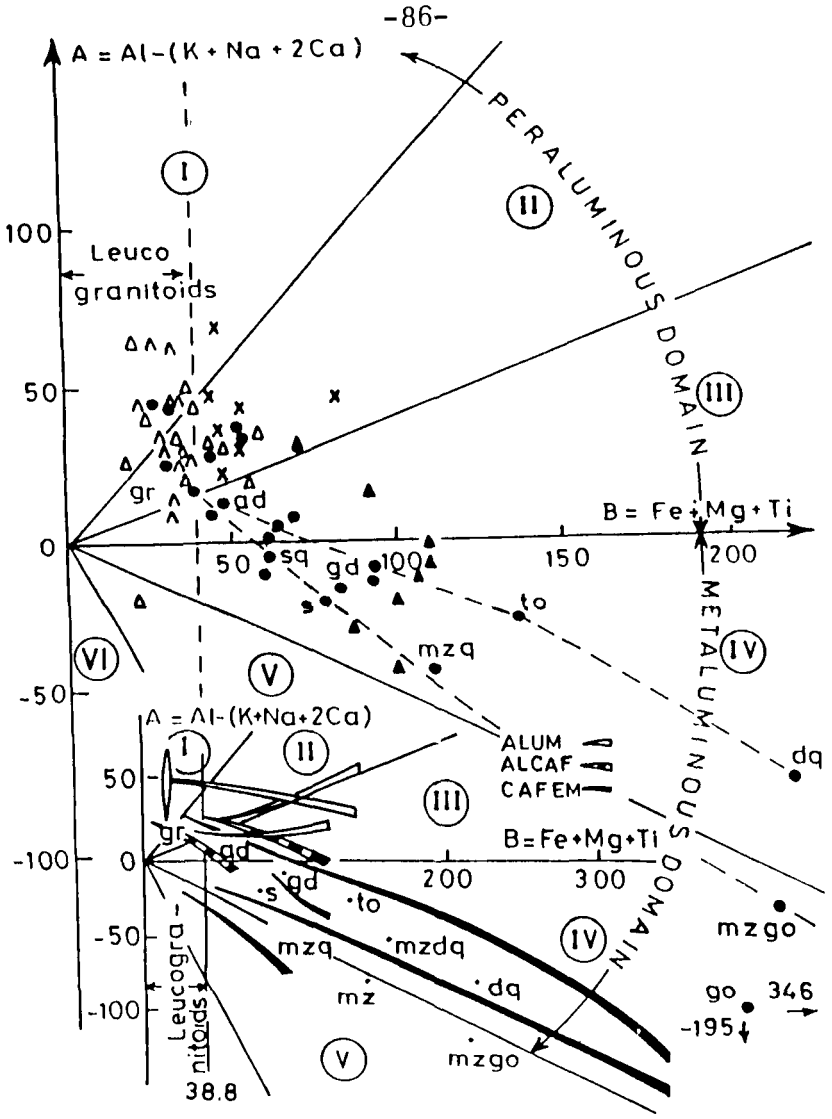

Figure 51. Distribution of the five types of Bundelkhand granites on the 'characteristic minerals' or 'A -B' diagram of Debon and Le Fort (1983). The two parameters are in millications; A is the 'aluminous index' and B is proportional to dark mineral content. Each of six sectors numbered from I to VI, corresponds to a specific mineralogical composition; I rocks with Mu > Bi (by volume), II Bi > Mu, III Bi, IV Bi+Amph±Cpx, V Cpx±Amph±Bi. The trends of the three main types of magmatic associations (see the index) are distinguished: ALUM aluminous, ALCAF alumino-cafemic, CAFEM cafemic. Other explanations as in Figure 50.

Debon and Le Fort (1983) suggested that the cafemic associations always start with the amphibole and/or pyroxene but often end with biotite alone or two mica rocks, whereas the alumino-cafemic associations are located mainly or totally within peraluminous domain and are essentially micaceous (biotite and sometimes two micas); amphiboles are commonly present in the dark members. Aluminous associations are confined in peraluminous domain and they bear micas but no amphiboles; sometimes secondary sphenes may be present. They have also suggested that these three associations may have peraluminous composition. The presence of hornblende, in the three older types of granite and biotite and sphene in all the types suggest that the Bundelkhand granites have similar features with the cafemic to alumino-cafemic associations.

The plots of Bundelkhand granite on "Q-B-F" diagram (Figure 52) reveal a compositional variation from granodiorite to granite; the two younger granites are restricted in the leucogranite field. The trend follows from calc-alkaline to subalkaline field.

The compositional range and nature of Bundelkhand granite, deduced from Debon and Le Fort (1983, 1988) nomenclature scheme, indicate a cafemic to alumino-cafemic magmatic association of rocks. The granite varies in composition from granodiorite to granite and corresponds to calc-alkaline to sub-alkaline type and is similar to I-type granite of Chappell and White (1974). Debon et al (1987) concluded that the granites with cafemic and alumino-cafemic character

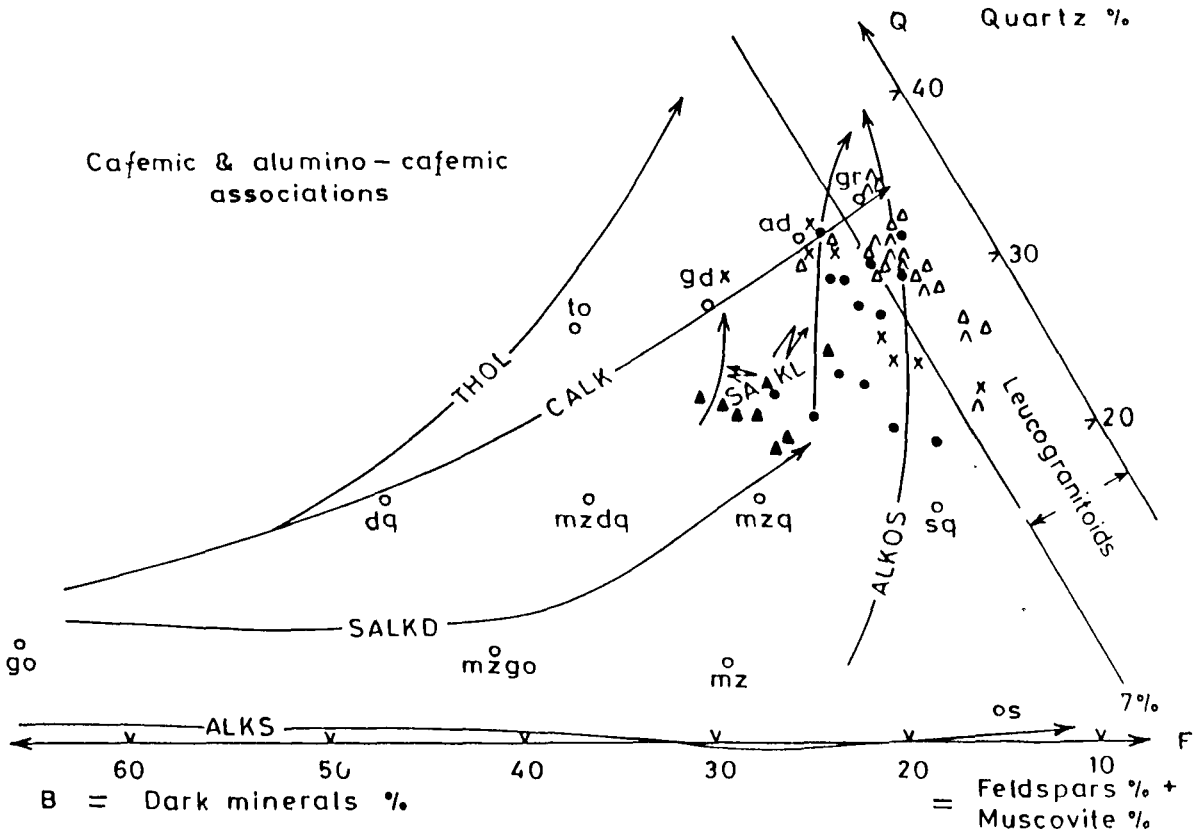

Figure 52. Distribution of Bundelkhand granites in the triangular quartz- dark minerals-feldspar+muscovite diagram ('Q-B-F' diagram) of Debon & Le Fort (1983). The parameters in millications. The different subtypes among the CAFEM and ALCAF types (Figure 51) of magmatic associations are distinguished: THOL, CALK, SALKD, SALKL, ALKS, and ALKOS (typical trends are shown). Other explanation as in Figure 50.

and calc-alkaline to sub-alkaline nature are related with the oceanic subduction processes.

Nature of Bundelkhand granites

The chemical composition of Bundelkhand granite, plotted on AFM diagram (Figure 53), reveals its calc-alkaline affinity. All the plots are concentrated within the region of calc-alkaline volcanic and plutonic rocks and are similar to the trend of Sierra Nevada batholith which is inferred to be calc-alkaline in nature (Bateman et al, 1963).

Wright (1969) proposed a classification scheme to distinguish among strongly alkaline, alkaline and calc-alkaline rocks over the full range of silica content. He proposed a simple alkalinity ratio: $(Al_2O_3 + CaO + alkalis)/(Al_2O_3 + CaO - alkalis)$ vs SiO_2 to identify the characteristics . Almost all the plots of Bundelkhand granite on alkalinity vs silica diagram (Figure 54) lie in the calc-alkaline field.

Rogers and Greenberg (1981) have distinguished the calc-alkaline rocks from alkaline granite suite using plot of SiO_2 vs Log_{10} (K_2O/MgO). All the known calc-alkaline granites plot within the calc-alkaline field on Rogers' diagram. However, the plots for Sierra Nevada batholith lie in both the calc-alkaline as well as alkaline granite fields. It is inferred that the Sierra Nevada granite is calc-alkaline in nature; their plot in the alkaline field is attributed to the enrichment of alkalis in the magma from the

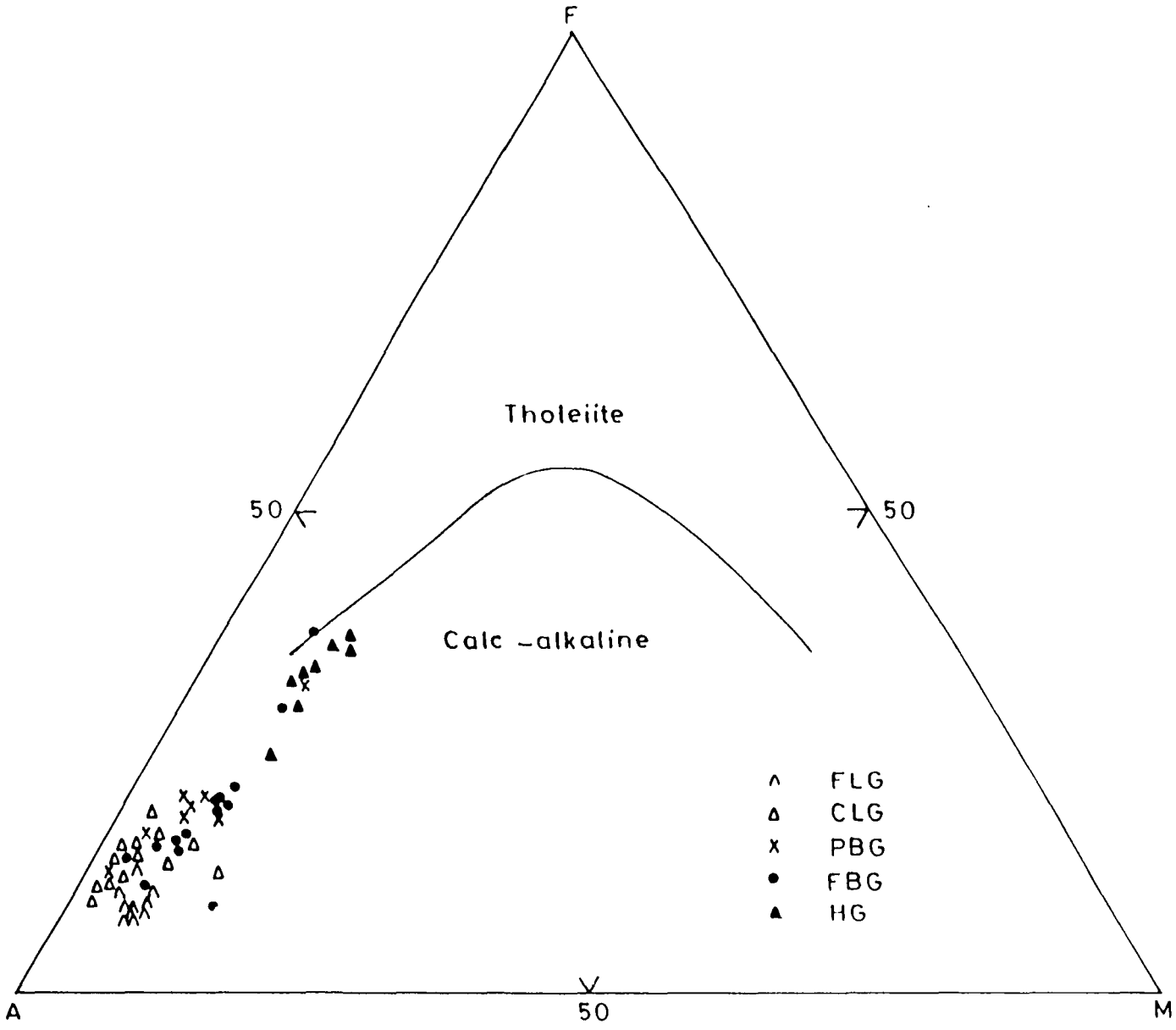

Figure 53. Chemical composition of Bundelkhand granites plotted on AFM diagram.

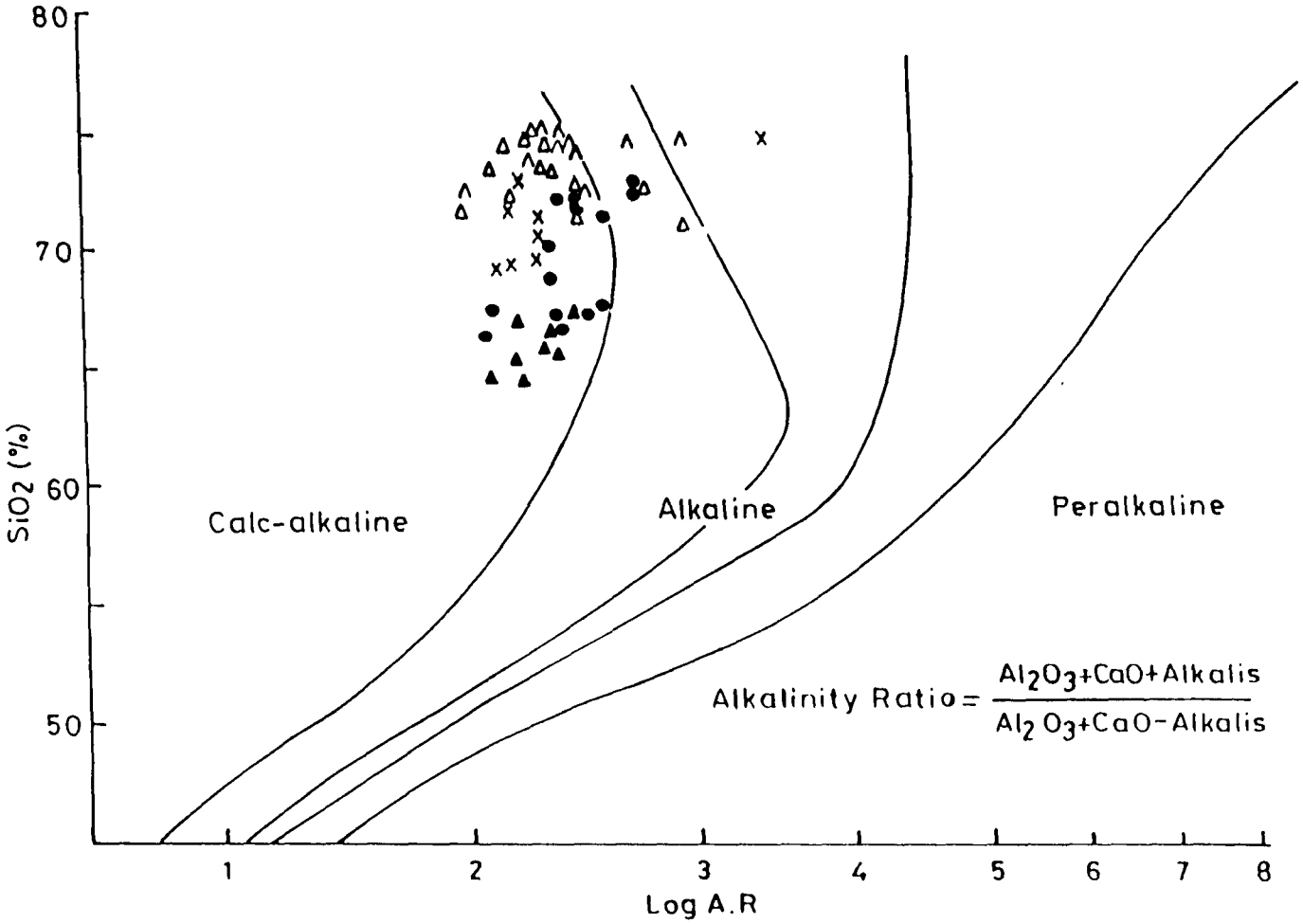

Figure 54. Alkalinity ratio vs SiO_2 diagram of Bundelkhand granites (after Wright, 1969). For explanation of symbols see Figure 53.

continental crust. Sierra Nevada batholith, being farther inland from the continental margin, probably traversed through a thick continental crust when it was emplaced. Rogers et al (1980) have also observed a similar trend for Ben Ghnema batholith and concluded that the alkali granites are differentiation product of calc-alkaline suites, differentiation apparently occurs in continental-margin environments. The plots of Bundelkhand granaites on Rogers and Greenberg's (1981) diagram (Figure 55) cover both the calc-alkaline and alkaline fields and follow the trend similar to that of Sierra Nevada batholith and Ben Ghnema batholith.

Sylvester (1989) classified the granites into three types, calc-alkaline granitoids, strongly peraluminous granitoids and alkaline granites. A fourth type, highly fractionated calc-alkaline granitoid is also recognised, but he considered it to be a variety of alkaline granitoids. He proposed a discriminant diagram based on $(Al_2O_3 + CaO)/(FeO_T + Na_2O + K_2O)$ vs $100\ (MgO + FeO_T + TiO_2)/SiO_2$ to differentiate various types of granite.

The data of Bundelkhand granitoids were plotted on Sylvester's diagram (Figure 56). The three older granites plot in the calc-alkaline and strongly peraluminous fields, whereas the plots of the two younger leucogranites in the highly fractionated calc-alkaline field. Sylvester (1989) observed that some highly fractionated differentiates of co-magmatic "normal" calc-alkaline granites plot in the alkaline field on the diagram. The close similarities between

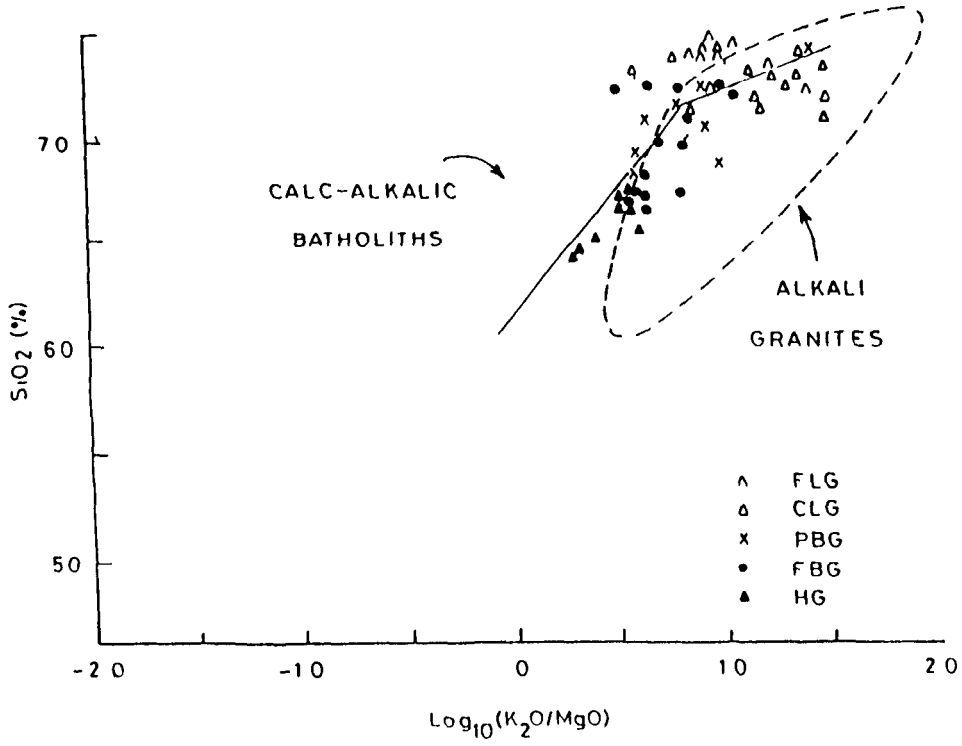

Figure 55. Distinction between calc-alkalic and alkali granite suites using the plots of SiO_2 vs $Log_{10}(K_2O/MgO)$, after Rogers and Greenberg (1981). The solid line represents the trend of Sierra Nevada and Ben Ghnema batholiths.

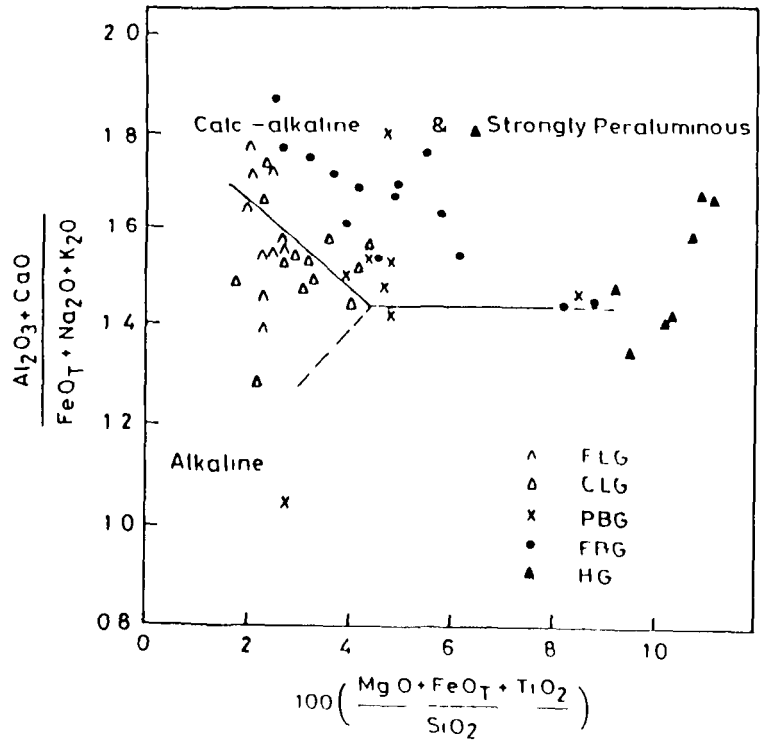

Figure 56. Major element discrimination diagrams of Bundelkhand granites (after Sylvester, 1989).

highly fractionated calc-alkaline granites and "normal" alkaline A-tpe granites have been reported earlier by Whalen et al (1987). They proposed plots of Zr + Nb + Ce + Y vs FeO_T/MgO or $(K_2O + Na_2O)CaO$ to discriminate the highly fractionated calc-alkaline granites from alkaline A-type granites. Sylvester, however, considered these highly fractionated felsic calc-alkaline granites as a variety of alkaline granites.

Sylvester (1989), correlated his classification of granites with the genetic classification of White and Chappell (1983) and found that the alkaline granites based on compositional classification are equivalent to A-type of White and Chappell (1983); the calc-alkaline and highly fractionated felsic calc-alkaline correspond to I-types, and the strongly peraluminous granites are related either to S-type or I-type granites.

It may be inferred from the plots of Bundelkhand granites (Figure 53, 54, 55 and 56) that all the five types of granite have calc-alkaline affinity, the younger intrusions which exhibit alkaline affinity correspond to highly fractionated calc-alkaline granites. The Bundelkhand granite correlates with the Sierra Nevada batholith and Ben Ghnema batholith which have been considered to be calc-alkaline inland continental margin magmatism (Rogers et al, 1980; Rogers and Greenberg, 1981).

Calc-alkaline rocks are developed near compressive plate boundaries and they are associated in some way with subducted lithospheric slab (Wyllie et al, 1976; Middlemost, 1985; Defand et al , 1988). The calc-alkaline nature of the Bundelkhand granites suggests its generation in a subduction related tectonic setting.

CHAPTER - V

TECTONIC SETTING OF BUNDELKHAND GRANITE

The granite controversy is significant from two points of view; their confinement to relatively near the surface and their virtual restriction to continental crust with almost total absence in the oceanic crust. With the advent of the theory of plate tectonics, a great revolution came in the field of geology which abandones many older views and hypotheses and sought to explain the geological phenomena with a unified dynamic model. Granite problem acquired a new dimension as a consequence of the concept of plate tectonics. It is realised that some tectonic activity, either extensional or compressional, must be invoked to explain the initiating trigger of magma production and to provide 'room' to the huge granite batholiths.

The Bundelkhand massif occupies the heart of present Indian plate and is delineated by the Indo-Gangetic alluvium in the northeast, the Son-Narmada lineament in the south and the Great Boundary Fault in the west (Figure 57). A huge batholithic body like that of Bundelkhand granite in the central portion of the present Indian plate deserves special attention with regard to its evolution from the tectonic point of view.

Various major and trace element discriminant diagrams have widely been employed to elucidate the tectonic setting of basic

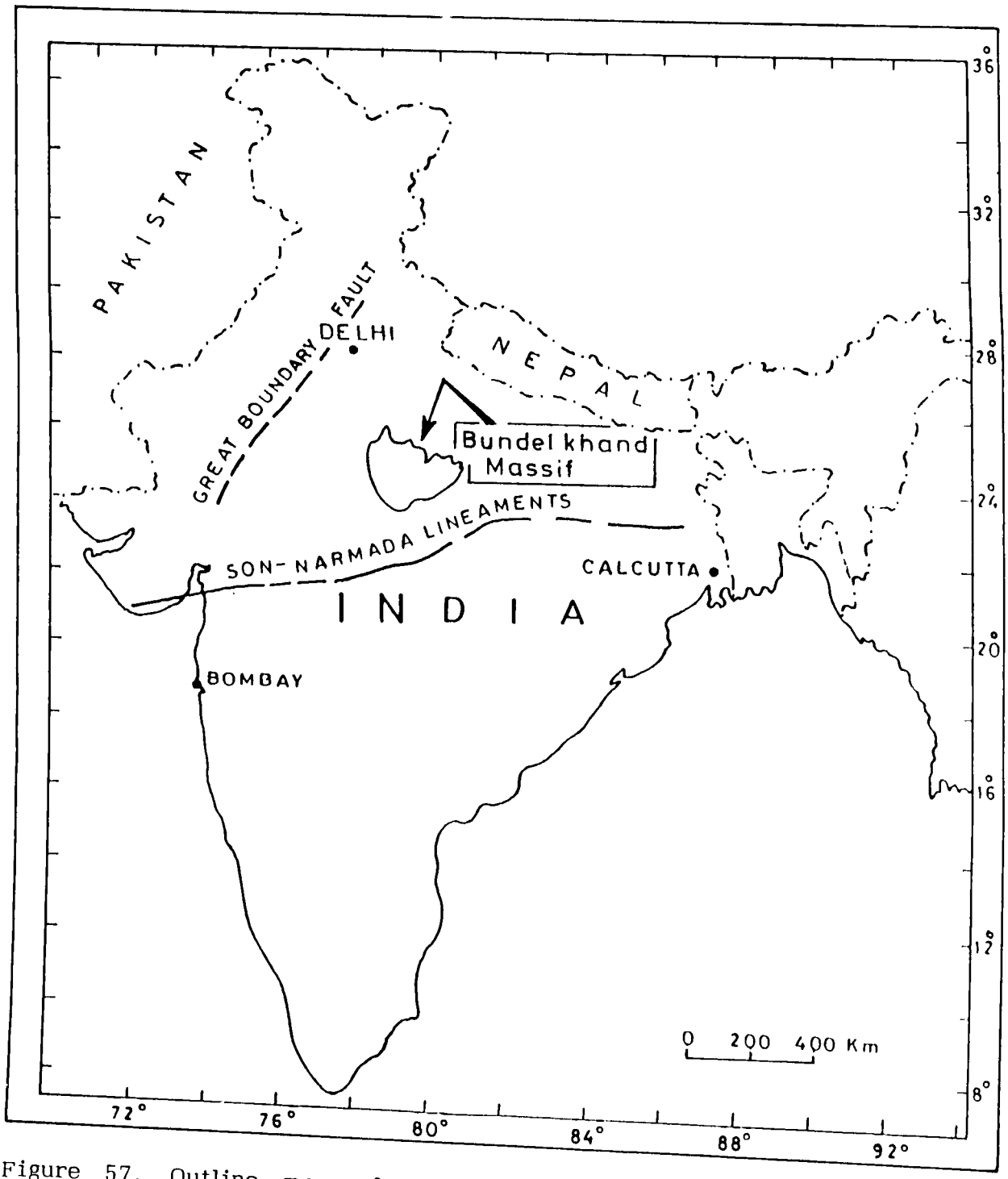

Figure 57. Outline map of India showing Son-Narmada lineament, Great boundary fault and Bundelkhand massif in between them.

volcanic rocks. However, these diagrams have not found such wide applications for the plutonic rocks, particularly granites, due chiefly to the complicated petrogenetic history of granite which involves continental crust, besides other factors like pressure, temperature, volatile content and source rocks which control the magma dynamics. Crystallization of trace element-rich phases which are of generally little relevance to basalt genesis can obscure many important geochemical signatures of granites thereby making the chemical composition of granites difficult to interpret (Pearce et al, 1984). In the present study, an attempt has been made to understand the tectonic setting of the Bundelkhand granite by using Maniar and Piccoli's (1989) discrimination diagram based on major elements and the trace element spidergrams of granites from known tectonic set-up (Sun et al, 1979; Wood et al, 1979). An approach of this kind may reveal a different configuration of the erstwhile Indian plate in relation to Son-Narmada lineament.

Maniar and Piccoli (1989) proposed a classification scheme for the tectonic discrimination of granitic rocks based on major element chemistry. By applying various discriminant plots, they have sequentially distinguished the different tectonic environments, in which granitic rocks were emplaced. They distinguished seven types of granitoid based on their tectonic setting; these are, (1) island arc granitoids (IAG), (2) continental arc granitoids (CAG), (3) continental collision granitoids (CCG), (4) post-orogenic granitoids

(POG), (5) rift related granitoids (RRG), (6) continental epirogenic uplift granitoids (CEUG), and (7) ocean plagiogranitoids (OP). Of these, the IAG, CAG, CCG, and POG are considered as orogenic granitoids, whereas RRG, CEUG and OP are believed to be anorogenic granitoids. The steps involved in discriminating between various tectonic environments on the basis of the major element chemistry of granitoids are as follows:

OP is discriminated from the rest of the granitoid rocks using the K_2O vs SiO_2 variation plots. Discrimination between group I (IAG, CCG, CAG), group II (RRG, CEUG), and group III (POG) can be achieved by using plots of Al_2O_3 vs SiO_2, FeO (T)/FeO (T) + MgO vs SiO_2, and AFM and ACF ternary diagrams. Distinction between CCG and IAG + CAG can be made on the basis of molar concentration $Al_2O_3/(CaO + K_2O + Na_2O)$ (A/CNK). CCG has the A/CNK ratio of more than 1.05, whereas IAG + CAG have A/CNK values less than 1.15. If, however, the ratio is between 1.05 and 1.15, it may not be possible to distinguish CCG from IAG + CAG. Discrimination between RRG and CEUG is possible by the TiO_2 vs SiO_2 plots. However , they suggested that the proposed discrimination scheme is emperical and have pointed out a few limitations in their approach.

An attempt has been made to classify the Bundelkhand granites by applying the Maniar and Piccoli (1989) classification scheme.

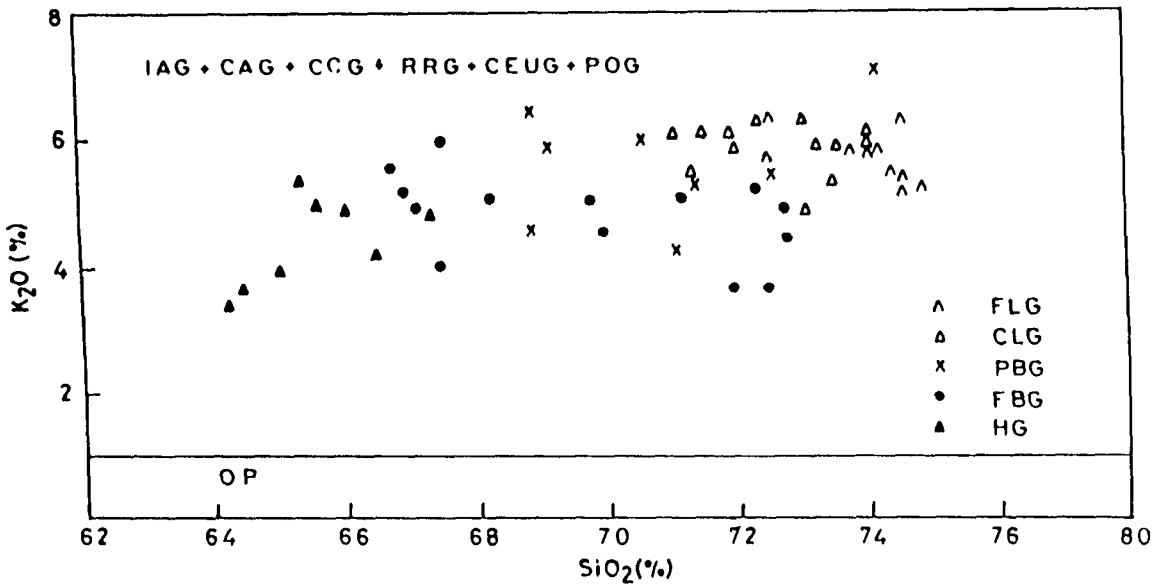

Figure 58. Distinctioon between oceanic plagiogranites (OP) and granitoids from other tectonic setting on K_2O vs SiO_2 diagram.

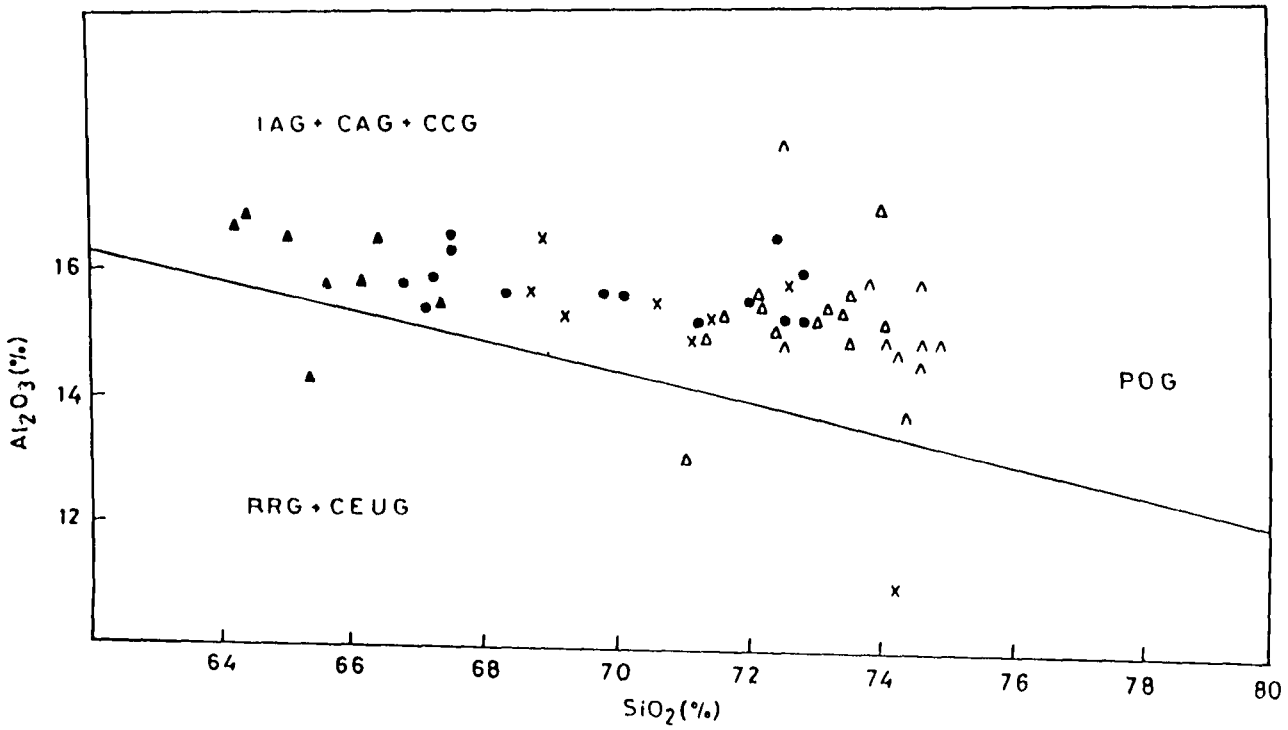

Figure 59. Al_2O_3 vs SiO_2 diagram. Distinction between group I (IAG+CAG+CCG), group II (RRG+CEUG) and group III (POG). For explanation of symbols see Figure 58.

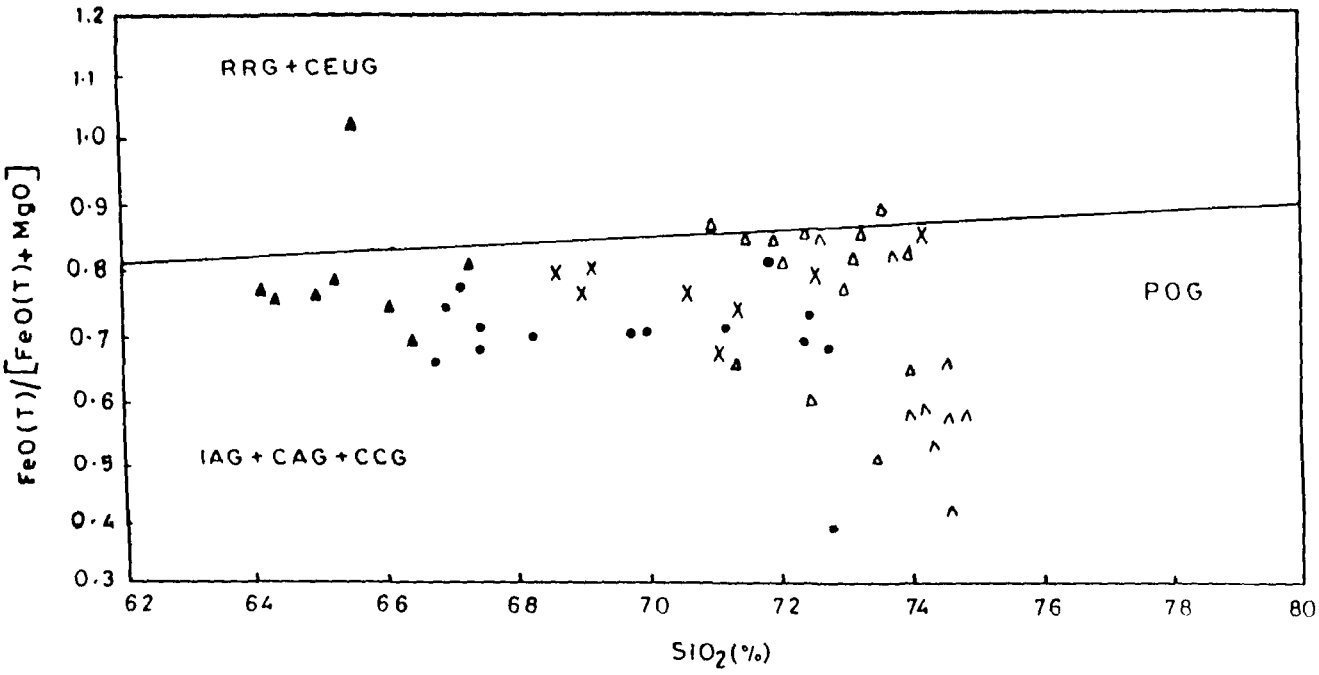

Figure 60. FeO(T)/[FeO(T)+MgO] vs SiO_2 plots. Distinction between group I (IAG+CAG+CCG), group II (RRG+CEUG) and group III (POG). Symbols as in Figure 58.

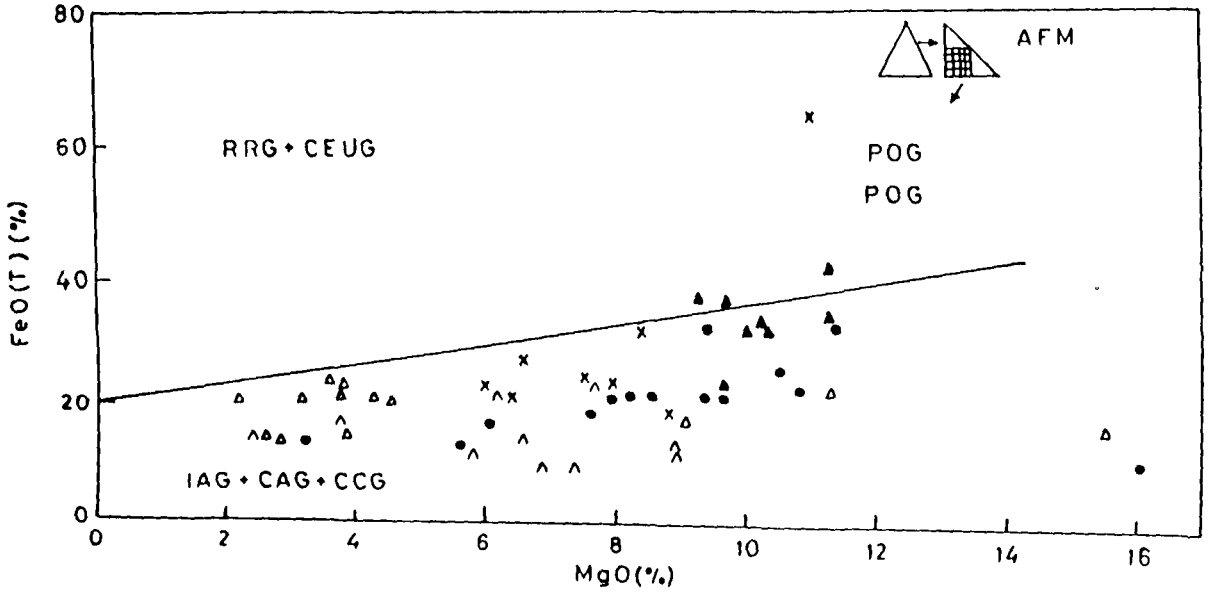

Figure 61. Plots on (Al_2O_3-Na_2O-K_2O)- [FeO(T)]-(MgO) ternary diagram. Distinction between group I (IAG+CAG+CCG), group II (RRG+CEUG) and group III (POG). Symbols as in Figure 58.

Discrimination between OP and rest of the granitoids was achieved by K_2O vs SiO_2 plots (Figure 58); all the data of Bundelkhand granites correspond to the field of CAG, IAG, CCG, PRG, CEUG, and POG. Al_2O_3 vs SiO_2, FeO(T)/FeO(T)+ MgO vs SiO_2,(Al_2O_3-Na_2O-K_2O) - [FeO(T)] - (MgO), and (Al_2O_3-Na_2O-K_2O) - [FeO(T)+MgO]-(CaO) plots were applied to differentiate group I (IAG, CAG, CCG), group II (RRG, CEUG) and group III (POG) rocks. Figures 59, 60, 61 and 62 show that the plots of Bundelkhand granites are concentrated in the field identified for group I (IAG, CAG, CCG) rocks. However, some plots of the two youngest leucogranites lie in the (POG) field. To discriminate between the various rocks (IAG, CAG and CCG) belonging to group I, molar Al_2O_3/(CaO + K_2O + Na_2O) (A/CNK) ratio was used (Figure 63). It is evident from the figure that all the samples of Bundelkhand granites have A/CNK values greater than 1.2. The chemical composition of the five types of Bundelkhand granite is compared with the granites of different tectonic setting in Table 8. As such, the Bundelkhand granites are inferred to have continental collision affinity. It may be concluded that the Bundelkhand granites were emplaced in a continental collision tectonic setting. The younger leucogranites may be of post-collision setting.

Sun et al (1979) and Wood et al (1979) proposed a mantle normalised incompatible element spidergram for genetic interpretation

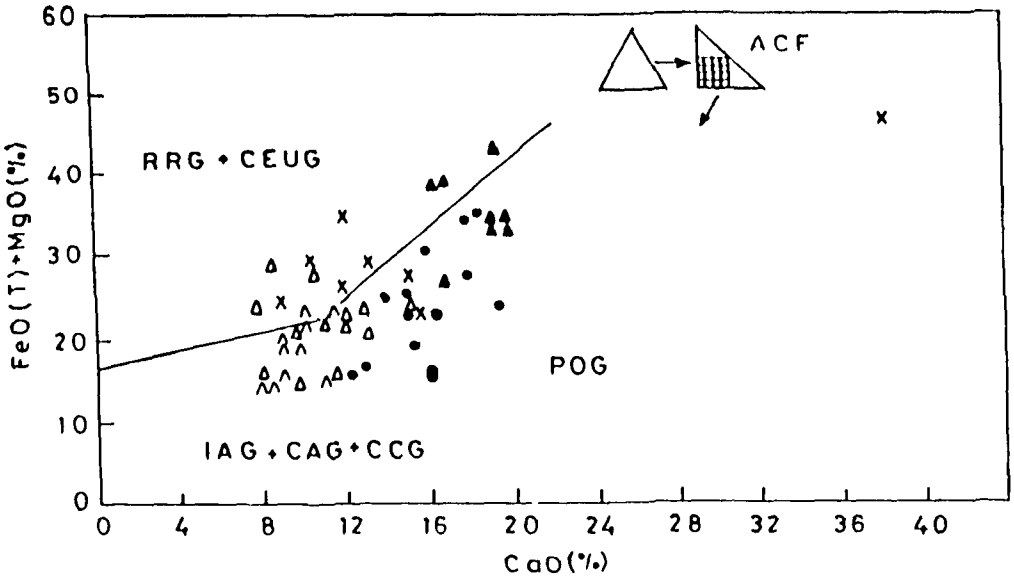

Figure 62. Bundelkhand granites plotted on (Al_2O_3-Na_2O-K_2O)-[FeO(T)+MgO]-(CaO) ternary diagram. Distinction between group I (IAG+CAG+CCG), group II (RRG+CEUG) and group III (POG). Symbols as in Figure 58.

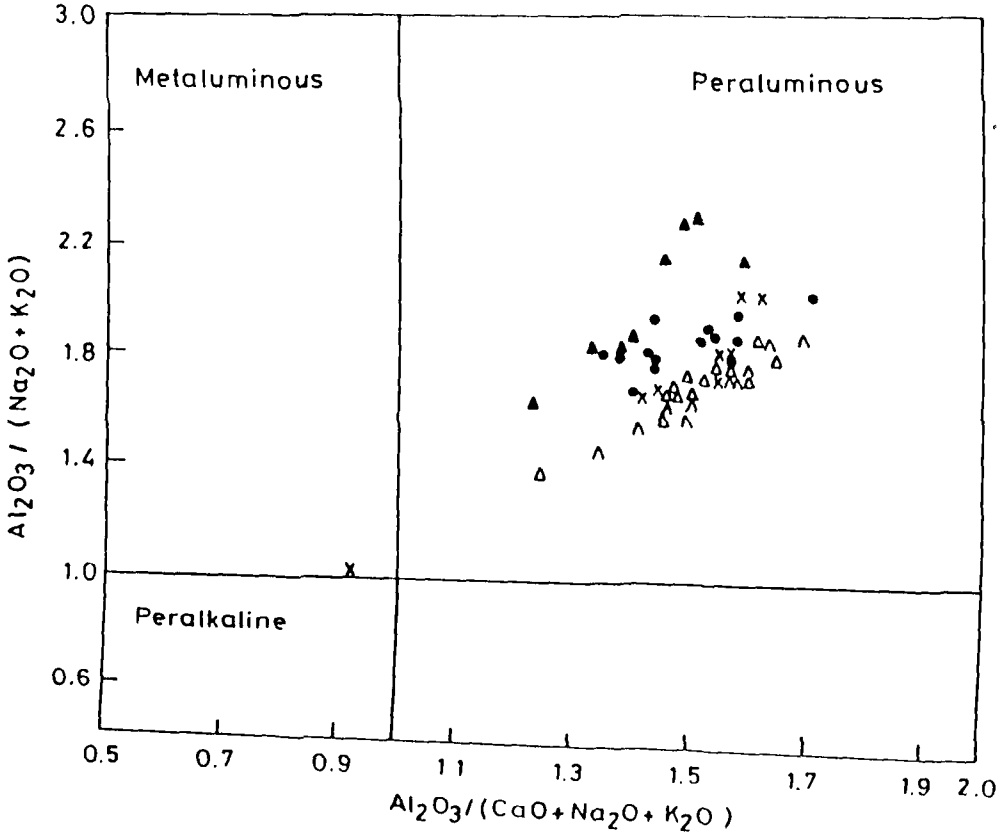

Figure 63. Discrimination of granites based on Shand's index (symbols as in Figure 58).

Table 8 Chemical characteristics of Granitoids by Tectonic Environment compared with Bundelkhund granite

	AG	CAG	CCG	POG	RRG	CEUG	OP	B U N D E L K H A N D G R A N I T E		
								Hornblende Granite (8 samples	Foliated Biotite Granite (14 samples)	Porphyritic Biotite Granite (8 samples	Coarse grained Leucogranite (13 samples)	Fine grained Leucogranite (10 samples)
Silica range (wt %)	64-68	62-76	72-76	72-76	72-78	71-77	61-78	64 21 - 67 28	67 08 - 72 82	68 91 - 74 22	70 95 - 74 07	72 51 - 74 67
Alkali-lime index	Calcic to calc-alkaline	Calc-alkaline	Calc-alkaline to alkali-calcic	Alkali-calcic	Alkalic	Alkalic	Calcic	Calc-alkaline	Calc-alkaline	Calc-alkaline	Calc-alkaline	Calc-alkaline
Shand's index	Predominantly ne a luminous	Metaluminous peraluminous	Peraluminous	Peraluminous metaluminous peralkaline (minor)	Peraluminous (minor) metaluminous peralkaline	Peralu-minous (minor) metalum-inous peralka-line	Peraluminous metaluminous	Peraluminous	Peraluminous	Peraluminous	Peraluminous	Peraluminous
Na_2O/CaO (wt %)	~1 0	~4 0	~2 0-10 0	~2 0-18 0	~2 0-25 0	~1 0-12 0	~4 0	0 99 - 1 56	1 17 - 3 33	1 67 - 3 47	2 24 - 5 21	1 64 - 4 95
Na_2O/K_2O (wt %)	~0 4-3 0	~0 4-2 0	~0 4-1 5	~0 6-1 2	~0 7-1 0	~0 6-1 0	0 0-50 0	0 66 - 1 18	0 58 - 1 24	0 49 - 0 75	0 48 - 0 73	0 53 - 0 66
MgO/FeO(T) (wt %)	0 3-0 85	0 10-0 50	0 50-0 6	0 02-0 30	0 02-0 20	0 02-0 12	0 02-0 70	0 25 - 0 43	0 23 - 1 53	0 17 - 0 47	0 1 - 0 97	0 17 - 0 88
MgO/MnO (wt %)	12 0-28 0	2 0-38 0	2 0-45 0	2 0-15 0	0 0-7 5	0 0-7 5	0 0-50 0	18 33 - 23 33	4 41 - 44 36	6 66 - 17 05	5 66 -60 83	9 69 -33 15
$Al_2O_3/(Na_2O+K_2O)$	>1 5	>1 1	>1 1	0 9-1 4	<1 15	<1 15	>1 0	1 6 - 2 29	1 66 - 2 02	1 05 - 2 01	1 56 - 1 83	1 54 - 1 85

Source Maniar and Piccoli (1989)

of basalts. Their spidergram was applied by Harmon et al (1984) to study the trace element variation in different suites of British Caledonian granite. Sheraton and Black (1988) plotted the data of granitic rocks from the East Antarctic shield on the incompatible element spidergram to determine the chemical evolution of granitic rocks. The normalised incompatible pattern of Y-depleted granitic rocks are relatively smooth, enriched in highly incompatible elements (Pb, Ce) but with large negative Nb anomalies. The Y-undepleted granites have more irregular pattern; most elements other than Sr are relatively enriched. Y, Zr, Nb, La and Ce are higher and most LILE also tend to be enriched compared to undepleted granites. The late- to post- orogenic granites show features similar to undepleted granites, but the pattern is more irregular with large negative Sr and Ti anomalies.

Incompatible trace element pattern for Bundelkhand granites (Figure 64) shows a relatively smooth pattern with significant depletion in Y content for the oldest granite (HG) in relation to the other types. The pattern of hornblende granite correlates with Y-depleted granitic rocks of East Antarctic shield which are inferred to be syn-collision granite. The pattern for younger varieties of Bundelkhand granite shows significant enrichment in Y with larger negative Sr and Ti anomalies; other LILE are also enriched in relation to oldest type. The pattern is similar to undepleted granite of East Antarctic shield.

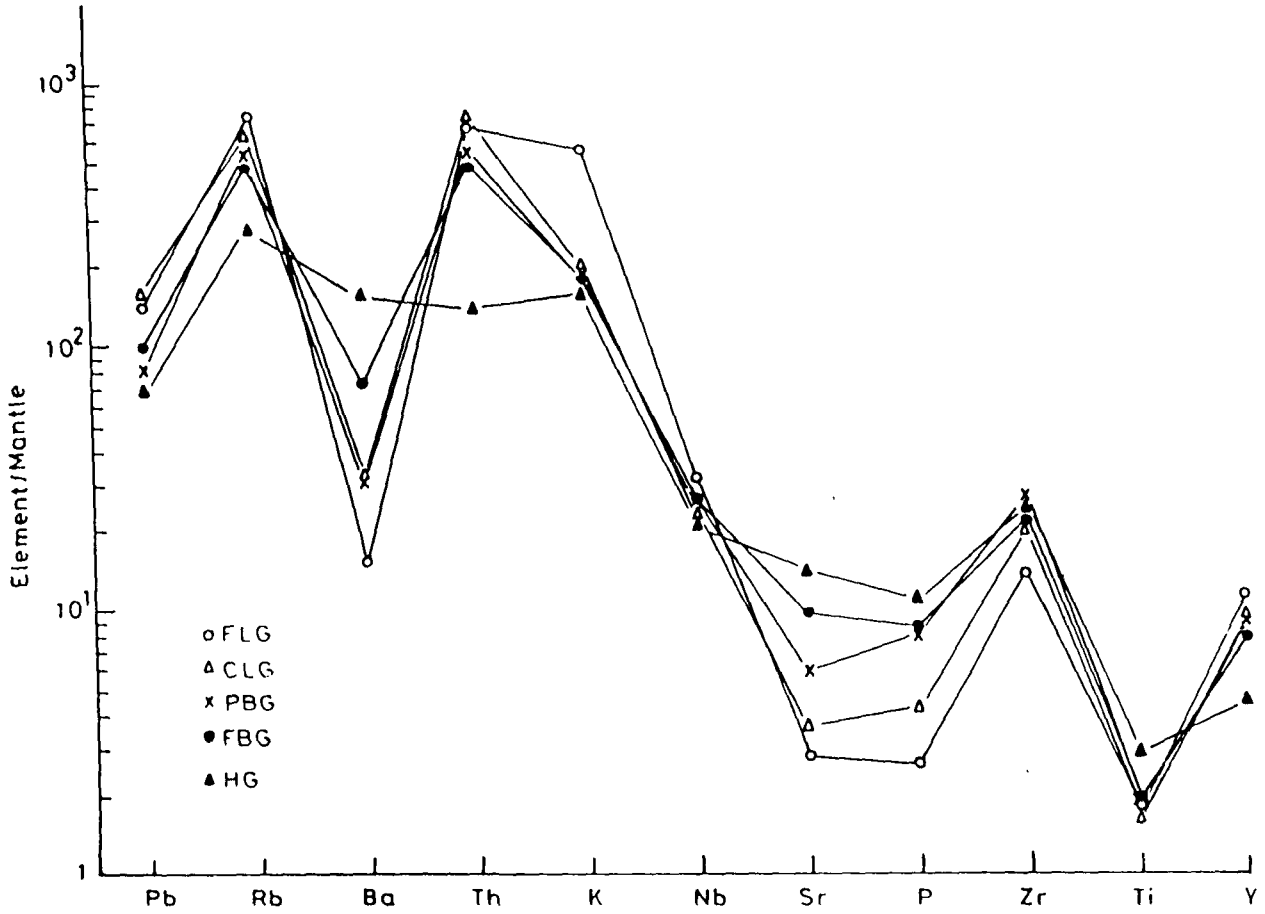

Figure 64. Normalised incompatible trace elements abundance pattern of Bundelkhand granite. Normalising values are estimated primordial mantle concentrations taken from Sheraton & Black (1988).

In relation to oldest hornblende granite, the younger varieties of granite in Bundelkhand have higher Y, Nb, Ga/Al ratio and lower CaO, Sr and Mg (Atomic $Mg/Mg+FeO_T$) values. These features are typical of worldwide I-type granitic rocks and are consistent with relatively dry melting of crustal rocks (Sheraton et al, 1985).

The geochemical signatures of Bundelkhand granites revcal a spectrum of tectonic setting of intrusions. The oldest hornblende granite has a Y-depleted pattern which is consistent with hydrous partial melting of a hornblende and/or garnet bearing mafic source (Sheraton et al, 1985). High geothermal gradient in Archean may have resulted in more extensive melting of garnet bearing subducted oceanic crust and may have caused an enhanced production of depleted magma (Tarney & Saunders, 1979).

The younger foliated biotite granite and porphyritic biotite granite show an undepleted pattern, similar to Y-undepleted granites of East Antarctic shield. The granites are believed to be syn-orogenic which were formed by melting of felsic crust during the collision of the lithospheric plates. Post-Archean subduction related calc-alkaline granite magmatism is typically undepleted I-type (Cordilleran type of Pitcher, 1983).

The late-to post-orogenic melting event is represented by the youngest two leucogranites in the area; they show marked enrichment of Y, Zr, Th, K, & Rb and depletion of P, Sr, Ti & Ba. The leucogranites correlate with highly fractionated felsic I-type granites, which show characteristics similar to A-type.

A secular evolution from depleted to more potassic undepleted type granitic magmatism in Bundelkhand is similar to many Archean cratonic blocks; these includes southern Indian shield (Glikson 1982), western Australia (Glikson and Lambert, 1976, northeastern Minnesota (Arth and Hanson, 1975), north Atlantic craton (Bridgwater et al, 1978; Collerson and Bridgwater 1979; McGregor, 1979).

The geochemistry of Bundelkhand massif reveals its calc-alkaline affinity, the plots on the AFM diagram are concentrated in the calc-alkaline field and closely resemble the trend of Sierra Nevada batholith which has been inferred to be inland continental margin magmatism (Rogers and Greenberg, 1981). The classification scheme of Wright (Figure 54) based on alkalinity ratio vs SiO_2 also reveals the calc-alkaline nature of Bundelkhand granites.

Plots of Bundelkhand granites on Rogers and Greenberg's (1981)SiO_2 vs Log_{10} (K_2O/MgO) diagram (Figure 55) lie in the fields of both calc-alkaline and alkaline granites. The plots on Sylvester's discrimination diagrams (Figure 56) indicate that the three older granites correspond to calc-alkaline and peraluminous type, whereas the two younger types correlate with the highly fractionated calc-alkaline I-type granite which is considered to be a variety of alkaline type although they may have a distinct origin. Stoeser and Elliot (1980) and Bentor (1985) suggested that alkaline granites make up the majority of the post-collisional suite, whereas

the calc-alkaline granites dominate the preceeding syn-collisional subduction related magmatism.

The tectonic map of India (prepared by ONGC and GSI) shows that the Indian plate is not a single unit but a composite of three protoplates juxtaposed on each other with a Y-shaped Son-Narmada-Godavari lineament in between them (Naqvi et al, 1974). The three protoplates termed as Dharwar, Aravalli - Bundelkhand, and Singhbhum protoplates, are defined by low values of seismicity and heat flow, whereas the lineaments in between them have relatively high seismicity and heat flow values. These protoplates came into existence as discrete isolated nuclei in the Gondwanaland during pre-Gondwana period. These nuclei grew in size due to accretion of new sialic material from the mantle and also by supracrustal elements (Goodwin, 1971).

It is proposed that during the Precambrian time, the protoplates might have collided along the Son-Narmada lineament; the emplacement of Bundelkhand granites is a result of this collision tectonics. This inference is supported by the calc-alkaline composition of the Bundelkhand granites and the close similarity with the Sierra Nevada and Ben Ghnema batholiths and the east Antarctic shield granites which are believed to be subduction related. The highly fractionated younger I-type leucogranites, some of which plot in alkaline field (Figure 55) may belong to post-collisional setting.

Convergent tectonics is characterized by the presence of features, like ophiolites, blue schist facies of metamorphism and paired metamorphic belt. However, these features cannot be extrapolated back in the Precambrian since the nature of the Archean plates and the tectonic regime may have been quite different from their present day counterparts.

The thermal regime in the Archean was probably different, the heat flow was higher. An immediate consequence of this was that major heat loss was through the large number of spreading centres thereby making the plates smaller and larger in number (Taylor and McLennan, 1985). The controversy of whether the plate tectonics prevailed in the Archean or not should be resolved by the Archean data themselves and not by the present data (Glikson, 1982). The ophiolites in and around Bundelkhand were probably hindered as happened elsewhere. Phinney (1985), observed that the ophiolites in the Archean convergent belts have been hindered in a number of cases as a result of heavy sediment cover.

SUMMARY AND CONCLUSION

The Bundelkhand granite occupying the central portion of India has been mapped as a single undifferentiated granitic massif. Detailed field and laboratory investigations, however, reveal that it is a composite body comprising of several magmatic episodes. Five genetically different types of granite were deciphered and delineated in Mahoba area.

The oldest granitic phase termed hornblende granite is a dark grey coloured medium grained rock with small phenocrysts of feldspars. Enclaves of hornblende granite are found in all the younger granites. The foliated biotite granite exhibits porphyritic texture with two generations of feldspar phenocrysts, pre-tectonic and syn-to post-tectonic. This is intruded by porphyritic biotite granite which is a coarse grained rock with large phenocrysts of feldspar. The coarse grained leucogranite has intruded into the porphyritic biotite granite; xenoliths of foliated biotite granite in coarse grained leucogranite indicate a younger age of the latter. This granite has been intruded by a fine grained rock which has been termed fine grained leucogranite. The fine grained leucogranite is the youngest granitic rock in the area. It is intrusive into all the older types of granite.

The five types of granite have an overall similar mineralogy with differences in relative proportions of individual mineral phases.

The three older granites are characterised by the abundance of ferromagnesian minerals including biotite, hornblende, plagioclase and low K-feldspar content, whereas the younger leucogranites have lower content of ferromagnesian constituents and plagioclase with an increase in K-feldspars and quartz. Hornblende is conspicuously lacking in the two younger leucogranites.

The plots of hornblende granite and foliated biotite granite are concentrated in the granodiorite and granite fields of Streckeisen's (1976) modal quartz, K-feldspar and plagioclase diagram ; the porphyritic biotite granite, coarse grained leucogranite and the fine grained leucogranite occupy the granite field. Plots of all the five types of granite were concentrated mainly in the central part of the Orthoclase-Albite-Quartz phase diagram. The plots of the two older granites are restricted towards the plagioclase field, whereas the three younger granites plot towards K-feldspar field which reflects an enrichment of potassium in progressively younger granites. The plots of all the five types are restricted in and around the area of low temperature trough suggesting that the granites maintained equilibrium throughout cooling.

Various types of perthite are present in all the types of granite; sometimes veins of albite from plagioclase extend into K-feldspar suggesting the exsolution origin of the perthite. Myrmekitic intergrowth is fairly common in all the granites except the hornblende granite and porphyritic biotitte granite where it is rare. Evolution

of the granitic liquid through fractional crystallization is indicated by the presence of zoned euhedral crystals of zircon in the rock.

Plagioclase in all the five types of granite is generally sodic in nature; however, the plagioclase in oldest hornblende granite is relativity more calcic. The plagioclase crystals in the granites exhibit normal zoning with calcic core, intensely altered to serecite surrounded by sodic shell. Abundance of Calrsbad twinning in plagioclase in all the types of Bundelkhand granite suggests a magmatic origin of the granites.

Trace element concentration and their ratios in different types of Bundelkhand granite on Harker's diagram show a good positive linear correlation with U, TH and Rb and strong negative correlation with Sr, Ba and V. Rb/Sr and K/Ba show strong positive correlation, whereas K/Rb and Ra/Rb show negative correlation. K/Rb vs Rb/Sr plots for the Bundelkhand granite follow the trend of fractional crystallization. A progressive increase in Rb/Sr in the younger granites is evident in Rb vs Sr plots. The trends resemble those of a granitic melt produced by fractional crystallization of a common parental co-magmatic source.

The plots of Bundelkhand granites on various major and trace element discriminant diagrams (Figure 45) lie in the orogenic (I- & S- type) granite field and also in the field of fractionated I-type granite. The plots define a negative linear correlation between CaO

and SiO_2 on Harker's diagram (Figure 33). This type of linear array is characteristic of I-type granites. A significant geochemical characteristic of the Bundelkhand granite is its peraluminous composition.

The compositional range and nature of Bundelkhand granite determined from Debon and Le Fort (1983, 1988) nomenclature scheme indicates that the granites vary in composition from granodiorite to granite and correspond to cafemic and alumino-cafemic association of magmatic rocks and calc-alkaline to sub-alkaline in nature. The chemical composition of Bundelkhand granite plotted on AFM diagram and Wright's alkalinity ratio vs SiO_2 diagram reveals a calc-alkaline nature of the granites. The plots on Rogers and Greenberg's (1981) diagram (Figure 55) lie in the field of both calc-alkaline and alkaline composition. Similar trend emerges from Sylvester's (1989) diagram where older three types plot in calc-alkaline and strongly peraluminous fields, whereas the younger two leucogranites lie in the highly fractionated calc-alkaline field.

The Bundelkhand granites closely resemble with Sierra Nevada batholith on AFM diagram and on Rogers and Greenberg's (1981) diagram, it correlates with the Sierra Nevada and Ben Ghnema batholiths. On the basis of close similarity with Sierra Nevada batholith which has been considered to be calc-alkaline inland continental margin magmatism, it is concluded that Bundelkhand granite represents a subduction related magmatism.

The Bundelkhand granites when plotted sequentially on Maniar and Piccoli (1989) tectonic discrimination diagram reveal a continental collision tectonic setting for these rocks. The incompatible trace element patterns of Bundelkhand granite reveal a spectrum of tectonic setting of intrusion. The oldest hornblende granite has a Y-depleted incompatible trace element pattern consistent with that of the Y-depleted granitic rocks of East Antarctic shield which is inferred to be subduction related granite. The pattern of the younger varieties show significant enrichment in Y content and correlates with the trend of undepleted granites of East Antarctic shield. The Y-undepleted granites of East Antarctic shield have been concluded to be syn-orogenic formed by partial melting of felsic crust during the collision of lithospheric plates.

This corroborates the inference based on the plots of Bundelkhand granites on Rogers and Greenberg's (1981) SiO_2 vs Log_{10} (K_2O/MgO) diagram which reveals its calc-alkaline as well as alkaline nature. The plots on Sylvester's diagram (Figure 56) indicate that the three older granites correspond to calc-alkaline type, whereas the two younger leucogranites correlate with the highly fractionated calc-alkaline I-type granite considered to be a variety of alkaline granite.

The Indian plate is a composite one with at least three protoplates coalesced with a Y-shaped Son-Narmada-Godavari lineament

in between them (Naqvi et al, 1974). These protoplates came into existence as discrete isolated nuclei during pre-Gondwana period in the Gondwanaland. Later, they grew in size due to accretion. It is proposed that these protoplates might have collided along the Son-Narmada lineament and the emplacement of Bundelkhand granite is a result of this collision tectonics. This is supported by the I-type calc-alkaline nature and close similarity of Bundelkhand with Sierra Nevada and East-Antarctic shield granites, both believed to be subduction related. It is concluded that the three older types of Bundelkhand granite belong to collisional setting, whereas the two younger leucogranites which plot in the alkaline field (Figure 55) may represent post-collisional magmatism.

LIST OF REFERENCES

Abbott, R.N., and Clarke, D.B., 1979, Hypothetical liquidus relationships in the subsystem Al_2O_3-FeO-MgO projected from quartz, alkali feldspar and plagioclase for a_{H_2O}=1: Cand. Miner., V. 17, pp. 549-560.

Abbott, R.N., JR., 1981, AFM liquidus projections for granitic magmas, with special reference to hornblende, biotite, and garnet : Cand. Miner., V. 19, pp. 103-110.

Adamson, O.J., 1942, Minerals of the Varutrask pegmatite. XXXI. The feldspar group : Geol. Foren. Forh. (Stockholm), V. 64, pp. 19-54.

Alam, S., 1979, Petrology of the granitic rocks in Mahoba, District Hamir Pur (U.P.) : M.Phil. Disser., 62 pp. Aligarh Muslim University.

Anderson, A.T., Jr., 1966, Mineralogy of the Labrieville anorthosite, Quebec : Amer. Miner., V. 51, pp. 1671-1711.

Arth, J.G. and Hanson, G.N., 1975, Geochemistry and origin of the early Precambrian crust of northeastern Minnesota : Geochim. et Cosmochim. Acta, V. 39, pp. 325-362.

Bailey, E.H. and Stevens, R.E., 1960, Selected staining of K-feldspar and plagioclase on rock slabs and thin sections : Amer. Miner., V. 45, pp. 1020-1025.

Barr, S.M., Macdonald, A.S. and Blenkinsop, J., 1986, The Cheticamp pluton : a Cambrian granodioritic intrusion in the western Cape Breton Highlands, Nova Scotia : Cand. Jour. Earth Sci., V. 23, pp. 1686-1699.

Barth, T.F.W., 1962, The feldspar geologic thermometers : Norsk. Geol. Tidsskr., V. 42, pp. 330-339.

_____, 1969, Feldspars : John Wiley and Sons, New York, 261 pp.

Basu, A.K., 1986, Geology of parts of the Bundelkhand granite massif, central India : Rec. Geol. Surv. India, V. 117, pp. 61-124.

Bateman, P.C., Clark, L.D., Huber, N.K., Moore, J.G. and Rinehart, C.D., 1963, The Sierra Nevada batholith : A synthesis of recent work across the central part, U.S. Geol. Surv. Prof. Paper 414-D, 46 pp.

Beckinsale, R.D., 1979, Granite magmatism in the tin belt of southeast Asia. In : M.P. Atherton, J. Tarney (Editors), Origin of Granite Batholiths Geochemical Evidence. 148 pp. Shiva Pub. Co. London.

Bentor, Y.K., 1985, The crustal evolution of the Arabo-Nubian Massif with special reference to the Sinai Peninsula : Precamb. Res., V. 28, pp. 1-74.

Bridgwater, D., Collerson, K.D. and Myers, J.S., 1978, The development of the Archean gneiss complex of the North Atlantic region. In : D. Tarling (Editors), Evolution of the earth's crust. Academic Press, London, pp. 19-69.

Butler, J.R., Bowden, P. and Smith, A.Z., 1962, K/Rb ratios in the evolution of the younger granites of northern Nigeria: Geochim. et Cosmochim. Acta, V. 26, pp. 89-100.

Cawthorn, R.G. and Brown, P.A., 1976, A model for the formation and crystallization of corundum-normative calc-alkaline magmas through amphibole fractionation : Jour. Geol., V. 84, pp. 467-476.

_____, Strong, D.F. and Brown, P.A., 1976, Origin of corundum-normative intrusive and extrusive magmas : Nature, V. 259, pp. 102-104.

Chappell, B.W. and White, A.J.R., 1974, Two contrasting granite types : Paci. Geol., V. 8, pp. 173-174.

_____, 1984, Source rocks of I - and S - type granites in the Lachlan Fold Belt, southeastern Australia : Philos. Trans. Roy. Soc. London, Series A, V. 310, pp. 709-742.

Charoy, B., 1986, The genesis of the Cornubian Batholith (southwest England) : the example of the Carnmenellis pluton, Jour. Petr., V. 27, pp. 571-604.

Chatterji, G.C., Ray, D.K. and Banerjee, P.K., 1971, Stratigraphic sub-division and nomenclature of the Precambrian rock of India : Rec. Geol. Surv. India, V. 101, pp. 1-14.

Chayes, F., 1956, Petrographic modal analyses : 113 pp. Wiley, New York.

Clemens, J.D. and Wall, V.J., 1988, Controls on the mineralogy of S-type volcanic and plutonic rocks : Lithos, V. 21, pp. 53-66.

Collerson, K.D. and Bridgwater, D., 1979, Metamorphic development of early Archean tonalitic and trondhjemitic gneisses : Saglek area, Labrador. In : F. Barker (Editors), Trondhjemites, Dacites and Related Rocks. Elsevier, Amsterdam, pp. 205-273.

Collins, W.J., Beams, S.D., White, A.J.R. and Chappell, B.W., 1982, Nature and origin of A-type granites with particular reference to southeastern Australia : Contr. Miner. Petr., V. 80, pp. 189-200.

Crawford, A.R., 1970, Precambrian geochronology of Rajasthan and Bundelkhand, northern India : Cand. Jour. Earth Sci., V. 7, pp. 91-110.

Czamanske, G.K., Ishihara, S. and Atkin, S.A., 1981, Chemistry of rock forming minerals of the Cretaceous-Paleocene batholith in southwestern Japan and implications for magma genesis : Jour. Geophy. Res., V. 86, pp. 10431-10469.

Das, G.R.N., Bhattacharya, A.K., Dattanarayana, T.A. and Kaul, R., 1982, Radioactive mineral occurrences in the northwestern part of Bundelkhand massif in central India. In : K.S. Valdiya, S.B. Bhatia and V.K. Gaur (Editors), Geology of Vindhyachal, pp. 30-46. Hindustan Pub. Co., New Delhi.

Debon, F. and Le Fort, P., 1983, A chemical - mineralogical classification of common plutonic rocks and associations : Tran. Roy. Soc. Edin : Earth Sc., V. 73, pp. 135-149.

_____ , Le Fort, P., Dautel, D, Sonet, J. and Zimmermann, J.L., 1987, Granites of western Karakorum and northern Kohistan (Pakistan) : A composite Mid-Cretaceous to upper Cenozoic magmatism, Lithos, V. 20, pp. 19-40.

_____ , and Le Fort, P., 1988, A cationic classification of common plutonic rocks and their magmatic associations : principles, method, applications, Bull. Mineral. III. pp. 493-510.

Defant, M.J., Drummond, M.S., Arthur, J.D. and Ragland, P.C., 1988, An example of trondhjemite petrogenesis : the Blackes Ferry pluton, Alabama, U.S.A., Lithos, V. 21, pp. 161-181.

Drake, M.J. and Weill, D.F., 1975, Partition of Sr, Ba, Ca, Y, Eu^{2+}, Eu^{3+}, and other REE between plagioclase feldspar and magmatic Liquid : an experimental study, Geochim. et Cosmochim. Acta, V. 39, pp. 689-712.

Drescher - Kaden, F.K., 1948, Die Feldspat-Quartz - Reaktionsgefuge der Granite und Gneise. 259 pp. Berlin-Gottingen - Heidelberg : Springer.

Eby, G.N., 1987, The Monteregian Hills and White Mountain alkaline igneous provinces, eastern North America. In : J.G. Fitton and B.G.J. Upton (Editors), Alkaline Igneous Rocks, Geol. Soc. Spec. Publ., No. 30, pp. 433-448.

_____ ,and Kochhar, N., 1990, Geochemistry and petrogenesis of the Malani Igneous Suite, north peninsular India : Jour. Geol. Soc. India, V. 36, pp. 109-130.

El-Bouseilly, A.M. and El-Sokkary, A.A. 1975, The relation Rb, Ba and Sr in granitic rocks : Chem. Geol., V. 16, pp. 207-219.

Emmons, R.C., 1943, The universal stage : Geol. Soc. America, Mem. 8, 204 pp.

Erlank, A.J., 1968, The terrestrial abundance relationship between potassium and rubidium. In : L.H. Ahrens (Editor), Origin and Distribution of the Elements. 1178 pp. Pergamon Press.

Fermor, L.L., 1909, Manganese ore deposits of India : Mem. Geol. Surv. India, V. 37, pp. 58-62.

Gast, P.W., 1968, Trace element fractionation and the origins of tholeiitic and alkaline magma types : Geochem. et Cosmochim. Acta, V. 32, pp. 1057-1086.

Glikson, A.Y. and Lambert, I.B., 1976, Vertical zonation and petrogenesis of the early Precambrian crust in western Australia : Tectonophysics, V. 30, pp. 55-89.

_____, 1982, The early Precambrian crust with reference to the Indian Shield : An essay : Jour. Geol. Soc. India, V. 23, pp. 581-603.

Goodwin, A.M., 1971, Metallogenic patterns and evolution of the Canadian Shield : Geol. Soc. Australia, Spec. Publ., V. 3, pp. 157-174.

Gorai, M., 1951, Petrological studies of plagioclase twins : Amer. Miner., V. 36, pp. 884-901.

Halliday, A.N., Stephens, W.E. and Harmon, R.S., 1981, Isotope and chemical constraints on the development of peraluminous Caledonian and Acadian granites : Cand. Miner., V. 19, pp. 205-216.

Hanson, G., 1978, The application of trace elements to the petrogenesis of igneous rocks of granitic composition : Earth Planet. Sci., Lett., V. 38, pp. 26-43.

Harker, A, 1909, The natural history of igneous rocks : pp. New York.

Harmon, R.S., Halliday, A.N., Clayburn, J.A.P. and Stephens, W.E., 1984, Chemical and isotopic systematics of the Caledonian intrusions of Scotland and Northern England : a guide to magma source region and magma-crust interaction : Philos. Trans. Roy. Soc. London, Series, A, V. 310, pp. 709-742.

Haskin, L.A., Allen, R.O., Halmke, P.A., Paster, T.P., Anderson, M.R., Korotev, R.L. and Zweifel, K.A., 1970, Rare earths and other trace elements in Apollo II lunar samples : Proc. Apollo II Lunar Sci. Conf., Geochim. et Cosmochim. Acta, Suppl. 1, V. 2, pp. 1213-1231. Pergamon Press.

Heier, K.S. and Taylor, S.R., 1959, The distribution of Li, Na, K, Rb, Cs, Pb and Tl in southern Norwegian Precambrian alkali-feldspars : Geochim. et Cosmochim. Acta, V. 15 pp. 284-304.

Helz, R.T., 1976, Phase relations of basalts in their melting ranges at PH_2O = 5 Kbar. Part II. Mett compositions: Jour. Petr., V. 17, pp. 139-193.

Herms, O.D., Gromet, L.P. and Zartman, R.E., 1981, Zircon geochronology and petrology of plutonic rocks in Rhode Island. In : J.C. Boothroyd (Editor), Guidebook to geologic field studies in Rhode Island and adjacent areas, Annual Meeting New England Intercollegiate Geological Conference, pp. 315-338.

Heron, A.M., 1935, Pre-Vindhyan geology of Rajasthan : Curr. Sci. V. 83, pp. 10-12.

Hine, R., Williams, I.S. Chappell, B.W. and White, J.R., 1978, Contrast between I- and S-type granitoids of the Kosciusko batholith : Jour. Geol. Soc. Australia, V. 25, pp. 219-234.

Hubbard, F.H., 1966, Myrmekite in charnokite from southwest Nigeria : Amer. Minor., V. 51, pp. 762-773.

_____, 1967, Exsolution myrmekite : geologiska Foreningnesi Stockholm Forhandlingar, V. 89, pp. 410-422.

Hubbard, N.J., Gast, P.W., Meyer, C., Nyquist, L.E., Shih, C. and Weismann, H., 1971, Chemical composition of lunar anorthosites and their parent liquids : Earth Planet. Sci. Lett., V. 13, pp. 71-75.

Imeokparia, E.G., 1984, Geochemistry of the granitic rocks from the Kwandonkaya Complex north Nigeria : Lithos, V. 17, pp. 103-115.

Ischihara, S., 1977, The magnetite-series and ilmenite-series granitic rocks : Ming. Geol., V. 27, pp. 293-305.

Jackson, N.J., Walsh, J.N. and Pegran, E., 1984, Geology, geochemistry and petrogenesis of the late Precambrian granitoids in the central Hijaz region of the Arabian shield : Contr. Miner. Petro., V. 87, pp. 205-219.

James, R.S. and Hamilton, D.L., 1969, Phase relations in the system $NaAlSi_3O_8$-$KAlSi_3O_8$ - $CaAl_2Si_2O_8$ - SiO_2 at 1 Kilobar water vapour pressure : Contr. Miner. Petro., V. 21, pp. 111-141.

Jhingran, A.G., 1958, The problems of Bundelkhand granites and gneisses : Presidential Address, Section Geol. Geog., 45th. Ind. Sci. Congr., Madras.

Kleemann, G.J. and Twist, D., 1989, The compositionally-zoned sheet-like granite pluton of the Bushveld Complex : evidence bearing on the nature of A-type magmatism : Jour. Petro., V. 30, pp. 1383-1414.

Kuno, H., 1956, High-temperature optics of natural sodic plagioclase : Mineral. J. (Tokyo).

Loiselle, M.C. and Wones, D.R., 1979, Characteristics and origin of anorogenic granites : Geol. Soc. Amer. Abstr. with progs., V. 11, pp. 468.

Macrae, N.D. and Nesbitt, H.W., 1980, Partial melting of common sedimentary rocks : a mass balance approach : Contr. Miner. Petro., V. 75, pp. 21-26.

Mallet, F.R., 1869, Vindhyan rocks in Bundelkhand : Mem. Geol. Surv. India, V. 7.

Maniar, P.D. and Piccoli, P.M., 1989, Tectonic discrimination of granitoids : Geol. Soc. Amer. Bull., V. 101, pp. 635-643.

Martin, H., 1987, Petrogenesis of Archean trondhjemites, tonalites, and granodiorites from eastern Finland : major and trace element geochemistry, Jour. Petro., V. 28, pp. 921-953.

Mason,. B. and Moore, C.B., 1985, Principles of Geochemistry (4th Edi.) : 350 pp. Wiley Eastern Limited.

Mathur, P.C., 1954, A note on granitization of quartzites in Bundelkhand : Sci. Cult., V. 20(5), pp. 242-243.

McCarthy, T.S. and Hasty, R.A., 1976, Trace element distribution patterns and their relationship to the crystallization of granitic melts : Geochim. et Cosmochim. Acta, V. 40, pp. 1351-1358.

_____, and Fripp, R.E.P., 1978, The crystalliziation history of a granitic magma, as revealed by trace element abundances : Jour. Geol., V. 88, pp. 211-224.

_____, and Groves, D.I., 1979, The Blue Tie batholith, northeastern Tasmania. A cumulate-like product of fractional crystallization : Contr. Mine. Petr., V. 71, pp. 193-209.

McGregor, V.R., 1979, Archaean grey gneiss and the origin of the continental crust : evidence from the Godthab region, West Greenland. In : F. Barker (Editors), Trondhjemite, Dacites, and Related Rocks. Elsevier, Amsterdam, pp. 169-204.

Michot, P., 1961, Struktur der mesoperthite : Neu. Jahr. Miner. Abte., V. 96, pp. 213-216.

Middlemost, E.A.K., 1985, Magmas and magmatic rocks : 266 pp. Longman Group Limited.

Millar, C.F., 1985, Are strongly peraluminous magmas derived from pelitic sedimentary sources? Jour. Geol., V. 93, pp. 673-689.

Misra, R.C., 1945, Geology of Mahoba area : Proc. Ind. Sci. Congr. Assoc., 32nd Session.

_____, 1948, Hybrid gneisses in Bundelkhand granites of Mahoba, Hamirpur Distt. U.P.: Proc. Ind. Sci. Congr. Assoc., 35th Session, 144 pp.

_____, and Sharma, R.P., 1974, Petrochemistry of Bundelkhand granites and associated rocks of central India : Ind. Miner., V. 15, pp. 43-50.

Misra, R.C. and Sharma, R.P., 1975, New data on the geology of the Bundelkhand Complex of central India : Rec. Reser. Geol., V. 2, pp. 311-346. Hindustan Pub. Co., New Delhi.

Mittlefehldt, D.W. and Miller, C.F., 1983, Geochemistry of the Sweetwater Wash pluton, California : Implications for "anomalous" trace element behaviour during differentiation of felsic magmas: Geochim. et Cosmochim. Acta, V. 47, pp. 109-124.

Naney, M.T., 1983, Phase equilibria of rock forming ferromagnesian silicates in granitic systems : Amer. Jour. Sci., V. 283, pp. 993-1033.

Naqvi, S.M., Rao, D. and Narain, H., 1974, The protocontinental growth of the Indian shield and the antiquity of its rift valleys : Precamb. Res. V. 1, pp. 345-398.

_____, and Rogers, J.J.W., 1987, Precambrian Geology of India: Oxford Mono. Geol. Geophy. 6, 223 pp. Oxford Univ. Press.

Noyes, H.J., Frey, F.A. and Wones, D.R., 1983, A tale of two plutons : geochemical evidence bearing on the origin and differentiation of the Red lake and Eagle Peak pluton, central Sierra Nevada, California : Jour. Geol., V. 91, pp. 487-509.

_____, Wones, D.R. and Frey, F.A., 1983, A tale of two plutons : petrographic and mineralogic constraints on the petrogenesis of the Red lake and Eagle peak plutons, central Sierra Nevada, California, Jour. Geol., V. 91, pp. 353-379.

Onion, R.K. and Pankhurst, R.J., 1978, Early Archean rocks and geochemical evolution of the earth's crust : Earth Planet. Sci. Lett., V. 38, pp. 211-236.

Pascoe, E.H., 1950, A manual of the geology of India and Burma: V. 1, Geol. Surv. India, Calcutta.

Pearce, J.A., Harris, N.B.W. and Tindle, A.G., 1984, Trace element discrimination diagrams for the tectonic interpretation of granitic rocks : Jour. Petr., V. 25, pp. 956-983.

Pitcher, W.S., 1982, Granite types and tectonic environment. In: K.J. Hsu (Editor), Mountain Building Processes, Ch. 1-3, pp. 19-40. Academic Press, London.

_____, 1983, Granite : typology, geological environment and melting relationships. In : M.P. Atherton and C.D. Gribble (Editors), Migmatites, Melting and Metamorphism. Shiva, Nantwich, pp. 277-285.

Phinney, R.A., 1985, A Seismic cross-section of the New England Appalachians : the origin exposed : AGU Spec. Mon.

Raju, R.D., Varma, H.M., Padmanabhan, N. and Mahadevan, T.M., 1983, I- and S-type classification of the Precambrian granitoids of southern India and its possible relevance to mineral exploration. In : S.M. Naqvi and J.J.W. Rogers (Editors), Precambrian of South India. Geol. Soc. India, Mem. 4, pp. 389-400.

Roday, P.P. and Bhatt, A.K., 1980, Tectonic history of the Bijawar rocks at the Barmhanghat Section of the Narmada Valley : Jour. Geol. Soc. India, V. 21, pp. 546-57.

Rogers, J.J.W., Hodges, K.V. and Ghuma, M.A., 1980, Trace elements in continental margin magmatism : part II. Trace elements in Ben Ghnema batholith and nature of the Precambrian crust in central North Africa : Geol. Soc. Amer. Bull.,Vol. 91 Part II, pp. 1742-1788.

_____and Greenberg, J.K., 1981, Trace elements in continental-margin magmatism : Part III. Alkali granites and their relationship to cratonization : Geol. Soc. Amer. Bull., V. 92, pp. 57-93.

Santosh, M. and Drury, S.A., 1988, Alkali granites with Pan-African affinities from Kerala, S. India : Jour. Geol., V. 96, pp. 616-626.

Sarkar, S.N., Polkanov, A.A., Gerling, E.K. and Churkov, F.V., 1964, Precambrian geochronology of Peninsular India : Proc. 22nd Int. Geol. Congr., pp. 158-159.

_____, Saha, A.K. and Miller, J.A., 1969, Geochronology of the Precambrian rocks of Singhbhum and adjacent regions, Eastern India : Geol. Mag., V. 106, pp. 15-45.

Sarma, S.R. and Raja, N., 1958 Some observations on the myrmekite structures in Hyderabad granites : Quart. J. Geol. Mining Metall. Soc. India, V. 30, pp. 215-220.

_____ and Raja, N., 1959, On myrmekite : Quart. J. Geol. Mining Metall. Soc. India, V. 31, pp. 127.

Sastry, V.V., Bhandari, L.L., Raju, T.R. and Datta, A.K., 1971, Tectonic framework and subsurface stratigraphy of the Ganga basin : Jour. Geol. Soc. India, V. 12, pp. 223-233.

Saxena, M.N., 1953, Agmatites in Bundelkhand granites : Curr. Sci., V. 22, pp. 376.

_____, 1956, Trends of variation in the heavy mineral percentages during the course of granitization of the country rocks of the type area : Sci. Cult., V. 22, pp. 544.

_____,1961, Bundelkhand granites and associated rocks from Kabrai and Mau Ranipur areas of Hamirpur and Jhansi Distt. U.P., India : Res. Bull. Punj. Univ., V. 12 (I,II), pp. 85-107.

Seifert, K.E., 1964, The genesis of plagioclase twinning in the Nonewag granite : Amer. Miner., V. 49, pp. 297-320.

Shapiro, L. and Brannock, W.W., 1962, U.S. Geol. Surv. Bulletin, 1144-A.

Sharma, R.P., 1982, Lithostratigraphy structure and petrology of the Bundelkhand group. In : K.S. Valdiya, S.B. Bhatia and V.K. Gaur (Editors), Geology of Vindhyachal, pp. 30-46. Hindustan Pub. Co., New Delhi.

_____ , 1983, Structure and tectonic of the Bundelkhand Complex : Central India, Rec. Reser. Geol., V. 10, pp. 198-210.

Sheraton, J.W. and Black, L.P., 1988, Chemical evolution of granitic rocks in the east Antractic Shield, with particular reference to post-orogenic granites : Lithos, V. 21, pp. 37-52.

_____ , Ellis, D.J. and Kuehner, S.M., 1985, Rare earth element geochemistry of Archean orthogneisses and evolution of the East Antarctic Shield : Bur. Miner. Resour. J. Aust. Geol. Geophys. V. 9, pp. 207-218.

Smith, J.V., 1974, Feldspar Minerals, 2, chemical and textural properties : 690 pp. Springer - Verlag Berlin Heidelberg New York.

Soldatos, K., 1962, Uber die kryptoperthitische Albite-Ausscheidung in mikroklinperthiten : Norsk Geologisk Tidskrifft, V. 42, pp. 180-192.

Stavrov, O.D., 1971, Ore content in granite and the geochemistry of Rb : Geochemistry Int., V. 8, pp. 739-754.

Stoeser, D.B. and Elliot, J.E., 1980, Post-orogenic peralkaline and calc-alkaline granites and associated mineralization of the Arabian Shield, Kingdom of Saudi Arabia. In : Al-Shanti, A.M. (Editors), Evolution and Mineralization of the Arabian-Nubian Shield, Bull. Inst. Appl. Geol. King Abdul Aziz University, V. 4, pp. 1-23.

Streckeisen, A.L., 1976, To each plutonic rock its proper name : Earth Sci. Rev., V. 12, pp. 1-33.

Sun, S-S., Nesbitt, R.W. and Sharaskin, A.Y., 1979, Geochemical characteristics of mid-ocean ridge basalts : Earth Planet. Sci. Lett., V. 44, pp. 119-138.

Sylvester, P.J., 1989, Post-collisional alkaline granites : Jour. Geol., V. 97, pp. 261-280.

Tarney, J. and Saunders, A.D., 1979, Trace element constraints on the origin of cordilleran batholiths. In : M.P. Atherton and J. Tarney (Editors), Origin of Granitic Batholiths : Geochemical Evidence. Shiva, Nantwich, pp. 90-105.

Tauson, L.V., 1965, Factors in the distribution of the trace elements during the crystallization of magmas : Phys. Chem. Earth, V. 6, pp. 215-249.

_____, 1968, Distribution regularities of trace elements in granitoid intrusions of the batholiths and hypabyssal type. In : L.H. Ahrens (Editors), Origin and distribution of the elements, pp. 1178. Pergamon Press.

Taylor, S.R., Emeleus, C.H. and Exley, C.S., 1956, Some anomalous K/Rb ratios in igneous rocks and their petrological significance : Geochim. et Cosmochim. Acta, V. 10, pp. 224-229.

_____ and Heier, K.S., 1958, Alkali elements in potash feldspars from the Precambrian of southern Norway : Geochim. et Cosmochim. Acta, V. 13, pp. 293-302.

Taylor, S.R. and Heier, K.S., 1960, The petrological significance of trace element variations in alkali feldspars : Proc. XXI Int. Geol. Congr., Norden, part 14, pp. 47-61.

_____, 1965, The application of trace element data to problems in petrology : Phys. Chem. Earth, V. 6, pp. 133-213.

_____ and McLennan, S.M., 1985, The continental Crust : its composition and evolution, 311 pp. Blackwell Sci. Publ.

Tobi, A.C., 1962, Characteristic patterns of plagioclase twinning : Norsk. Geol. Tidsskr., V. 42, pp. 264-271.

Tuach, J., Davenport, P.H., Dickson, W.L. and Strong, D.F., 1986, Geochemical trends in the Ackley granite, southeast Newfoundland : their relevance to magmatic - metallogenic processos in high-silica granitoid systems : Cand. Jour. Earth Sci., V. 23, 747-765.

Valsov, K.A., 1966, Geochemistry of rare elements, V.I., Israel program for Scientific Translations, Jerusalem, 688 pp.

Vance, J.A., 1961, Polysynthetic twinning in plagioclase : Amer. Miner., V. 46, pp. 1097-1119.

Weill, D.F., McKay, G., Kridelbaugh, S. and Grutzeck, M., 1974, Modeling the evolution of Sm and Eu abundances during lunar igneous differentiation : Proc. 5th Lunar Sci. Conf., Geochim. et Cosmochim. Acta Suppl. 5, V. 2, pp. 1337-1352.

Whalen, J.B., 1983, The Ackley city batholith, southeastern Newfoundland : evidence for crystal versus liquid - state fractionation, Geochim. et Cosmochim. Acta, V. 47, pp. 1443-1457.

_____ , Currie, K.I. and Chappell, B. W., 1987, A-type granites : geochemical characteristics, discrimination and petrogenesis : Contr. Miner. Petr., V. 95, pp. 407-419.

White, A.J.R. and Chappell, B.W., 1977, Ultrametamorphism and granitoid genesis : Tectonophysics, V. 43, pp. 7-22.

_____ and Chappell, B.W., 1983, Granitoid types and their distribution in the Lachlan fold belt, southeastern Australia : Geol. Soc. America, Mem., V. 159, pp. 21-34.

Whitney, J.A., Lois, M.J. and Walker, R.L., 1976, Age and origin of the Stone mountain granite, Lithonia district, Georgia : Geol. Soc. Amer. Bull., V. 87, pp. 1067-1077.

Wood, D.A., Tarney, J., Varet, J., Saunders, A.D., Bougault, H., Joron, J.L., Treuil, M. and Cann, J.R., 1979, Geochemistry of basalts drilled in the North Atlantic by IPOD Leg 49 : implications for the mantle heterogeneity : Earth Planet. Sci. Lett., V. 42, pp. 77-97.

Wright, J.B., 1969, A simple alkalinity ratio and its application to questions of non-orogenic granite genesis : Geol. Mag., V. 106, pp. 370-384.

Wyllie, P.J., Huang, W., Stern, C.R. and Maalque, S., 1976, Granitic magmas : possible and impossible sources, water contents, and crystallization sequences : Cand. Jour. Earth Sci., V. 13, pp. 1007-1019.

Zielinski, R.A. and Frey, F.A., 1970, Gough Island : evaluation of a fractional crystallization model : Contr. Miner. Petro., V. 29, pp. 242-254.

Zen, E. and Hammarstrom, J.M., 1982, Magmatic epidote : host rocks, mineral compositions, and significance : Geol. Soc. Amer. (Abs. with Prog.) , V. 14, pp. 652.

Zlobin, B.I. and Lebedev, V.I., 1960, Geochemical relationship of Li, Na, K, Rb, and Tl in alkalic magma and its petrogenetic significance : Geokhimiya, No.2, pp. 101-124.

APPENDIX - A

Chemical Analysis of Five Types of Bundelkhand Granite

	Hornblende Granite							
Major Elements (Oxide Wt. %)	73	75	76	77	81	83	85	87
SiO_2	66.43	65.03	64.35	66.10	65.36	65.60	67.28	64.21
TiO_2	0.28	0.60	0.54	0.48	0.80	0.68	0.66	0.57
Al_2O_3	16.34	16.43	16.76	15.73	14.18	15.70	15.26	16.55
Fe_2O_3*	2.80	4.90	5.00	4.16	4.60	4.80	4.60	4.90
MnO	0.065	0.084	0.069	0.062	0.068	0.067	0.054	0.076
MgO	1.21	1.54	1.61	1.42	1.25	1.28	1.15	1.59
CaO	2.57	3.57	3.75	3.13	2.67	2.68	2.47	3.76
Na_2O	3.55	3.81	3.70	3.85	3.50	3.60	3.85	3.96
K_2O	4.12	3.90	3.61	4.80	5.32	4.90	4.71	3.36
P_2O_5	0.15	0.24	0.22	0.20	0.29	0.27	0.26	0.22
Total	97.52	100.10	99.61	99.93	98.03	99.57	100.29	99.20
Trace Elements (ppm)								
Ba	623	1092	1216	731	771	1062	796	902
Rb	222	169	155	209	218	238	259	142
Sr	243	291	510	221	260	266	259	298
Cr	63	58	52	49	58	42	52	58
Ni	45	41	39	29	32	32	29	45
Cu	11	8	18	12	15	8	18	14
Zn	68	81	73	67	82	74	69	76
Co	20	26	21	25	22	21	21	25
Pb	14	15	15	14	16	16	17	13
Ni	32	42	34	30	34	31	38	37
V	45	-	-	-	-	-	-	70
Nb	21	-	-	-	15	-	-	27
Y	28	17	19	-	26	-	-	30
Zr	-	177	188	-	-	-	-	-
Ga	-	12	13	-	11	-	-	-
U	-	3	3	-	6	-	-	-
Th	-	16	8	-	12	-	-	-
$Al_2O_3/CaO+Na_2O+K_2O$	1.59	1.45	1.51	1.33	1.23	1.40	1.38	1.49
K_2O/Na_2O	1.16	1.02	0.98	1.25	1.52	1.36	1.22	0.85
K/Rb	154	192	193	190	202	171	151	196
K/Ba	42.43	29.67	24.64	54.44	52.20	38.30	49.12	31.98
Rb/Sr	0.85	0.58	0.30	0.94	0.84	0.89	1.00	0.40
U/Th	-	0.19	0.38	-	0.50	-	-	-
Ni/Co	2.25	1.58	1.86	1.16	1.45	1.52	1.38	1.60
Zr/Y	-	10.41	9.89	-	-	-	-	-
Ti/Zr	-	20.43	17.22	-	-	-	-	-
Ti/Nb	80.95	-	-	-	319.73	-	-	126.56

*Fe_2O_3 was determined as total iron.

Appendix-A contd

	Foliated Biotite Granite													
Major Elements (Oxide Wt %)	88	89	90	91	93	132	171	180	181	184	197	202	189	194
SiO_2	67 21	68 47	69 84	70 07	71 21	72 85	65 08	66 83	72 43	72 49	72 82	67 52	71 96	67 58
TiO_2	0 38	0 40	0 35	0 41	0 33	0 54	0 53	0 46	0 24	0 24	0 16	0 36	0 21	0 26
Al_2O_3	15 86	15 63	15 73	15 56	15 13	15 14	15 35	15 82	16 44	15 17	15 93	16 48	15 42	16 34
Fe_2O_3*	4 00	2 70	1 80	2 20	1 80	2 10	4 00	2 30	1 20	1 50	1 00	2 40	1 30	1 90
MnO	0 055	0 060	0 042	0 050	0 041	0 054	0 063	0 048	0 060	0 074	0 033	0 055	0 068	0 052
MgO	1 15	1 12	0 74	0 87	0 71	0 95	1 37	1 14	0 52	0 55	1 53	0 96	0 30	0 89
CaO	2 68	2 04	1 76	1 78	1 80	1 86	2 82	2 29	1 46	1 68	1 20	2 80	1 33	1 79
Na_2O	3 92	3 72	3 54	3 55	3 65	3 65	3 30	3 25	3 70	4 50	4 00	4 60	4 03	3 96
K_2O	4 89	5 05	5 00	4 50	5 05	4 38	5 18	5 52	5 20	3 62	4 91	3 99	3 61	5 90
P_2O_5	0 17	0 18	0 14	0 16	0 13	0 16	0 20	0 19	0 10	0 10	0 08	0 18	0 09	0 10
Total	100 31	99 17	99 31	99 15	99 85	101 68	99 89	97 84	101 35	99 92	101 66	99 34	98 31	98 77
Trace Elements (ppm)														
Ba	610	584	228	207	310	504	988	925	705	274	233	469	173	515
Rb	307	329	336	296	350	324	388	405	429	211	263	243	367	306
Sr	262	239	203	185	224	202	253	241	149	115	108	258	92	130
Cr	52	58	42	37	68	62	-	58	31	21	31	68	31	31
Ni	27	34	34	24	36	-	43	29	32	17	-	34	22	27
Cu	11	8	11	9	9	10	15	15	7	4	7	11	5	6
Zn	69	66	57	63	57	59	67	58	53	73	49	61	66	47
Co	21	25	26	14	30	36	17	18	19	19	24	23	19	18
Pb	16	20	20	24	18	45	34	22	17	27	17	10	16	15
Li	50	47	39	35	40	41	-	45	-	-	17	40	59	12
V	35	-	-	-	-	-	61	-	-	-	-	-	-	-
Nb	22	16	22	21	-	-	26	20	-	-	-	-	-	-
Y	27	32	36	44	-	-	33	37	-	-	-	-	-	-
Zr	-	201	199	212	-	-	-	208	-	-	-	-	-	-
Ga	-	16	16	17	-	-	-	14	-	-	-	-	-	-
U	-	9	14	17	-	-	-	15	-	-	-	-	-	-
Th	-	24	40	-	-	-	-	62	-	-	-	-	-	-
$Al_2O_3/CaO+Na_2O+K_2O$	1 38	1 44	1 52	1 58	1 44	1 53	1 35	1 43	1 58	1 54	1 57	1 44	1 71	1 40
K_2O/Na_2O	1 24	1 36	1 41	1 26	1 38	1 20	1 56	1 69	1 40	0 80	1 22	0 86	0 89	1 48
K/Rb	132	127	123	126	120	112	111	113	101	142	155	136	82	160
K/Ba	65	72	102	100	135	72	44	50	61	110	175	71	173	95
Rb/Sr	1 10	1 37	1 65	1 60	1 56	1 60	1 39	1 68	2 87	1 83	2 43	0 94	3 98	2 3
U/Th	-	0 38	0 30	-	-	-	-	0 24	-	-	-	-	-	-
Ni/Co	1 29	1 36	1 31	1 71	1 20	-	2 53	1 61	1 68	0 89	-	1 48	1 16	1 50
Zr/Y	-	6 28	5 53	4 82	-	-	-	7 78	-	-	-	-	-	-
Ti/Zr	-	11 93	10 54	11 59	-	-	-	9 57	-	-	-	-	-	-
Ti/Nb	103 64	149 87	95 16	117 04	-	-	122 19	137 90	-	-	-	-	-	-

* Fe_2O_3 was determined as total iron

Appendix-A contd.

	Porphyritic Biotite Granite							
Major Elements (Oxide Wt. %)	68	69	72	79	80	86	139/1	141
SiO_2	68.91	71.08	69.21	70.60	68.77	72.64	71.10	74.22
TiO_2	0.33	0.33	0.24	0.46	0.52	0.37	0.57	0.33
Al_2O_3	16.14	15.22	15.22	15.47	15.62	15.70	14.92	11.09
Fe_2O_3*	1.90	2.50	2.50	2.20	4.20	2.30	1.90	1.50
MnO	0.034	0.045	0.045	0.049	0.067	0.041	0.059	0.039
MgO	0.58	0.61	0.61	0.67	1.11	0.59	0.91	0.26
CaO	0 95	1.34	1.34	1.61	1.87	1.38	1.92	1.46
Na_2O	3.30	3.25	3.33	3.45	3.26	3.32	3.21	3.50
K_2O	6.35	5.20	5.79	5.90	4.50	5.40	4.24	7.02
P_2O_5	0.19	0.13	0.16	0.15	0.20	0.14	0.18	0.14
Total	98.98	99.88	98.44	100.55	98.26	101.88	99.00	99.56
Trace Elements (ppm)								
Ba	206	100	273	159	212	206	128	466
Rb	402	358	356	415	333	355	375	580
Sr	120	129	158	176	168	129	127	135
Cr	31	42	45	36	42	26	42	26
Ni	22	22	17	27	24	27	29	-
Cu	13	13	7	8	15	10	9	11
Zn	53	66	64	56	82	64	76	69
Co	17	20	18	21	19	28	22	31
Pb	16	15	19	22	20	18	20	51
I	44	54	51	34	42	48	61	25
V	-	-	-	46	-	-	38	31
Nb	20	-	-	40	20	20	40	24
Y	41	-	-	51	41	38	52	28
Zr	254	-	-	-	291	283	-	-
Ga	17	-	-	-	12	15	-	-
U	13	-	-	-	12	18	-	-
Th	52	-	-	-	46	50	-	-
$Al_2O_3/CaO+Na_2O+K_2O$	1.55	1.57	1.45	1.41	1.62	1.55	1.59	0.92
K_2O/Na_2O	1.92	1.60	1.73	1.71	1.38	1.62	1.32	2.00
K/Rb	131	121	135	118	112	126	94	100
K/Ba	256	432	176	308	176	218	275	125
Rb/Sr	3.35	2.77	2.25	2.36	1.98	2.75	2.95	4.30
U/Th	0.25	-	-	-	0.26	0.36	-	-
Ni/Co	1.29	1.10	0 94	1.29	1.26	0.96	1.32	-
Zr/Y	6.20	-	-	-	7.10	7.45	-	-
Ti/Zr	7.79	-	-	-	10.71	7.84	-	-
Ti/Nb	98.90	-	-	68.95	155.85	110.90	85.42	82.42

*Fe_2O_3 was determinod as total iron.

Appendix -A contd.

Coarse Grained Leucogranite

Major Elements (Oxide Wt. %)	119	121	125	127	133	146	147	148	152	155	157	159	161
SiO_2	71.50	72.01	74.22	71.49	72.41	73.04	73.28	70.95	74.07	73.57	73.97	71.29	73.51
TiO_2	0.60	0.18	0.32	0.13	0.39	0.21	0.31	0.23	0.24	0.26	0.23	0.15	0.21
Al_2O_3	15.21	15.56	15.35	15.41	14.98	15.19	15.31	13.07	16.84	14.74	15.06	14.89	15.60
Fe_2O_3*	2.00	1.80	1.70	1.00	1.60	1.20	1.60	1.20	1.20	1.60	1.80	1.40	1.50
MnO	0.026	0.028	0.025	0.027	0.026	0.037	0.039	0.019	0.031	0.030	0.033	0.027	0.024
MgO	0.33	0.40	0.35	0.18	0.29	0.32	0.25	0.18	0.25	0.17	0.97	0.74	1.46
CaO	1.29	1.26	1.12	0.74	0.97	1.11	1.22	0.89	0.79	0.86	0.82	0.65	1.11
Na_2O	2.89	3.05	3.15	3.86	3.00	3.49	3.40	3.50	3.44	3.25	3.30	3.30	3.40
K_2O	6.01	5.79	6.15	5.98	6.20	4.78	5.80	6.05	6.00	5.29	5.9	5.41	5.75
P_2O_5	0.10	0.10	0.10	0.07	0.09	0.08	0.10	0.07	0.08	0.09	0.09	0.06	0.09
Total	99.95	100.37	101.48	99.38	99.95	99.45	101.30	96.13	102.94	99.86	102.17	97.91	102.65
Trace Elements (ppm)													
Ba	287	195	295	341	109	260	526	233	170	465	653	335	477
Rb	374	373	361	465	378	356	568	656	640	465	363	418	450
Sr	97	96	98	115	96	83	122	71	76	90	95	56	136
Cr	33	31	32	31	31	24	26	31	31	31	16	21	31
Ni	24	22	24	23	24	41	13	22	22	24	12	17	27
Cu	10	10	8	9	8	9	10	11	9	13	11	10	8
Zn	53	66	55	57	55	51	53	55	50	63	57	59	49
Co	12	20	18	25	18	23	32	31	34	21	30	28	39
Pb	27	21	43	35	43	20	43	42	65	26	32	40	58
Li	15	24	21	19	21	49	33	35	33	31	35	29	36
V	-	-	-	-	29	-	-	-	-	29	-	-	19
Nb	-	24	-	-	38	12	-	-	21	33	-	-	20
Y	-	43	-	-	43	34	-	-	43	29	-	-	22
Zr	-	309	-	-	-	149	-	-	211	-	-	-	-
Ga	-	15	-	-	-	14	-	-	15	-	-	-	-
U	-	17	-	-	-	14	-	-	23	-	-	-	-
Th	-	73	-	-	-	43	-	-	89	-	-	-	-
$Al_2O_3/CaO+Na_2O+K_2O$	1.49	1.54	1.47	1.45	1.47	1.61	1.46	1.24	1.64	1.56	1.50	1.59	1.52
K_2O/Na_2O	2.14	1.89	1.95	1.54	2.06	1.36	1.70	1.72	1.74	1.72	1.78	1.63	1.69
K/Rb	137	129	141	107	136	111	85	77	78	94	135	107	106
K/Ba	174	246	173	146	136	153	91	216	293	140	75	135	98
Rb/Sr	3.85	3.88	3.68	4.04	5.32	4.28	4.65	9.23	8.42	6.54	3.82	7.46	3.62
U/Th	-	0.23	-	-	-	0.33	-	-	0.26	-	-	-	-
Ni/Co	2.0	1.1	1.33	0.92	1.33	1.78	0.41	0.71	0.65	1.14	0.4	0.61	0.69
Zr/Y	-	7.19	-	-	-	4.38	-	-	4.91	-	-	-	-
Ti/Zr	-	7.37	-	-	-	8.44	-	-	6.81	-	-	-	-
Ti/Nb	-	94.92	-	-	61.53	104.92	-	-	68.52	47.24	-	-	62.95

*Fe_2O_3 was determined as total iron

Appendix-A contd.

	Fine Grained Leucogranite									
Major Elements (Oxide Wt. %)	163	164	165	166	167	168	175	139/A	142	154
SiO_2	74.35	72.54	74.25	74.59	74.11	74.91	74.61	74.67	73.78	72.51
TiO_2	0.14	0.14	0.15	0.13	0.18	0.13	0.13	0.19	0.21	0.23
Al_2O_3	13.62	14.75	14.58	14.41	14.83	14.79	15.76	14.86	15.79	17.96
Fe_2O_3*	0.85	1.00	1.10	0.94	0.91	0.85	0.80	0.90	1.50	1.40
MnO	0.024	0.032	0.025	0.024	0.028	0.026	0.019	0.019	0.033	0.023
MgO	0.75	0.66	0.75	0.67	0.64	0.60	0.63	0.45	0.32	0.24
CaO	0.71	0.77	0.82	0.81	0.74	0.84	0.82	0.80	0.93	1.25
Na_2O	3.52	3.32	3.31	3.56	3.32	3.33	3.39	3.19	3.31	3.40
K_2O	5.39	5.68	5.79	6.31	5.85	5.23	5.11	5.31	5.83	6.35
P_2O_5	0.06	0.05	0.06	0.05	0.05	0.05	0.05	0.06	0.08	0.11
Total	99.39	98.94	100.82	101.49	100.61	100.75	101.32	100.45	101.78	103.47
Trace Elements (ppm)										
Ba	63	43	84	72	85	91	95	161	238	495
Rb	631	541	506	612	508	534	471	352	393	342
Sr	57	50	63	55	51	41	69	79	98	112
Cr	29	31	31	52	52	63	62	50	42	46
Ni	27	22	27	29	34	34	-	-	32	41
Cu	11	6	13	7	6	6	6	7	9	8
Zn	50	53	50	44	40	41	33	39	60	41
Co	41	20	45	27	27	45	20	24	23	24
Pb	48	31	33	30	27	28	35	17	22	14
Li	24	56	33	30	11	33	18	13	27	31
V	-	-	-	-	14	-	-	-	-	-
Nb	31	-	-	-	36	-	21	22	-	-
Y	52	-	-	-	41	-	50	41	-	-
Zr	139	-	-	-	-	-	119	169	-	-
Ga	13	-	-	-	-	-	18	13	-	-
U	29	-	-	-	-	-	28	22	-	-
Th	54	-	-	-	-	-	55	78	-	-
$Al_2O_3/CaO+Na_2O+K_2O$	1.41	1.50	1.46	1.34	1.49	1.57	1.69	1.59	1.56	1.63
K_2O/Na_2O	1.53	1.71	1.74	1.77	1.76	1.57	1.50	1.66	1.76	1.86
K/Rb	70.90	87.15	94.98	85.31	138.72	81.30	90.06	125.22	123.14	154.13
K/Ba	710.20	1096.50	572.19	727.50	829.05	477.08	446.50	273.78	203.34	106.49
Rb/Sr	11	11	8	11	10	13	7	4.45	4.01	3.05
U/Th	0.54	-	-	-	-	-	0.51	0.28	-	-
Ni/Co	0.66	1.10	0.60	1.07	1.26	0.76	-	-	1.39	1.71
Zr/Y	2.67	-	-	-	-	-	2.38	4.12	-	-
Ti/Zr	6.03	-	-	-	-	-	6.54	5.39	-	-
Ti/Nb	27.06	-	-	-	23.30	-	37.09	51.77	-	-

*Fe_2O_3 was determined as total iron.